5-7-2016

Quantifying Atmospheric Nitrogen Deposition to U.S. Waterways

Xuanwen Chen
University of Connecticut - Storrs, xuanwen.chen@uconn.edu

Quantifying Atmospheric Nitrogen Deposition to U.S. Waterways

Xuanwen Chen

B.E., Nanchang University, 2014

A Thesis

Submitted in Partial Fulfillment of the

Requirements for the Degree of

Masters of Science

At the

University of Connecticut

2016

APPROVAL PAGE

Masters of Science Thesis

Quantifying Atmospheric Nitrogen Deposition to U.S. Waterways

Presented by

Xuanwen Chen, B.E.

Major Advisor_____

Kristina Wagstrom

Associate Advisor_____

Leslie Shor

Associate Advisor_____

Marina Astitha

University of Connecticut

2016

ACKNOWLEDGEMENT

The completion of my Master's thesis could not be achieved without the help of many individuals.

First, my sincere thanks to my advisor, Dr. Kristina Wagstrom, for her great guidance on my research. She gave me considerable support and advice on writing my thesis.

Thanks to Dr. Leslie Shor from UConn Chemical Engineering and Dr. Marina Astithis from UConn Environmental Engineering for being willing to be a part of my Advisory Committee. I especially want to thank them for being flexible to set up my oral defense time as well as to receive my thesis draft.

My great thanks also go to my colleagues as well as friends, Fatema Parves and Carmen Lamancusa, who are always there to support and help me. They always had spare time for me to answer my questions and to explain things in detail to help me better understand concepts and programming.

Further thanks to the Booth Engineering Center for Advanced Technology (BECAT) from UConn, who helped our group install the software and provide us with the computational resources, which enabled us to complete the research. Thanks to my friends, especially Holly Robilllard, Nicole Beauregard, Lirong Ding, and Valeria Cooke, who helped me with my final thesis proof reading.

Finally, all my love and thanks to my parents, for their priceless love and support. Without their love and support, I would not have fulfilled my goal to further study in the United States and complete my degree.

Table of Contents

LIST OF FIGURES

ABSTRACT

Increasing atmospheric nitrogen deposition due to anthropogenic emissions released into the atmosphere contributes to water eutrophication in the recent years. Previous studies have discussed what major species contribute to the nitrogen deposition onto waterbodies. Few studies have quantified the contribution of these major nitrogen-containing species to individual U.S. watersheds. Seasonal dry and wet deposition of major nitrogen-containing species were quantified in this study, including ammonia (NH_3), nitric acid (HNO_3), nitrogen oxides (NOx), particulate ammonium (PNH_4) and particulate nitrate (PNO_3) onto watersheds in the contiguous United States.

A regional chemical transport model, the Comprehensive Air Quality Model with eXtension (CAMx), was used to get deposition information in the year 2011 in the contiguous United States. The watershed shapefile was obtained from the U.S. Geological Survey's website (USGS). A Geographic Information System (ArcGIS) was utilized to create a fishnet grid, which has the same information as the one in CAMx. ArcGIS was employed to combine the fishnet grid and the watershed file together to get the deposition information in each grid cell. Finally, a program was written in MATLAB to calculate how much each nitrogen-containing species was deposited onto each watershed.

It is shown that gaseous species are dominant in dry deposited mass per area, with ammonia (NH_3), nitric acid (HNO_3), and nitrogen dioxide (NO_2) contributing 40% to 60%, 20% to 40%, and 10% of the total nitrogen dry deposition, respectively. While for wet deposition, the major contribution is from nitric acid

(HNO_3) and particulate ammonium (PNH_4). HNO_3 contributes 40%-60% of the total nitrogen wet deposited mass per area, PNH_4 about 20%-40%, and NH_3 and particulate nitrate (PNO_3) altogether contribute about 10%. Gases receive less resistance while being dry deposited because they have smaller molecular size. Particulate matter acts as cloud nuclei and grows big to fall as precipitation by wet deposition. HNO_3 is highly soluble in water and can be easily removed by wet deposition in the atmosphere.

It is also concluded that spring and summer are the two seasons which consistently receive the most nitrogen deposited mass per area for both wet and dry deposition, while fall and winter receive the least deposited nitrogen mass. The maximum value of spring can be over twice that of fall. Because in spring and summer, there is more frequency of rainfall, which helps remove nitrogen-containing species by wet deposition. Vegetation starts to grow in spring and summer, which helps gases to be dry deposited.

For the annual deposition, the mass of nitrogen deposited per area through dry deposition, which ranges from 110 to 910 kgN/km^2, is over twice that of wet deposition, which ranges from 40 to 390 million kgN/km^2. It could be because there is less rainfall in the year 2011, which reduces the removal of nitrogen species by wet deposition.

Eastern United States, including Ohio, Mid Atlantic, Great Lakes, Upper Mississippi, Lower Mississippi, Tennessee and New England, and other watersheds such as California, Texas-Gulf, and Arkansas-White-Red watersheds receive more deposition throughout the year. Because nitrogen emission sources

are mainly vehicular emissions, power plants, and fertilizer use. These watersheds are highly populated. Additionally, power plants are concentrated in these areas. Both of these two factors can result in the higher deposition in the watersheds mentioned above.

Chapter 1 INTRODUCTION

1.1 Impacts of Nitrogen Deposition to the Environment

Industrialization and anthropogenic emissions have contributed to the continuing deposition of atmospheric nitrogen to terrestrial and aquatic systems. This excess of nitrogen loading leads to soil acidification, loss of biodiversity, decrease in water visibility, and eutrophication of waters (Zhao et al., 2015). Soil acidification is the accumulation of protons, which reduces the soil pH. The donor can be an acid, such as nitric acid (HNO_3). Soil acidification causes plants unable to grow. Decrease in water visibility declines the sunlight penetrating the water. Aquatic life cannot get enough sunlight to survive, which leads to the loss of biodiversity in the water. Eutrophication results from the oversupply of chemical nutrients, typically compounds containing nitrogen, phosphorus, or both (Khan et al., 2013; Hautier et al., 2009). The excess of nutrients often stimulates the overgrowth of algae and vegetation (Diaz et al., 2008; Rebich et al., 2011), which results in a noticeable greening of the water that can be seen in the bottom figure in Fig. 1.1. After such organisms die, they sink to the bottom of the water. In the process, microbes, such as bacteria, decompose the organisms and consume the dissolved oxygen in the water (Diaz et al., 2008; Werner et al., 2006; Khan et al., 2013; Kemker, 2013). Hypoxia takes place when the dissolved oxygen level falls below 2 mg/L (or approximately 30% saturation) (Diaz, 2001; Diaz et al., 2008). Starting from this level, organisms begin to feel the effects of oxygen deprivation (Diaz et al., 2008; Sotto et al., 2014). Most aquatic life, such as fish, invertebrates, plants and bacteria, cannot live below normal dissolved oxygen levels (Kemker,

2013). For instance, bottom creatures in the water, including crabs, oysters and worms need a minimal amount of oxygen, which is approximately 1-6 mg/L (Kemker, 2013); fish, such as shallow water fish which need 5-15 mg/L to survive, are unable to live below 30% saturation (Mallya et al., 2007; Kemker, 2013). Eutrophication in water results in a decrease in biodiversity. Eutrophication can also decline the visibility of water, which shows the sharp difference between clear water and polluted water.

Fig. 1.1 (Up: Clear Water; Down: Polluted Water, https://www.epa.gov/nutrientpollution/problem)

1.2 Sources of Atmospheric Nitrogen Emissions

Atmospheric nitrogen emissions are mainly from ammonia (NH_3) and nitrogen oxides (NO_x, including NO and NO_2) (Zhao et al., 2015; Pitcairn et al., 1995). NH_3 and NOx are mainly emitted from anthropogenic sources, including vehicular and transportation combustion, animal husbandry, and power plants (Luo et al., 2002). NH_3 is primarily emitted from agriculture, including fertilizer, animal waste, as well as industrial and vehicular emissions (Behera et al., 2013; Zhao et al., 2015; Pitcairn et al., 1995). Nitric oxide (NO) can be produced through biological processes, including nitrification and denitrification in soils by bacteria (Yu et al., 2010; Liu et al., 2015). NO can be released through the flux of soil into the atmosphere. NO can also be produced during the combustion of fuel cells (Qian et al., 2011). Nitrogen dioxide (NO_2) comes from traffic emission and other combustion sources, such as power plants (Son et al., 2004). NO_2 can also be produced by the oxidation of NO in the atmosphere (Seinfeld et al., 2006). The sum of NO and NO_2 is usually known as nitrogen oxides (NO_x) (Seinfeld et al., 2006).

In the atmosphere, nitrogen dioxide (NO_2) is then oxidized into nitric acid (HNO_3), which is soluble in water and can be removed from the atmosphere by wet and dry deposition (Zhao et al., 2015; Martin et al., 2003). HNO_3 is one of the components of acid rain. Deposition of HNO_3 contributes to acidification of soil and surface water (EPA, 2012). NH_3 can react with HNO_3 and sulfuric acid (H_2SO_4) to produce nitrate particles and ammonium sulfate (Zhang et al., 2012).

The figure below shows major sources of nitrogen emissions and reaction processes for nitrogen-containing species in the atmosphere (Fig. 1.2). The words in the orange rounded rectangular shape represent the major nitrogen-containing species which were considered in the research; the words in the black oval shape mean the main sources of nitrogen-containing species in the atmosphere; the words in blue refer to the removal processes of nitrogen species from the environment.

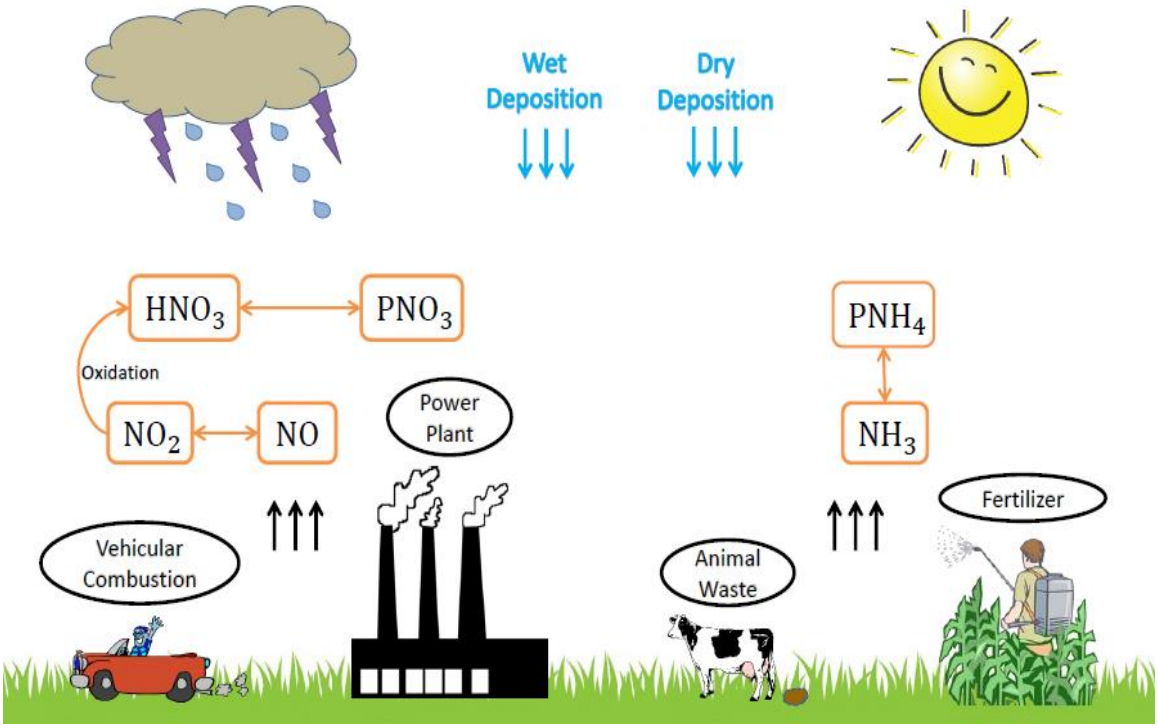

Fig. 1.2 Emission Sources and Reaction Processes for Nitrogen-Containing Species

Nitrogen dioxide (NO_2) and nitric oxide (NO) can be formed into each other in the atmosphere. NO_2 can be oxidized into nitric acid (HNO_3). There is a thermodynamics balance between nitric acid (HNO_3) and particulate nitrate (PNO_3) in the atmosphere. Ammonia (NH_3) can be formed into particulate ammonium (PNH_4) and vice versa.

1.3 Deposition of Nitrogen-Containing Species

Atmospheric nitrogen deposition (both wet and dry) is one of the major contributors to nutrient loading in waterways (Rebich et al., 2011; Elser et al., 2009). Dry deposition is the transport of gaseous species and particulate matter directly from the atmosphere to surfaces without any precipitation (Seinfeld et al., 2006). Wet deposition is the removal of species from the atmosphere by atmospheric hydrometeors, such as rain and snow (Seinfeld et al., 2006). Particulate matter is a mixture of solid particles and liquid droplets, which can be found in the air. Atmospheric nitrogen deposition is mostly in the forms of particulate nitrate (PNO_3) and particulate ammonium (PNH_4) from wet deposition, as well as gaseous nitric acid (HNO_3), ammonia (NH_3) and nitrogen dioxide (NO_2) from dry deposition (Pitcairn et al., 1995; Luo et al., 2002). Additionally, PNO_3 and PNH_4 have smaller inputs to the dry deposition process (Pitcairn et al., 1995).

Rebich et al. (2011) used a regional water-quality model, SPAtially Referenced Regression On Watershed attributes (SPARROW), to estimate nutrient inputs to the northwestern part of the Gulf of Mexico, from streams in the South-Central United States, during the year 2002. They found that the largest nitrogen contribution to the northwestern part of the Gulf of Mexico was from atmospheric deposition, representing 42%, with two other sources, including commercial fertilizer and livestock manure, making up 20% and 17% respectively.

Poor et al. (2013) used a regional chemical transport model, Community Multiscale Air Quality (CMAQ) to estimate the deposition of reactive nitrogen, including nitrogen oxides (NOx), ammonia (NH_3), nitrous oxide and nitrate, to

Tampa Bay and its watershed in the year 2002. The size of the grid cell was 12x12 km. They concluded that there were 1080 metric tons of nitrogen and 1490 metric tons of nitrogen for direct and indirect loading rates respectively, assuming the transfer rate of 18% from watershed to bay for indirect loading. They also found that atmospheric loading contributed to 71% of the total nitrogen loading to the Bay.

Elser et al. (2009) suggested that one of the major pathways of the anthropogenic nitrogen input into the ecosystem was from the atmospheric deposition. They investigated the atmospheric nitrogen deposition in the lakes in Norway, Sweden, and Colorado, the United States. They found that atmospheric nitrogen deposition increased the stoichiometric ratio of nitrogen and phosphorus in those lakes. This increase shifted the nutrient limitation from nitrogen to phosphorus and in the long run, this would shift the structure of the ecosystem.

Kim et al. (2011) investigated the relative abundance of nitrogen over phosphorus in waters of the East Asian marginal seas, which includes the East China Sea, the coastal waters of Korea, the East Sea, and the Pacific coast of Japan in the years 1980 to 2010. They divided the study area into 46 boxed regions, each 2° latitude by 2.5° longitude. They concluded that the increase in nitrogen availability within the study area was mainly driven by the increase of nitrogen concentrations, which was most likely due to atmospheric nitrogen deposition.

Recent studies focus on the considerable impacts of deposited nitrogen-containing atmospheric species on waterbodies, including Lake Tahoe (Dolislager et al., 2012), King River Watershed (Hunsaker et al., 2007), and Miyun reservoir

(Yang et al., 2005), and which nitrogen-containing species contribute more to nitrogen loading.

Dolislager et al. (2012) summarized the Lake Tahoe Atmospheric Deposition Study (LTADS), which was conducted by the California Air Resources Board (CARB). The studied areas were taken in three different locations around Lake Tahoe. Different measurements were combined to estimate the direct atmospheric nitrogen deposition onto the lake surface during the year 2003. They concluded that 185 metric tons of nitrogen were directly deposited from the atmosphere to the lake and that ammonia (NH_3) gas was the major component of nitrogen loading on to the Lake.

Hunsaker et al. (2007) conducted research on nitrogen monitoring on the Kings River Experimental Watershed (KREW), which includes four watersheds in total, in the years 2003 and 2004. The bulk deposition collectors were positioned under the forest canopy and in a nearby collector on each watershed. The sample was collected every two weeks during the wet season, which is typically November through May. They concluded that KREW received high exposures to nitrogen compounds, which may cause severe effects on the ecosystems in the western United States.

Yang et al. (2005) studied the water quality in the Miyun reservoir region. They collected the precipitation chemical data from the year 1990 to 2001, along with the atmospheric wet and dry deposition data from the year 2002-2003 at Shangdianzi Station. They used a Dionex500 ion chromatograph (IC) and a HITACHI180-70 atomic absorption spectrophotometer (AA) to test nitrate and

ammonium ions. They suggested that the main deposited nitrogen species into the reservoir included nitrate and ammonium and that those deposited nitrogen species exacerbated the eutrophication and acidification of the reservoir water.

Doney et al. (2007) used a global transport model, Model for Ozone and Related Chemical Tracers (MOZART) model, to simulate preindustrial and current nitrogen deposition for the year 1890. The emissions for both sources were from the EDGAR-HYDE inventory. They considered the waters near major source regions in North America, Europe, as well as South and East Asia. Atmospheric inputs included strong acids, such as nitric acid, and bases, such as ammonia. Results demonstrated that about one-third of anthropogenic nitrogen oxides emissions, which are mostly from fossil fuel combustion, were deposited to the ocean. They quantified the biogeochemical impacts and concluded that the acidification caused by deposited nitrogen-containing species affected more on the ecosystem in coastal waters than bases. Studies also showed that the loading in watersheds is expected to continue to increase in the future (Duce et al., 2008; Kim et al., 2011; Zhao et al., 2015; Luo et al., 2002; Kim et al., 2014; Fisher et al., 1991).

Zhang et al. (2012) used a global chemical transport model, GEOS-Chem to simulate nitrogen deposition over North America and adjacent oceans in the years 2006 to 2008. The horizontal resolution was 1/2° by 2/3° in the model. They found that there was a total nitrogen deposition flux of 6.5 $TgNa^{-1}$ over the contiguous United States, including 4.2 as oxidized nitrogen species (NOy) and 2.3 as NHx (including ammonia gas and ammonium aerosol). They also found that domestic

anthropogenic, foreign anthropogenic, and natural sources contributed 78%, 6%, and 16% of total nitrogen deposition over the contiguous United States.

Select studies have quantified the contribution of wet and dry deposition to watersheds in the United States (Zhao et al., 2015; Hu et al., 1997; Luo et al, 2002). Zhao et al. (2015) used a global transport model, GEOS-Chem, to study the nitrogen deposition onto the northwestern Pacific. They used a temporal resolution of 6 h and a horizontal resolution of 1/2° latitude by 2/3° longitude in the model. They simulated the data from the year 2008 to 2010 and found that nitrogen-containing species were deposited into the Yellow Sea and the South China Sea by 11.9 kgN/ha and 5.6 kgN/ha annually, respectively, through wet and dry deposition.

Hu et al. (1997) set up two dry deposition monitoring sites along the shore of Long Island Sound in 1991. An Aero-Chem wet-dry sampler and an Anderson wet-dry sampler were employed to collect rain water. Additionally, two three-gallon polyethylene buckets were used in the samplers, one to collect wet deposition, the other dry deposition. Both wet and dry deposition were sampled and measured every week. All the chemical data analyzed in the laboratory for both wet and dry deposition were conducted under EPA standards. A two-layer model developed by Slinn and Slinn (1980) was adapted to calculate deposition velocities. They estimated that the total atmospheric nitrogen loading to the Sound was 2240 metric tons per year.

Luo et al. (2002) studied the atmospheric deposition of nitrogen onto the Long Island Sound from 1991 through 1994, and from 1997 through 1999. They set up

four monitoring stations along the Connecticut coastline, located in Old Greenwich and Bridgeport in Fairfield county, Hammonasset in New Haven county, and Avery Point in New London County. They used sensors to collect meteorological information, a two-stage filter pack to collect atmospheric concentration of nitrogen, and wet deposition collector to collect data during rain events. The laboratory analysis was performed in the analytical laboratory at the University of Connecticut. Luo et al. (2002) found that nitric acid (HNO_3) was predominant in dry deposition, taking up over 70% of the total dry flux, and that wet deposition is the major contributor to the total nitrogen loading along the coastline.

Wall et al. (2013) used a regional transport model, the Community Multiscale Air Quality (CMAQ), to estimate atmospheric nitrogen deposition for soil and each of the 8-digit Hydrologic Unit Code (HUC8) watersheds in Minnesota by wet and dry deposition in the year 2002. They found that wet and dry deposition accounted for 52% and 48% of the total atmospheric nitrogen deposition, respectively. Additionally, they found that wet and dry atmospheric inorganic nitrogen deposition contributed between 4 and 14 pounds per acre to Minnesota soil and water. The major species contributing to wet and dry deposition included 62% unoxidized (NHx – mostly ammonia and ammonium) and 38% oxidized (NOx – nitrite, nitrate, and other) nitrogen species.

Benedict et al. (2013) conducted a research on nitrogen deposition for Rocky Mountain National Park (RMNP) during a year-long study, from the November 2008 to November 2009. They used the IMPROVE and CASTNet programs for air monitoring. Denuders and filter packs were used to collect 24-hr samples for

determination of concentrations of ammonia (NH_3), nitric acid (HNO_3), ammonium, and nitrate. They found that wet deposition of ammonium and nitrate were the two largest deposition pathways and the next two largest pathways were the wet deposition of organic nitrogen and the dry deposition of ammonia in the atmosphere. They also found that monthly deposition fluxes ranged from 0.06 to 0.54 kgN/ha per year, with peak deposition in July and the least deposition in December. This is due to the lower precipitation in winter.

1.4 Research Preview

As shown in the previous section, studies concluded ammonia gas, nitrate and ammonium ions are the major contributors to waterbodies. However, few studies have been conducted to quantify seasonal variation of the major species, including ammonia (NH_3), nitric acid (HNO_3), nitrogen oxides (NOx), particulate ammonium (PNH_4) and particulate nitrate (PNO_3) which contribute to the atmospheric nitrogen deposition onto U.S. watersheds.

The following figure (Fig. 1.3) was obtained from the National Atmospheric Deposition Program (NADP) website. The maps result from the integration of modeled and measured results of the concentration and wet deposition of nitrate and ammonium in the contiguous United States in the year 2012. It can be seen that the map of concentration and wet deposition is distributed differently for both species, with concentration centering in the middle of United States and wet deposition concentrating on the eastern United States.

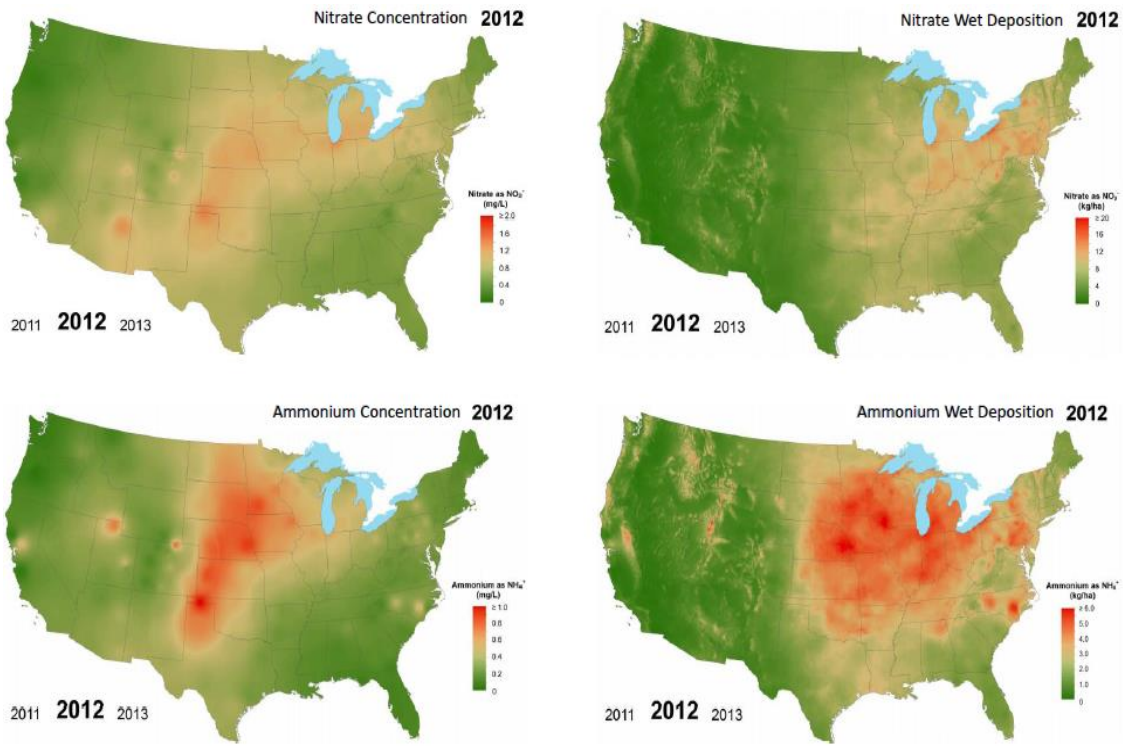

Fig. 1.3 Modeled and Measured Map of Airborne Concentration and Wet Deposition of Nitrate and Ammonium for the year 2012 in the United States (http://nadp.sws.uiuc.edu/ntn/annualmapsByYear.aspx#undefined)

In this study, a regional atmospheric chemical transport model, the Comprehensive Air Quality Model with eXtensions (CAMx) version 6.0 (ENVIRON, 2013), along with a geographic information system, ArcGIS by ESRI, is used to investigate the quantity of nitrogen deposited into watersheds in the contiguous United States in each season in the year 2011.

1.5 References

Behera, S. N., Sharma, M., Aneja, V. P., & Balasubramanian, R. (2013). Ammonia in the atmosphere: A review on emission sources, atmospheric chemistry and deposition on terrestrial bodies. *Environmental Science and Pollution Research*, 20(11), 8092–8131. http://doi.org/10.1007/s11356-013-2051-9

Benedict, K. B., Carrico, C. M., Kreidenweis, S. M., Schichtel, B., Malm, W. C., & Collett, J. L. (2013). A seasonal nitrogen deposition budget for Rocky Mountain National Park. *Ecological Applications : A Publication of the Ecological Society of America*, 23(5), 1156–69. http://doi.org/10.1890/12-1624.1

Davidson, E. a, & Kingerlee, W. (1997). A global inventory of nitric oxide emissions from soils. *Nutrient Cycling in Agroecosystems*, *48*(1-2), 37–50. http://doi.org/10.1023/A:1009738715891

Diaz, R. J. (2001). Overview of Hypoxia around the World, *30*(April), 275–281.

Diaz, R. J., & Rosenberg, R. (2008). Spreading dead zones and consequences for marine ecosystems. *Science (New York, N.Y.)*, *321*(5891), 926–9. http://doi.org/10.1126/science.1156401

Dolislager, L. J., VanCuren, R., Pederson, J. R., Lashgari, A., & McCauley, E. (2012). A summary of the Lake Tahoe Atmospheric Deposition Study (LTADS). *Atmospheric Environment*, *46*, 618–630. http://doi.org/10.1016/j.atmosenv.2009.09.020

Doney, S. C., Mahowald, N., Lima, I., Feely, R. a, Mackenzie, F. T., Lamarque, J.-F., & Rasch, P. J. (2007). Impact of anthropogenic atmospheric nitrogen and sulfur deposition on ocean acidification and the inorganic carbon system. *Proceedings of the National Academy of Sciences of the United States of America*, *104*(37), 14580–14585. http://doi.org/10.1073/pnas.0702218104

Duce, R. A., LaRoche, J., Altieri, K., Arrigo, K. R., Baker, A. R., Capone, D. G., … Zamora, L. (2008). Impacts of atmospheric anthropogenic nitrogen on the open ocean. *Science (New York, N.Y.)*, 320(5878), 893–7. doi:10.1126/science.1150369

Elser, J. J., Andersen, T., Baron, J. S., Bergström, A., Jansson, M., Kyle, M., … Hessen, D. O. (2009). Shifts in lake N: P stoichiometry and nutrient limitation driven by atmospheric nitrogen deposition. *Science*, 326(5954), 835–837. http://doi.org/10.1126/science.1176199

ENVIRON (2013). User's Guide COMPREHENSIVE AIR QUALITY MODEL WITH EXTENSIONS (CAMx) Version 6.0.

EPA (2012). Revision to New Source Performance Standards (Nsps) for Nitric Acid Plants. (X).

Fisher, A. D. C., & Oppenheimer, M. (1991). Atmospheric Nitrogen Deposition and the Chesapeake Bay Estuary. *Springer on behalf of Royal Swedish Academy of Sciences*, Ambio, 20(3), 102–108. Stable URL : http://www.jstor.org/stable/4313793.

Hautier, Y., Niklaus, P. A., Hector, A. (2009). Competition for Light Causes Plant Biodiversity Loss After Eutrophication, *Science*, *324*(5927), 636–638.

Hu, H. L., Chen, H. M., Nikolaidis, N. P., Miller, D. R., & Yang, X. S. (1997). Estimation of nutrient atmospheric decomposition to Long Island Sound. *Water Air and Soil Pollution*, *105*(3-4), 521–538.

Hunsaker, C., Bytnerowicz, A., Auman, J., & Cisneros, R. (2007). Air pollution and watershed research in the central Sierra Nevada of California: nitrogen and ozone. *TheScientificWorldJournal*, *7 Suppl 1*, 206–21. http://doi.org/10.1100/tsw.2007.82

Jacabson, M.Z. (2002). Atmospheric Pollution: History, Science, and Regulation. *Cambridge University Press*

Kemker, Christine (2013). "Dissolved Oxygen." Fundamentals of Environmental Measurements. *Fondriest Environmental, Inc. Web.* <http://www.fondriest.com/environmental-measurements/parameters/water-quality/dissolved-oxygen/>.

Khan, M. N., Mohammad, F. (2013): Eutrophication of Lakes. Eutrophication: causes, consequences and control. Springer Netherlands

Kim, T.-W., Lee, K., Duce, R., Liss, P. (2014). Impact of atmospheric nitrogen deposition on phytoplankton productivity in the South China Sea. *Geophysical Research Letters*, 1–7. http://doi.org/10.1002/2014GL059665.Received

Kim, T.-W., Lee, K., Najjar, R. G., Jeong, H.-D., & Jeong, H. J. (2011). Increasing N abundance in the northwestern Pacific Ocean due to atmospheric nitrogen deposition. *Science (New York, N.Y.)*, *334*(6055), 505–9. http://doi.org/10.1126/science.1206583

Liu, C., Yao, Z., Wang, K., & Zheng, X. (2015). Effects of increasing fertilization rates on nitric oxide emission and nitrogen use efficiency in low carbon calcareous soil. *Agriculture, Ecosystems & Environment*, *203*, 83–92. http://doi.org/10.1016/j.agee.2015.01.025

Luo, Y., Yang, X., Carley, R. J., & Perkins, C. (2002). Atmospheric deposition of nitrogen along the Connecticut coastline of Long Island Sound: A decade of measurements. *Atmospheric Environment*, *36*(28), 4517–4528. http://doi.org/10.1016/S1352-2310(02)00421-1

Mallya, Y. J. (2007). The Effect of Dissolved Oxygen on Fish Growth in Aquaculture, 30.

Martin, R. V. (2003). Global inventory of nitrogen oxide emissions constrained by space-based observations of NO2 columns. *Journal of Geophysical Research*, *108*(D17), 1–12. http://doi.org/10.1029/2003JD003453

Omidvarborna, H., Kumar, A., & Kim, D. S. (2015). NOx emissions from lowerature combustion of biodiesel made of various feedstocks and blends. *Fuel Processing Technology*, *140*(x), 113–118. http://doi.org/10.1016/j.fuproc.2015.08.031

Pitcairn, C. E. R., Fowler, D., & Grace, J. (1995). DEPOSITION OF FIXED ATMOSPHERIC NITROGEN AND FOLIAR NITROGEN CONTENT OF BRYOPHYTES AND Calluna vulgaris (L.) HULL. *Environmental Pollution*, 88, 193–205.

Poor, N. D., Pribble, J. R., & Schwede, D. B. (2013). Application of watershed deposition tool to estimate from CMAQ simulations the atmospheric deposition of nitrogen to Tampa Bay and its watershed. *Journal of the Air and Waste Management Association*, 63(1), 100–114. http://doi.org/10.1080/10962247.2012.739109

Qian, F. P., Chyang, C. S., Huang, K. S., & Tso, J. (2011). Combustion and NO emission of high nitrogen content biomass in a pilot-scale vortexing fluidized bed combustor. *Bioresource Technology*, *102*(2), 1892–1898. http://doi.org/10.1016/j.biortech.2010.08.008

Rebich, R. A., Houston, N. A., Mize, S. V., Pearson, D. K., Ging, P. B., & Evan Hornig, C. (2011). Sources and Delivery of Nutrients to the Northwestern Gulf of Mexico from Streams in the South-Central United States. *Journal of the American Water Resources Association*, *47*(5), 1061–1086. http://doi.org/10.1111/j.1752-1688.2011.00583.x

Seinfeld, J. H.; Pandis, S. N. (2006). Atmospheric Chemistry and Physics: From Air Pollution to Climate Change, 2nd ed.; *Wiley-Interscience*.

Son, B., Yang, W., Breysse, P., Chung, T., & Lee, Y. (2004). Estimation of occupational and nonoccupational nitrogen dioxide exposure for Korean taxi drivers using a microenvironmental model. *Environmental Research*, *94*(3), 291–296. http://doi.org/10.1016/j.envres.2003.08.004

Sotto, L. P. A., Jacinto, G. S., & Villanoy, C. L. (2014). Spatiotemporal variability of hypoxia and eutrophication in Manila Bay, Philippines during the northeast and southwest monsoons. *Marine Pollution Bulletin*, *85*(2), 446–454. http://doi.org/10.1016/j.marpolbul.2014.02.028

Wall, D., & Pearson, T. E. (2013). D3 . Atmospheric Deposition of Nitrogen in Minnesota Watersheds, (June), 1–12.

Werner, W. (2006): Fertilizers, 6. Environmental Aspects. Ullmann's Encyclopedia of Industrial Chemistry. *Wiley-Interscience.*

Yang, D. Z., Xu, X. D., Liu, X. D., Xu, Q., Ding, G. A., Cheng, X. H., Wang, W. Y. (2005). Complex sources of air-soil-water pollution processes in the Miyun reservoir region. *Science In China Series D-Earth Sciences*, *48*(<Go to ISI>://000235658700019), 230–245. http://doi.org/10.1360/02YD0358

Yu, J., Meixner, F. X., Sun, W., Mamtimin, B., Xia, C., & Xie, W. (2010). Biogenic nitric oxide emission of mountain soils sampled from different vertical landscape zones in the changbai mountains, Northeastern China.

Environmental Science and Technology, *44*(11), 4122–4128. http://doi.org/10.1021/es100380m

Zhang, L., Jacob, D. J., Knipping, E. M., Kumar, N., Munger, J. W., Carouge, C. C., … Chen, D. (2012). Nitrogen deposition to the United States: Distribution, sources, and processes. *Atmospheric Chemistry and Physics*, 12(10), 4539–4554. http://doi.org/10.5194/acp-12-4539-2012

Zhao, Y., Zhang, L., Pan, Y., Wang, Y., Paulot, F., & Henze, D. K. (2015). Atmospheric nitrogen deposition to the northwestern Pacific: Seasonal variation and source attribution. *Atmospheric Chemistry and Physics*, *15*(18), 10905–10924. http://doi.org/10.5194/acp-15-10905-2015

Chapter 2 METHODOLOGY

The goal of this study was to quantify deposited nitrogen in each season onto each of the major U.S. watersheds in the year 2011. Quantifying how much nitrogen was deposited throughout the year was achieved by a regional chemical transport model, the Comprehensive Air Quality Model with eXtension (CAMx) (ENVIRON, 2013). The time period for each season was defined as follows: January to March as winter, April to June as spring, July to September as summer, and October to December as fall.

In order to project the deposition data onto each of the major U.S. watersheds, the information about the U.S. watersheds was needed and obtained from National Hydrology Dataset (NHD) website. A Geographic Information System (ArcGIS) was used to obtain the features of the watershed file. Finally, the deposition data and the watershed information were combined to calculate how much nitrogen-containing species were deposited onto each watershed, which was achieved by MATLAB. This chapter has a detailed explanation about what models and program were used to conduct this research.

2.1 Comprehensive Air Quality Model with eXtension (CAMx)

In this study, a three-dimensional regional atmospheric chemical transport model, Comprehensive Air Quality Model with eXtension (CAMx) version 6.0 (ENVIRON, 2013), was employed to obtain the processed data for both wet and dry deposition of six major nitrogen-containing species, including nitric oxide (NO), nitrogen dioxide (NO_2), ammonia (NH_3), nitric acid (HNO_3), particulate ammonium (PNH_4), and particulate nitrate (PNO_3). The emissions data were simulated by

considering the whole contiguous United States as a large grid, containing 20 vertical layers of 396 columns and 246 rows of 12x12 km small horizontal grids. The Lambert Conformal Projection was chosen as the map projection.

CAMx treats the atmosphere as a large box. The box is divided into a series of grid cells of same size horizontally, considering each cell is well-mixed. Within each cell, the changes in the concentration of each species result from emissions, pollutant transport due to the wind flow (flow in and flow out), physical and chemical changes of chemical species due to gas- and aqueous-phase chemistry, aerosol dynamics, and deposition (both wet and dry). The processes within each grid cell are described in the following figure (Fig. 2.1).

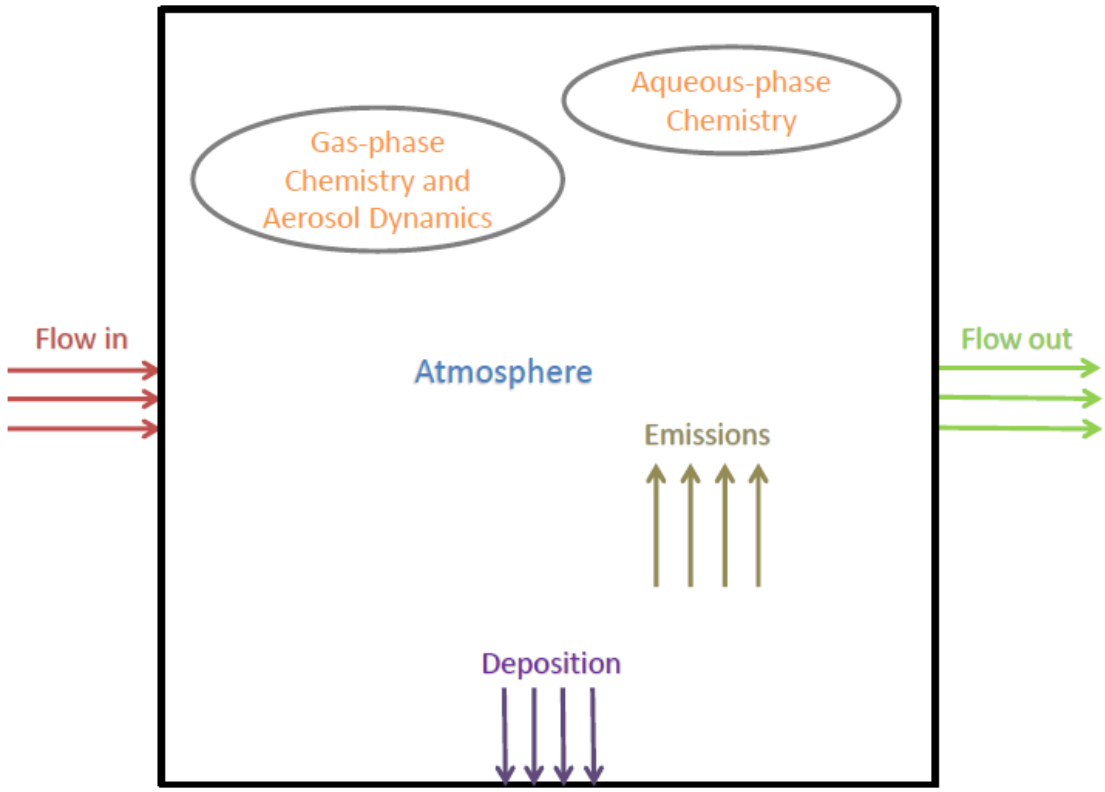

Fig. 2.1 Physical and Chemical Processes in CAMx

Wet and dry deposition are calculated separately in CAMx. The following two sub-sections describe how deposition is calculated in the model.

2.1.1 Wet Deposition

In wet deposition, the basic model used in CAMx is a scavenging method. The local rate of concentration change *c* depends on a scavenging coefficient *Λ*, which can be described in the following equation and *Λ* is different for particles and gases:

$$\frac{\partial c}{\partial t} = -\Lambda \times \mathrm{c}$$

Particles and relatively soluble gases can be removed by wet deposition. Particles serve as cloud condensation nuclei (CCN), which results in the growth of cloud droplets. When the droplets grow large, they fall as precipitation. Particles which exist within and below clouds are considered to be directly removed by precipitation (ENVIRON, 2013). The consideration of aerosols in CAMx is as follows:

a) Aqueous aerosols scavenging: It is assumed that all aerosols within clouds exist within cloud water. Therefore, $\Lambda = \Lambda_c$, where Λ_c is cloud water scavenging coefficient

$$\Lambda_c = 4.2 \times 10^{-7} \times \frac{E \times P}{d_d}$$

E is the collection efficiency and is a function of particle size d_p; *P* is rainfall rate in the unit of mm/hr.

b) Dry particles scavenging: Wet scavenging of dry particles only occurs below clouds. The scavenging coefficient is used the same as the expression for

Λ_c. The efficiency calculation for snow is complicated, so CAMx uses the value for *E* for rain and ice but also sets a lower limit of $1x10^{-3}$ based on the work of Sauter et al. (1988).

For relatively soluble gases, they can be absorbed by water droplets and then the droplets fall as precipitation. During these processes, the concentration of the gaseous pollutants depends on the Henry's Law constant, which is the ratio of concentration of a species in the liquid phase to the gas phase at equilibrium.

$$H = \frac{c_{aq}}{c_g}$$

The higher the Henry's Law constant is (greater than 10000 M/atm approximately), the stronger tendency the gas has to dissolve in water droplets (Seinfeld et al., 2006). Because the solubility of many pollutants greatly exceeds the concentration of the pollutants present in the air and is constant with time, it can be assumed that equilibrium conditions exist in the atmosphere.

For the gases existing within and below the precipitating clouds, the total gas concentration is considered differently. Below the cloud, the total gas concentration is ready for scavenging. Within the clouds, the total gas concentration has to be proportioned to an aqueous fraction c_{aq} at first, and then the remaining gaseous fraction c_g in the interstitial air. Aqueous and interstitial gases are ready for scavenging at different rates.

In conclusion, for gaseous species within clouds, scavenging coefficient is $\Lambda = \Lambda_g + \Lambda_a$, where Λ_g is gas-phase scavenging coefficient; for gaseous species below clouds, scavenging coefficient is $\Lambda = \Lambda_g$.

Additionally, if the rainfall is super-saturated and cannot take in any gases, the change of gas concentration is determined by

$$\Delta c = \left(c_{eq} - c_0\right) \times [1 - \exp(-\Lambda \times \Delta t)]$$

c_{eq} is the maximum possible gas in solution for the given condition and c_0 is the amount of pre-existing gas in solution from above layers. If Δc is positive, mass is added to the rain water and removed from the grid cell; if negative, mass is subtracted from rain water and added to the grid cell.

2.1.2 Dry Deposition

Dry deposition is often treated as a first-order removal mechanism because it is difficult to have a direct measurement of dry deposition and to have a suitable model parameterization. This means that the flux of a pollutant to a surface is the multiplication of a characteristic deposition velocity and its concentration in the lowest model layer. Deposition velocity is obtained from models which take into account of many factors, including the characteristics of gases (reactivity, solubility, and diffusivity), the size of particles, local meteorological conditions, and season-dependent surface characteristics.

For a given species, particle size and grid cell, CAMx determines a deposition velocity according to the land use type in that cell and combine the values together based on the fractional distribution of the land use. The files for aerosol size spectra and species-dependent properties, which are needed to calculate deposition velocity, are externally provided to CAMx through the chemistry parameters file; gridded land use is provided for the master grid and is optional for nested grids; the season is decided by the simulation date and location on earth.

CAMx offers two dry deposition models. In our research, we used the original method based on the work of Wesely (1989) and Slinn et al. (1980). The following part is a brief description of the Wesely/Slinn Model.

2.1.2.1 Dry Deposition of Gases

Deposition velocity v_d is calculated from three primary resistances r [s/m]:

$$v_d = \frac{1}{r_a + r_b + r_s}$$

r_a is the aerodynamic resistance, representing bulk transport through the lowest model layer by turbulent diffusion, which runs equivalently for all gases and small particles. r_b and r_s are quasi-laminar boundary resistance and surface resistance, respectively. The expressions for r_b and r_s are given in CAMx.

2.1.2.2 Dry Deposition of Aerosols

Surface deposition of particles takes place by diffusion, gravitational settling and impaction. Particle size plays a dominant role in these processes. CAMx adopted the resistance method of Slinn et al. (1980), as implemented in UAM-AERO by Kumar et al. (1996). The relationship between a given aerosol size and particle deposition velocity is expressed as follows:

$$v_d = v_{sed} + \frac{1}{r_a + r_b + r_a \times r_b \times v_{sed}}$$

v_{sed} is the gravitational settling velocity. It depends on aerosol size and density, which are influenced by aerosol water content.

Aerodynamic resistance r_a is the same as the value used for gaseous dry deposition. r_b is the boundary resistance.

2.1.3 Input Files

Emissions inputs were developed by the United States Environmental Protection Agency's (EPA) by using 2011 National Emissions Inventory (NEI) (EPA, 2014). We used mechanism 7 for gas-phase chemistry, which is based on Carbon Bond 6 (CB6) mechanism and includes aerosol chemistry (Yarwood et al., 2010). CAMx mechanism 7 includes 218 reactions for 77 gaseous species and 16 aerosol species. The gas-phase reaction of dinitrogen pentoxide (N_2O_5) with water vapor is slower in CB6, which reduces formation of nitric acid (HNO_3) at night (Brown et al., 2006).

The meteorology inventories were developed by the meteorology model, the Weather Research and Forecasting model (WRF). The evaluation of WRF was performed by the US EPA (EPA, 2014). The boundary conditions inputs were obtained from a global 3-D chemical transport model, GEOS-Chem. The ozone column and photolysis rates were obtained from NASA's aura satellite data, by using the Tropospheric Ultraviolet and Visible (TUV) script from ENVIRON. The following flowchart (Fig. 2.2) generalizes the sources of inputs information for CAMx. After running CAMx, gridded deposited mass for each nitrogen-containing species was obtained in the year 2011. Each species was totaled over each season.

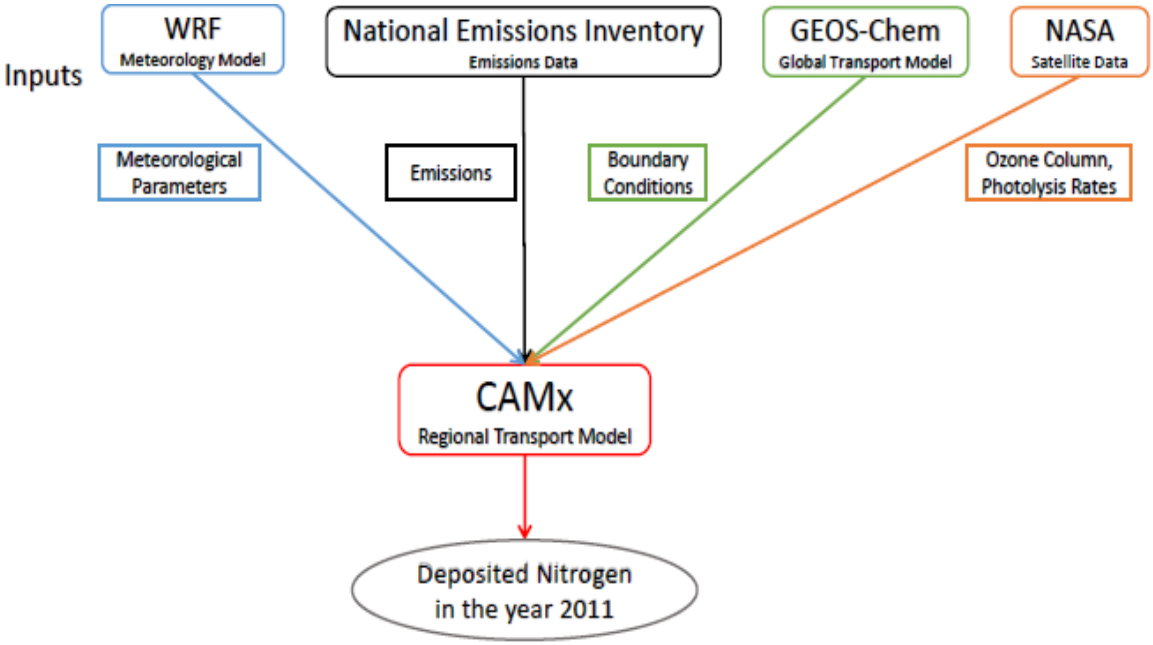

Fig. 2.2 Sources of Inputs Inventories in CAMx

2.2 Geographic Information System (ArcGIS)

A fishnet grid shapefile was created in a geographic information system, ArcGIS (version 10.2.2), with 396 columns and 246 rows of 12x12 km grid cells and the projection system is LAMBERT Conformal Projection. The fishnet grid information in ArcGIS aligns with the grid used in CAMx. The fishnet grid shapefile contains information about grid ID, and the area of each grid cell. The watershed shapefile was obtained from the U.S. Geological Survey's website (USGS). The watershed shapefile contains information about the area of each watershed, the name of each watershed, which states each watershed comprises of, and the 2-digit hydrologic unit code each watershed represents. There are 22 watersheds in total but only 18 of them are in our modeled domain. The other four watersheds, which are not in the contiguous United States, include Hawaii, Caribbean, South Pacific, and Alaska. A hydrologic unit code (HUC) is a series of numbers or letters

which identify a hydrological feature, such as a lake, river or basin. The United States is divided and subdivided into different hydrologic units and is classified into four levels, including regions, sub-regions, accounting units, and cataloging units. 2-digit Hydrologic Unit Codes means the largest aggregation of watersheds.

The following figure (Fig. 2.3) shows the Mid-Atlantic watershed with the fishnet grid to illustrate how the combined shapefile looks in ArcGIS. The attribute table of this combined shapefile contains the calculated area information using the union tool, grid ID, and which watershed each grid cell belongs to.

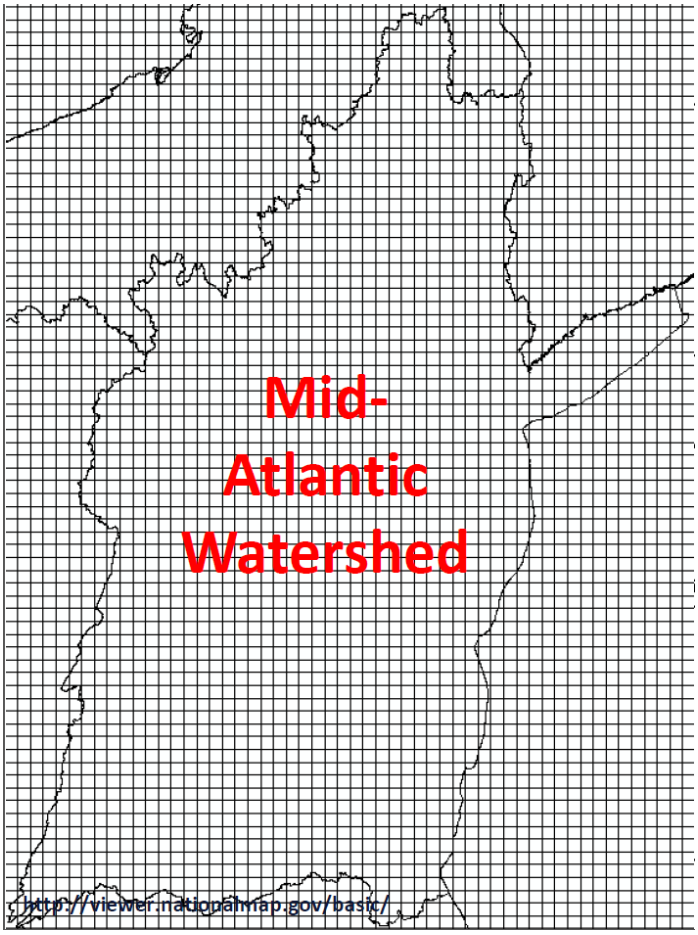

Fig. 2.3 Image of Combined Shapefile of Mid-Atlantic Watershed in ArcGIS

The gridded deposited mass, which was obtained from CAMx, gives the deposition information in each grid cell. There are some grids where the grid covers over two watersheds. In order to calculate the deposited mass in each watershed, how much each watershed occupies in each grid cell needs to be calculated. The union tool in ArcGIS was used to achieve this goal. The union tool combines the watershed and fishnet grid shapefile and can preserve the features of each shapefile, such as the polygon features. The following figure (Fig. 2.4) illustrates how union works in ArcGIS. For instance, three figures with the overlapped area is provided as an input. After using the union tool in ArcGIS, each of the area in the figures can be calculated separately.

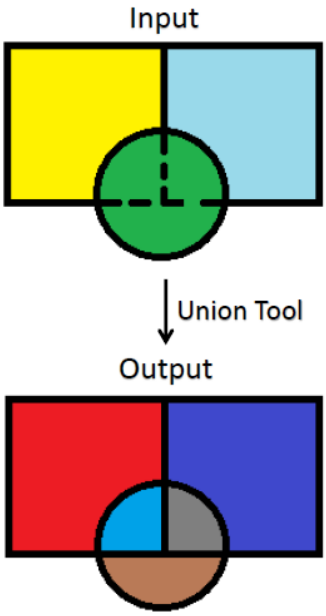

Fig. 2.4 How Union Tool Works in ArcGIS

The grid ID, watershed name, and the area information were saved in three columns in an Excel file. The names of the 18 watersheds were replaced with numbers so that it was easier to program in MATLAB. The naming convention is shown as follows:

Table 2.1 Watershed Name and Corresponding Numbers in MATLAB

Watershed Name	Number
Upper Mississippi	1
Souris-Red-Rainy	2
California	3
Upper Colorado	4
New England	5
Lower Colorado	6
Mid-Atlantic	7
Lower Mississippi	8
Arkansas-White-Red	9
South Atlantic-Gulf	10
Tennessee	11
Rio Grande	12
Great Basin	13
Texas-Gulf	14
Great Lakes	15
Pacific Northwest	16
Ohio	17
Missouri	18

The fishnet grid covers the contiguous United States and there are places which do not belong to any watersheds but are projected on the ocean. These places appear as 0 in grid ID in ArcGIS and are set to 0 in the Excel file.

2.3 MATLAB

The MATLAB code can be found in the Appendix A. The information of all the nitrogen-containing species for each season was copied and stored in four different Excel files. In each of these Excel file, each column contains dry/wet deposition for each species. There are 12 (6 species x 2 depositions) columns and 97416 (396x246) rows. Excel files for the other three seasons have the same format as the winter file but are stored with each season's data. The winter file is

taken for an example in the following description to demonstrate how the nitrogen deposition in each watershed was calculated.

In the Excel file for ArcGIS, grid ID (97416 in total) corresponds to the location of the deposition data in the winter file. First, a program was written in MATLAB to read the data from the winter file and then to read the calculated areas from the ArcGIS Excel file. When the grid ID matches the location of the deposition data (in the unit of g/ha or mol/ha, depending whether the species is gas or particulate matter), it calculates the deposition at that place and then divides it by 0.01, which is the conversion from hectare to km. It then multiplies the value by the calculated area (in the unit of km^2) at that place from ArcGIS Excel file. It is assumed that the deposition in each area is evenly distributed.

Using the above information, the deposited mass in each grid cell is ready to be calculated. The deposited mass with the same watershed number was added together to get how much each nitrogen species was deposited in winter in each watershed. The deposition data is in the unit of g and mol for gases and particulate matter, respectively.

The following conversions were used to unify the unit of all the species to kgN. For gases, including nitrogen dioxide (NO_2), nitric oxide (NO), nitric acid (HNO_3), and ammonia (NH_3), the data were multiplied by the molecular mass of N in each species, then were multiplied by 10^{-3} to convert g to kg. For particulate matter, including particulate ammonium (PNH_4) and particulate nitrate (PNO_3), the data were multiplied by the percentage of nitrogen in each species and then were multiplied by 10^{-3} to convert g to kg, i.e. PNO_3: $14/64 \times 10^{-3}$; PNH_4:$14/18 \times 10^{-3}$.

Deposited mass per area was also calculated by dividing nitrogen deposited mass by the area of each watershed. The following flowchart (Fig. 2.5) illustrates how models and program were used in this research.

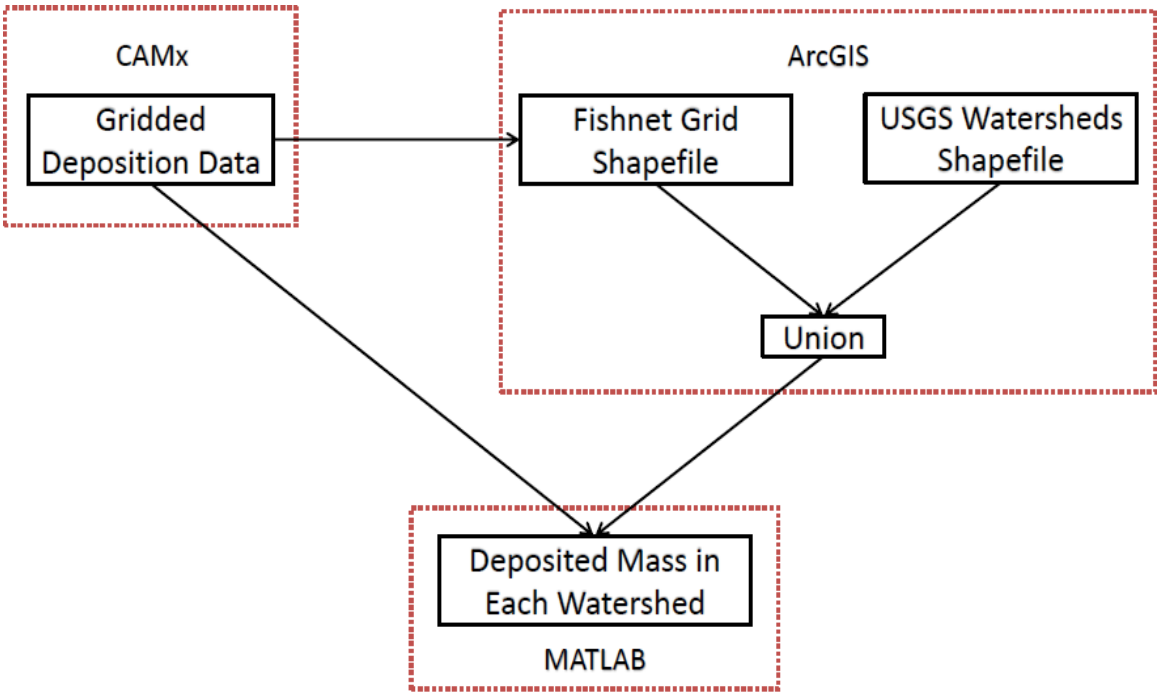

Fig. 2.5 Models and Program Used in the Research

2.4 Data Analysis

The deposited mass of nitrogen species (in the unit of kgN) in each watershed in each season and the deposited mass per area of each nitrogen species (in the unit of kgN/km^2) in each watershed in each season was quantified. This analysis includes: seasonal variation in each watershed for each species; comparison between different watersheds for different species; comparison between deposited mass and deposited mass per area for different species.

2.5 References

Brown, S. S., Ryerson, T. B., Wollny, A. G., Brock, C. A., Peltier, R., Sullivan, A. P., Weber, R. J., Dubé, W. P., Trainer, M., Meagher, J. F., Fehsenfeld, F. C., Ravishankara, A. R. (2006). *Nature*, 20(516), 493–494. http://doi.org/10.1038/020493a0

ENVIRN (2013). User's Guide COMPREHENSIVE AIR QUALITY MODEL WITH EXTENSIONS (CAMx) Version 6.0.

EPA (2014), The 2011 National Emissions Inventory. Environ. Prot. Agency, 2014 http://www.epa.gov/ttn/chief/net/2011inventory.html.

EPA (U.S. Environmental Protection Agency). *CASTNET Download Data module*.

EPA (2014), U.S. Meteorological Model Performance for Annual 2011 Simulation WRF v3.4. *U.S. Environ. Prot. Agency 2014a*, http://www.epa.gov/scram001/

ENVIRON International Corporation. http://www.camx.com/download/support-software.aspx

Huebert, B. J., & Robert, C. H. (1985). The dry deposition of nitric acid to grass. *Journal of Geophysical Research*, 90(D1), 2085–2090.

Hydrological Code. https://en.wikipedia.org/wiki/Hydrological_code

Kumar, N., & Russell, A. G. (1996). Development of a computationally efficient, reactive subgrid-scale plume model and the impact in the northeastern United States using increasing levels of chemical. *Journal of Geophysical Research*, 101(D11), 16737–16744.

Locatelli, J. D., & Hobbs, P. V. (1974). Fall speeds and masses of solid precipitation particles. *Journal of Geophysical Research*, 79(15), 2185–2197. http://doi.org/10.1029/JC079i015p02185

Sauter, D. P., Wang P. K. (1988). An Experimental Study of the Scavenging of Aerosol Particles by Natural Snow Crystals. *Journal of the Atmospheric Sciences*, 46(12), 1650-1655

Scott, B.C. (1978). Parameterization of sulfate removal by precipitation. *Appl. Meteor.*, 17, 1375-1389

Sehmel, G.A. (1980). Particle and Gas Deposition, a Review. *Atmospheric Environment*, 14, 983-1011.

Seinfeld, J. H., Pandis, S. N. (2006). Atmospheric Chemistry and Physics: From Air Pollution to Climate Change, 2nd ed.; *Wiley-Interscience*.

Slinn, S. A., W.G.N Slinn W. G. N. (1980). Predictions for particle deposition on natural waters. *Atmospheric Environment, 14*, 1013–1016

USGS Watershed Boundary Dataset. http://nhd.usgs.gov/wbd.html

U.S. Geological Survey, National Geospatial Technical Operations Center, 20140924, USGS National Watershed Boundary Dataset (WBD) 20140924 National Shapefile: U.S. Geological Survey: Reston, VA, https://prd-tnm.s3.amazonaws.com/StagedProducts/WBD/Shape/WBD_National.zip.

Wesely, M. L. (2007). Parameterization of surface resistances to gaseous dry deposition in regional-scale numerical models. *Atmospheric Environment*, 41(SUPPL.), 52–63. http://doi.org/10.1016/j.atmosenv.2007.10.058

Wesely, M. L., Hicks, B. B. (2000). A review of the current status of knowledge on dry deposition. *Atmospheric Environment*, 34(12-14), 2261–2282. http://doi.org/10.1016/S1352-2310(99)00467-7

Yarwood, G.; Jung, J.; Whitten, G. Z.; Heo, G.; Mellberg, J.; Estes, M. (2010). Updates to the Carbon Bond Mechanism for Version 6 (CB6). *Present. 9th Annu. C. Conf. Chapel Hill, NC,* Oct. 11-13, 6 (415), 1–4.

Chapter 3 MODEL EVALUATION

3.1 Total Dry and Wet Deposition Maps from NADP

The following two maps of total nitrogen dry and wet deposition (Fig. 3.1) were obtained from the National Atmospheric Deposition Program (NADP). The total dry and wet deposition were derived from monitoring and modeling data.

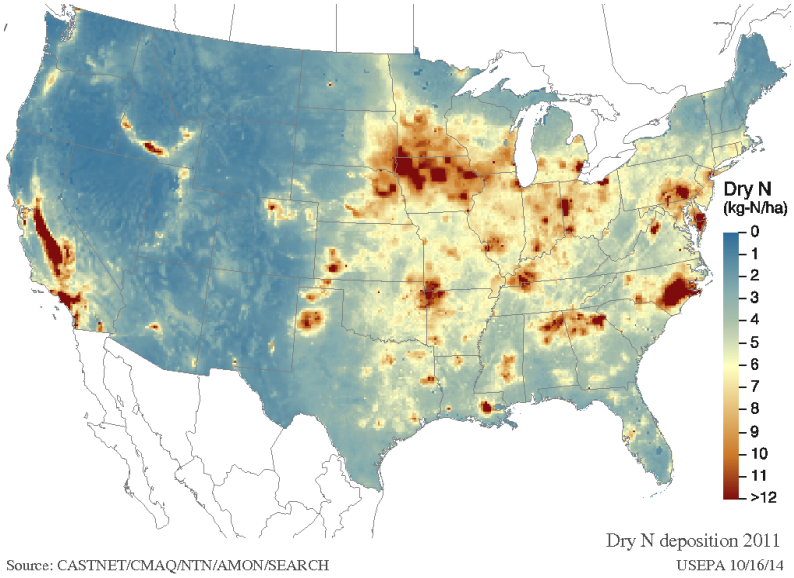

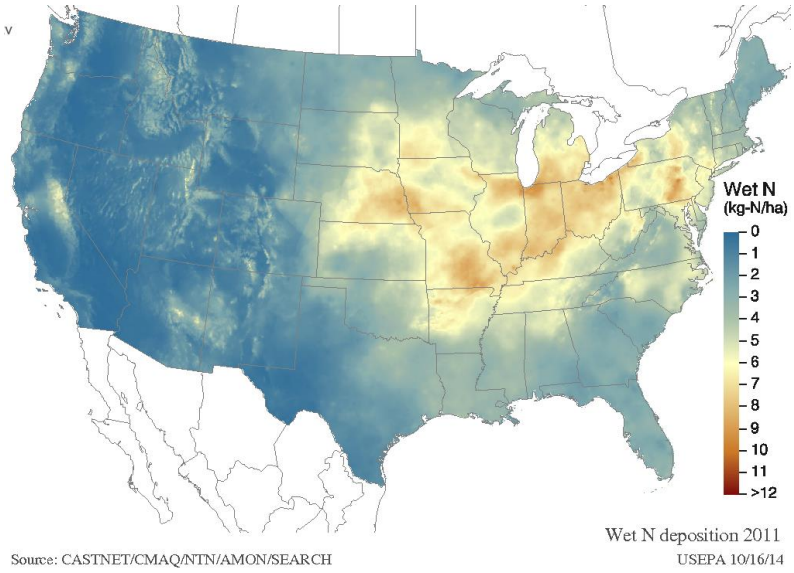

Fig. 3.1 Modeled and Simulated Total Nitrogen Deposited Mass Per Area in the United States in the year 2011, [kgN/ha] (up: dry deposition, down: wet deposition, http://nadp.sws.uiuc.edu/committees/tdep/tdepmaps/preview.aspx#n_wd)

Schwede et al. (2014) estimated dry deposition by combining monitoring data and modeling data. Monitoring data were from monitoring networks for the years 2000-2012, including:

- The Clean Air Status and Trends Network (CASTNET), which is coordinated by the U.S. Environmental Protection Agency (EPA);
- The Ammonia Monitoring Network (AMoN), which is operated by NADP;
- The Southeastern Aerosol Research and Characterization (SEARCH) network, which is operated by Atmospheric Research and Analysis, Inc.

Modeling data were from the regional transport model for the years 2002-2009, the Community Multiscale Ari Quality model (CMAQ) 4.7.1. Air concentration data were from monitoring networks and deposition velocities were estimated from CMAQ. Wet deposition values were obtained from combining the National Trends Network (NTN), which is operated by NADP, and measured values of precipitation chemistry with precipitation estimates from the Parameter-elevation Regression on Independent Slopes Model (PRISM). The PRISM model estimates precipitation across the U.S. based on elevation and slope.

The map of nitrogen dry deposition (Fig. 3.1) shows the highest contribution from the eastern United States and arid areas in the southwest. For CASTNET, deposition estimates were produced by multiplying site specific concentrations and modeled deposition velocities (Meyers et al., 1998). However, these estimates cannot be spatially interpolated but can be obtained from air quality models, such as CMAQ. The estimates obtained from CMAQ can include biases resulting from

errors or gaps in emissions and limitations in modeling the complete physics and chemistry of the atmosphere (Appel et al., 2011).

CMAQ requires gridded fields of meteorological variables which are provided by the Weather Research and Forecasting (WRF) model (Skamarock et al., 2008) or its predecessor, MM5 (Grell et al., 1995). Gridded and speciated emissions inventory is provided by the SMOKE processing system (UNC, 2013). Total dry deposition for nitrogen-containing species in CMAQ include PAN, N_2O_5, NO, NO_2, HONO and organic nitrate. For the years 2010-2013, the average annual deposition determined from the year 2009 was used. The resolution is 12x12 km. Schwede et al. (2014) concluded that due to the limited treatment of organic nitrogen in CMAQ version 4.7.1, the values likely underestimated the organic nitrogen deposition, which consequently might underestimate the total nitrogen deposition. They also suggested that dry deposition is typically measured only for intensive field studies while wet deposition is routinely monitored.

The map of nitrogen wet deposition shows highest values in the eastern United States, where it receives more precipitation (shown in Fig. 3.7).

3.2 Total Dry and Wet Deposition Maps from CAMx Output Data

The following maps (Fig. 3.2), with the U.S. map from ArcGIS in the front, of total dry and wet deposition were obtained from the outputs by CAMx. They have the same scale of deposition as the one from NADP. The nitrogen-containing species include nitrogen dioxide (NO_2), nitric oxide (NO), ammonia (NH_3), nitric acid (HNO_3), particulate ammonia (PNH_4), and particulate nitrate (PNO_3). The

code for the calculation of gridded nitrogen deposition, in the unit of kgN/ha, can be found in Appendix A.

The description of inputs inventories can be found in section 2.1 in Chapter 2 METHODOLOGY.

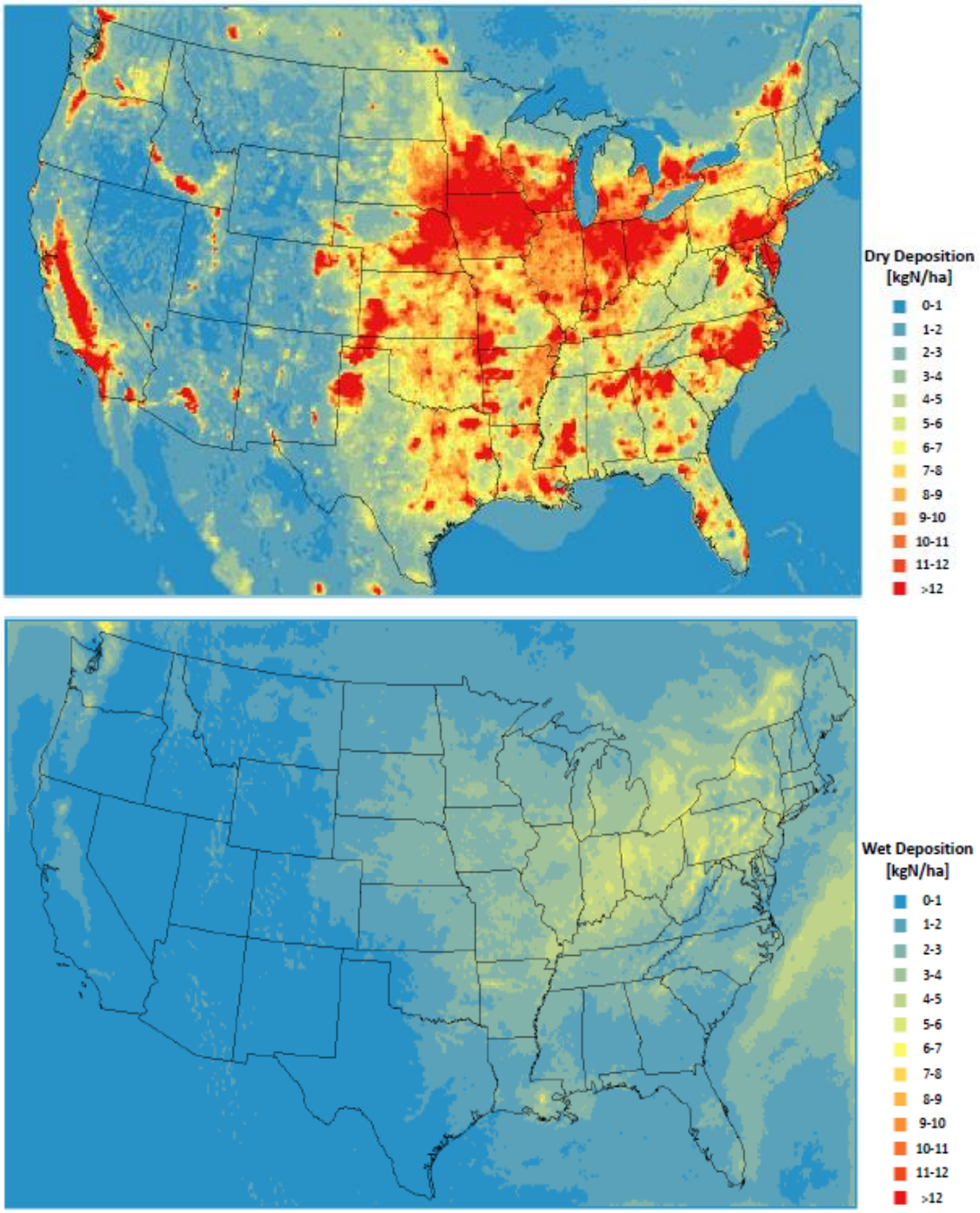

Fig. 3.2 Total Nitrogen Deposited Mass Per Area from CAMx Outputs in the United States in the year 2011, [kgN/ha] (up: dry deposition; down: wet deposition)

It can be concluded from the above maps (Fig. 3.2) that for dry deposition, eastern and southwestern United States received the most deposited mass per area. The watersheds include Upper Mississippi, Ohio, Mid-Atlantic, Great Lakes, Arkansas-White-Red, Texas-Gulf, South-Atlantic-Gulf, and California. For wet deposition, eastern United States received the most deposited mass per area. The watersheds include Upper Mississippi, Great Lakes, Ohio, and Mid-Atlantic. Both of the maps show the similar trend from CAMx output data as the one from NADP.

However, the maximum values obtained from CAMx are higher than the values from NADP. For dry deposition, some of the yellow spots from NADP maps in Fig. 3.1 turned to be the red spots in our maps, which means that our values are higher than the same spots in NADP maps. The watersheds where yellow spots are located include Great Lakes, Upper Mississippi, Ohio, Mid-Atlantic, Arkansas-White-Red, Texas Gulf, and South Atlantic-Gulf watersheds. For wet deposition, NADP map (Fig. 3.1), with more red areas in the map, has higher values in the same watersheds shown in our map (Fig. 3.2). First, different nitrogen-containing species were considered in both models. Different inputs inventories were used as well. These two factors can contribute to the difference in our deposition values from the ones from NADP.

3.3 Comparison between Individual Nitrogen-Containing Species

The following figures (Fig. 3.3) show the comparison between NADP and CAMx maps for dry deposition of ammonia (NH_3). The scales are the same, ranging from 0 to over 12 kgN/ha. It shows that both of the maps have the same watersheds with the highest deposition values. These watersheds include Upper

Mississippi, California, South Atlantic-Gulf. Some areas in other watersheds also show the highest deposition, such as Texas-Gulf, Arkansas-White-Red, Mid-Atlantic, Great Lakes, Lower Mississippi, and Pacific Northwest. Our map shows

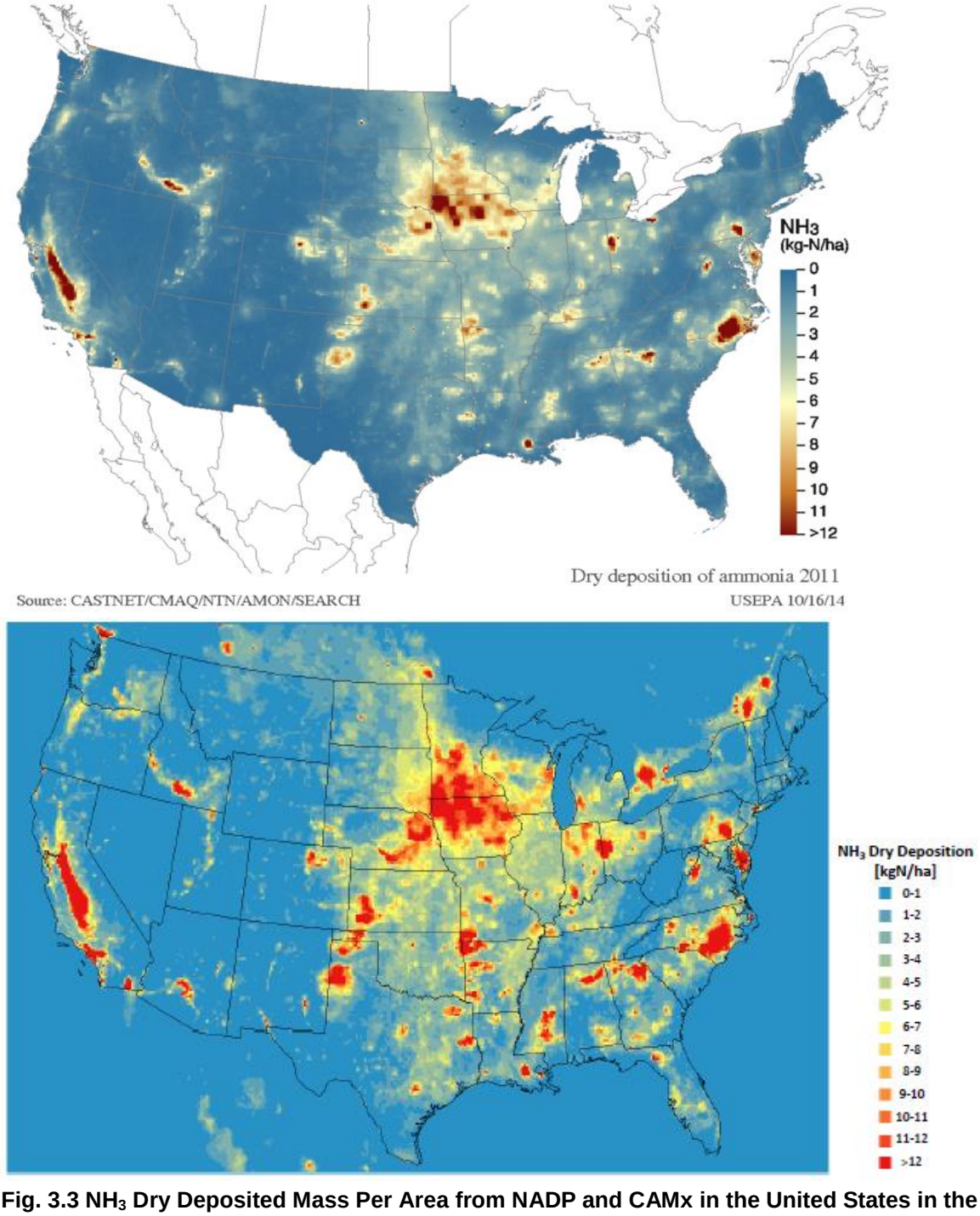

Fig. 3.3 NH_3 Dry Deposited Mass Per Area from NADP and CAMx in the United States in the year 2011, [kgN/ha] (up: NADP; down: CAMx http://nadp.sws.uiuc.edu/committees/tdep/tdepmaps/preview.aspx#n_dd)

higher values for NH_3 dry deposited mass per area, with more red spots in the same places in the NADP map.

Fig. 3.4 shows the difference between NADP and CAMx maps of dry deposited mass per area for nitric acid (HNO_3). Both of the scales range from 0 to over 6 kgN/ha. It can be observed that in some watersheds, the values are higher

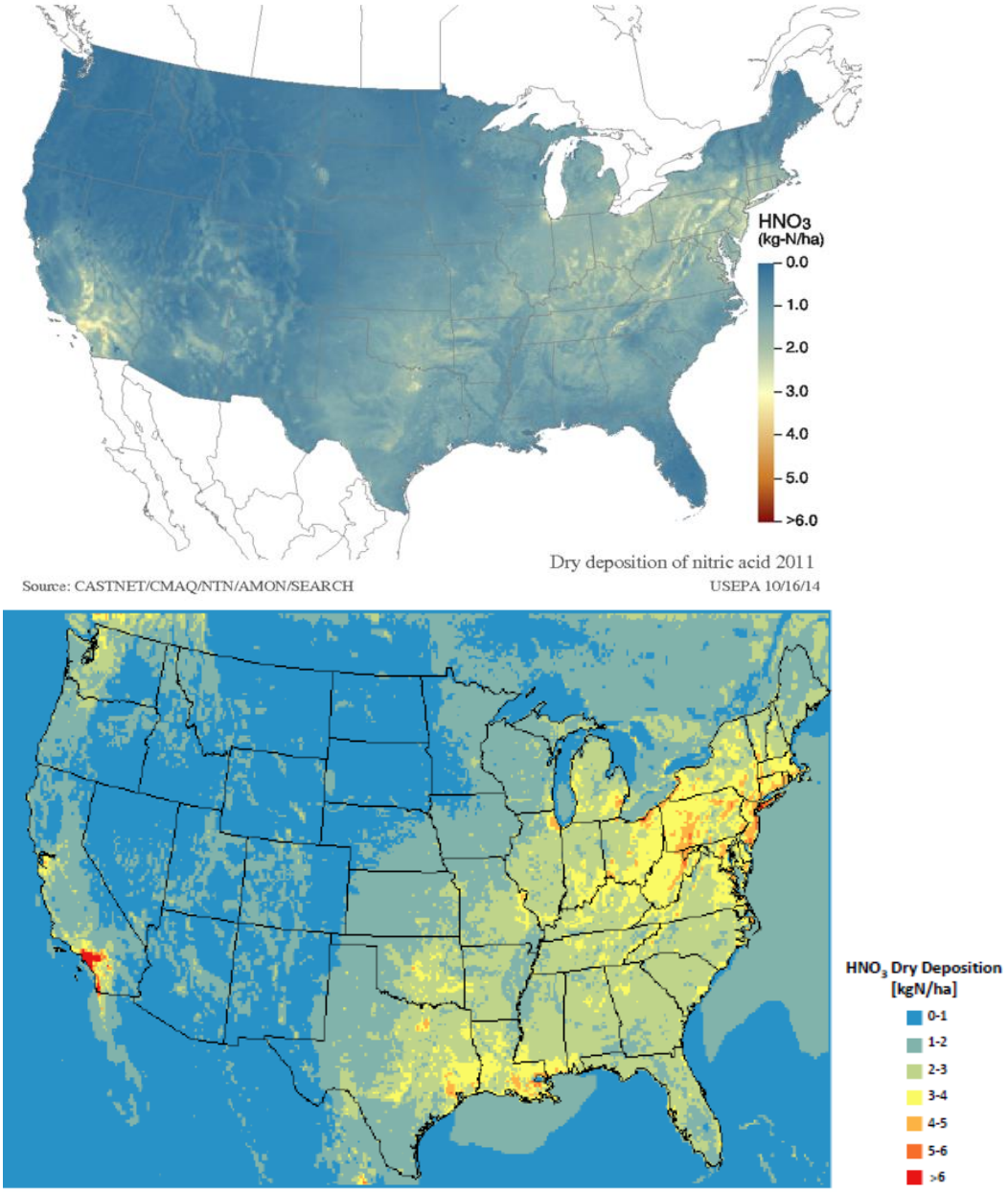

Fig. 3.4 HNO_3 Dry Deposited Mass Per Area from NADP and CAMx in the United States in the year 2011, [kgN/ha] (up: NADP; down: CAMx http://nadp.sws.uiuc.edu/committees/tdep/tdepmaps/preview.aspx#n_dd)

in our map. These watersheds include California, Mid-Atlantic, Ohio, and Lower Mississippi.

The difference between NADP and CAMx maps of dry deposited mass per area for particulate nitrate (PNO_3) can be seen in Fig. 3.5. The scale for PNO_3 in

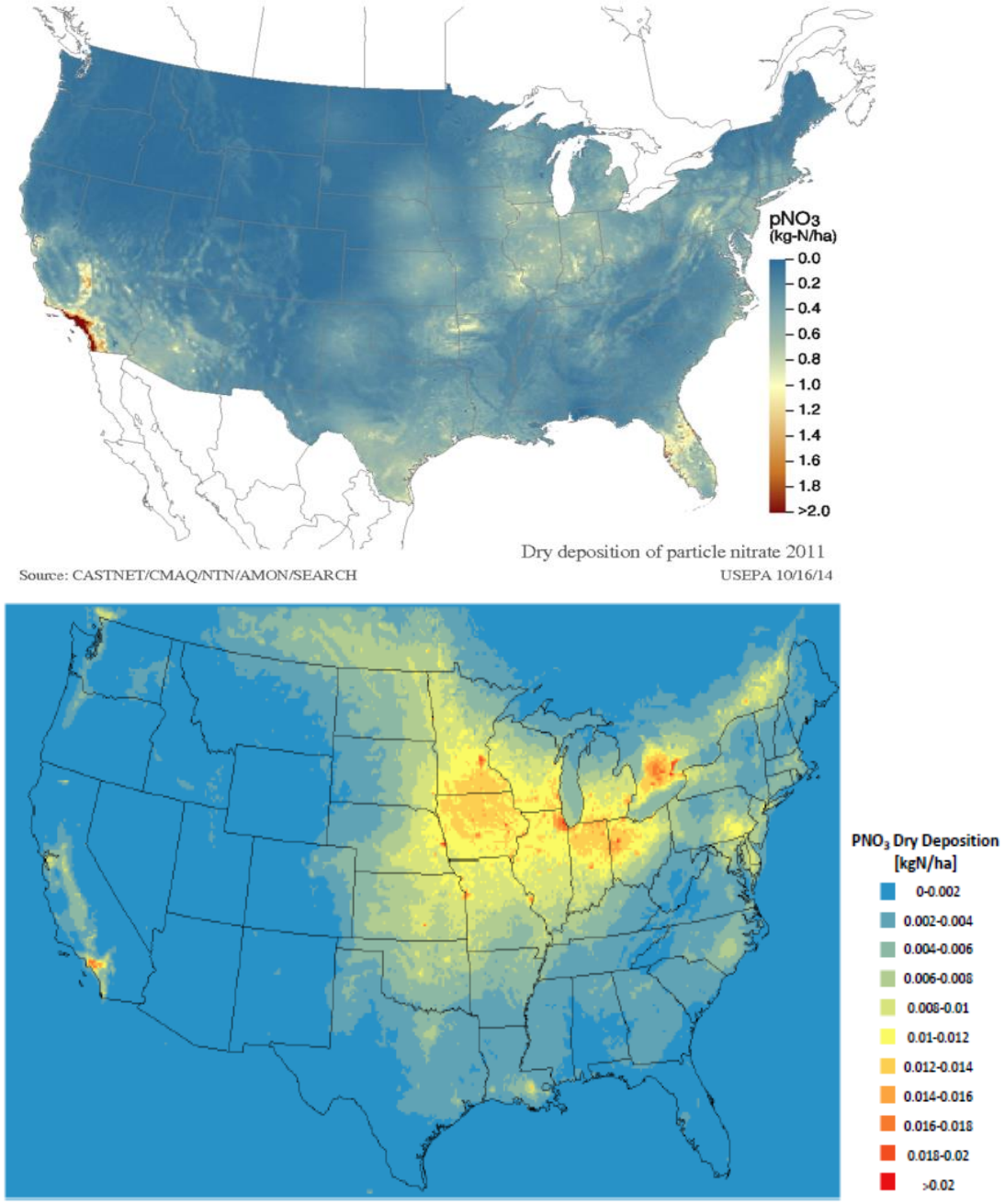

Fig. 3.5 PNO_3 Dry Deposited Mass Per Area from NADP and CAMx in the United States in the year 2011, [kgN/ha] (up: NADP; down: CAMx http://nadp.sws.uiuc.edu/committees/tdep/tdepmaps/preview.aspx#n_dd)

NADP, ranging from 0 to over 2 kgN/ha, is two magnitudes higher than that from CAMx, ranging from 0 to over 0.02 kgN/ha. It also can be seen that California receives the most dry deposited mass per area in the NADP map, while our map shows that the watersheds, which receive the most deposited mass per area, include Great Lakes, Upper Mississippi, Ohio, and California.

Dry deposition from NADP and CAMx maps for particulate ammonium (PNH_4) is shown in Fig. 3.6. The scale for both maps is different, with NADP from 0 to over 2 kgN/ha and CAMx from 0 to over 0.06 kgN/ha. It shows that the watersheds which receive the highest deposition are Ohio, Mid-Atlantic, Great Lakes, and Upper Mississippi in the NADP map. Our map also shows that those four watersheds receive the highest PNH_4 dry deposited mass per area. Other watersheds, including Missouri, Arkansas-White-Red, Lower Mississippi, and South Atlantic-Gulf also receive a relatively high dry deposited mass per area.

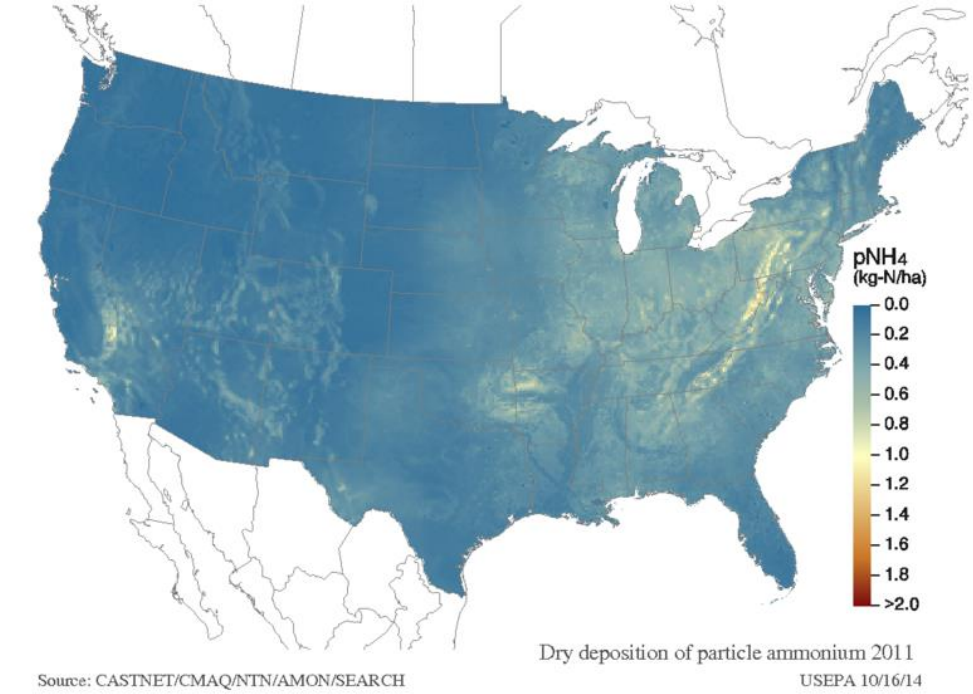

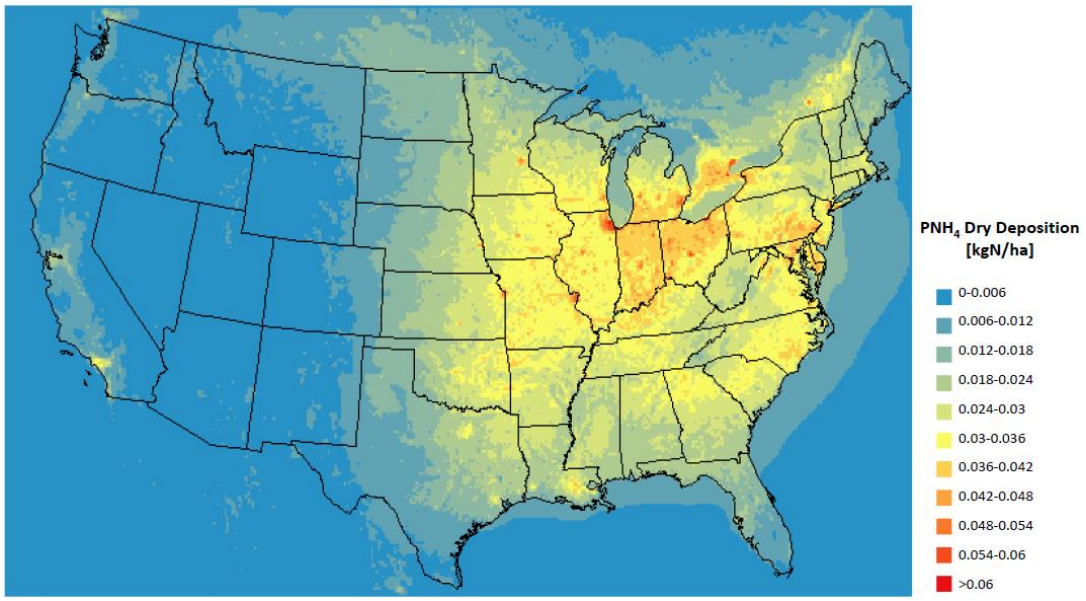

Fig. 3.6 PNH_4 Dry Deposited Mass Per Area from NADP and CAMx in the United States in the year 2011, [kgN/ha] (up: NADP; down: CAMx http://nadp.sws.uiuc.edu/committees/tdep/tdepmaps/preview.aspx#n_dd)

The following maps (Fig 3.7) show the wet deposited mass of nitrate (including nitric acid and particulate nitrate) in the unit of kg/ha. The range for nitrate in both maps is from 0 to over 20. It can be seen that in both maps, the same watersheds receive the highest wet deposited nitrate. These watersheds

include Great Lakes, Upper Mississippi, Ohio, and Mid-Atlantic.

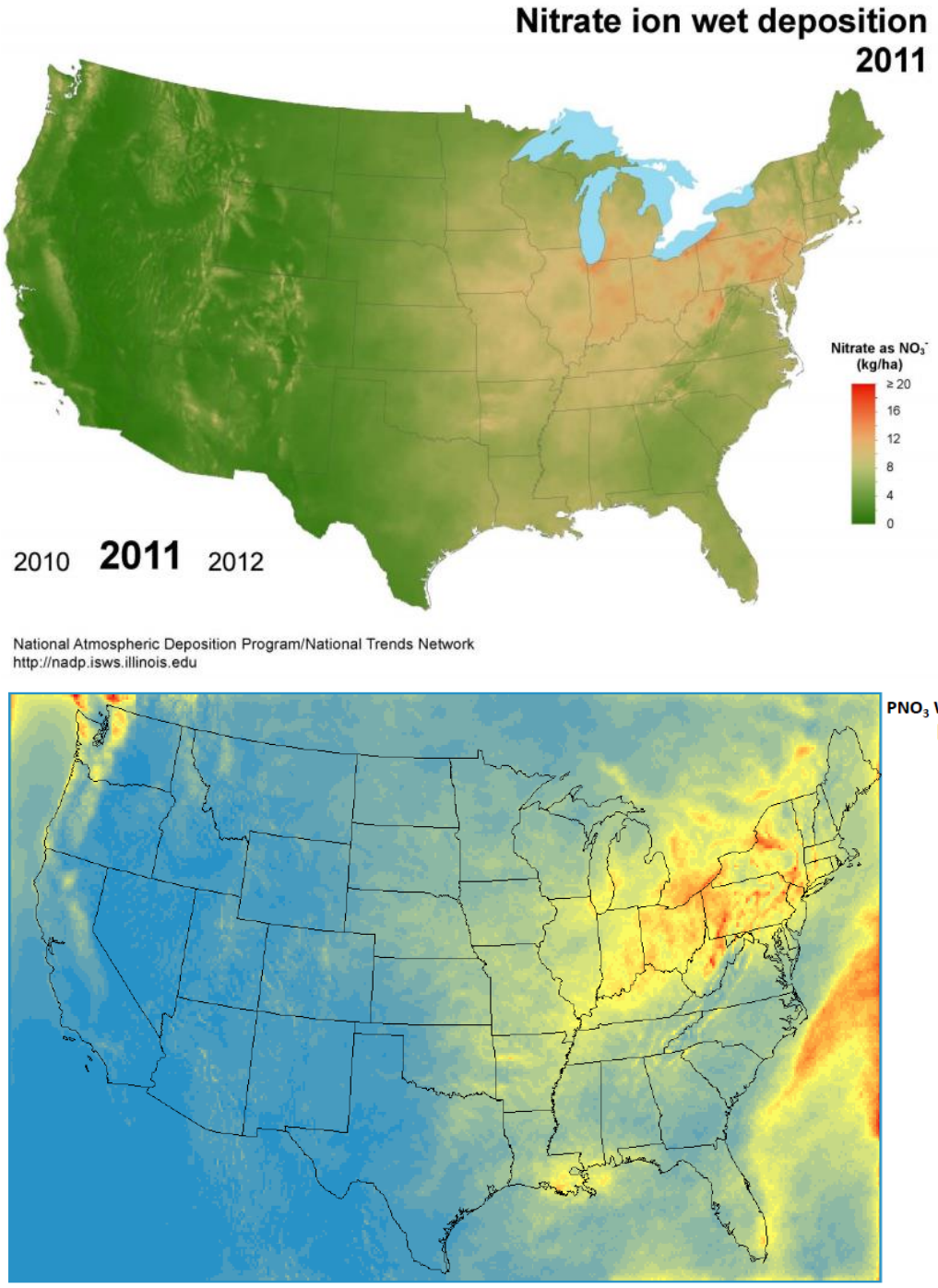

Fig. 3.7 Nitrate Wet Deposited Mass Per Area from NADP and CAMx in the United States in the year 2011, [kgN/ha] (up: NADP; down: CAMx http://nadp.sws.uiuc.edu/data/animaps.aspx)

Wet deposition of ammonium from both maps can be seen in Fig. 4.8, with both scale ranging from 0 to over 6 kg/ha. It shows that in NADP map, the watersheds which receive the highest wet deposited mass are Upper Mississippi,

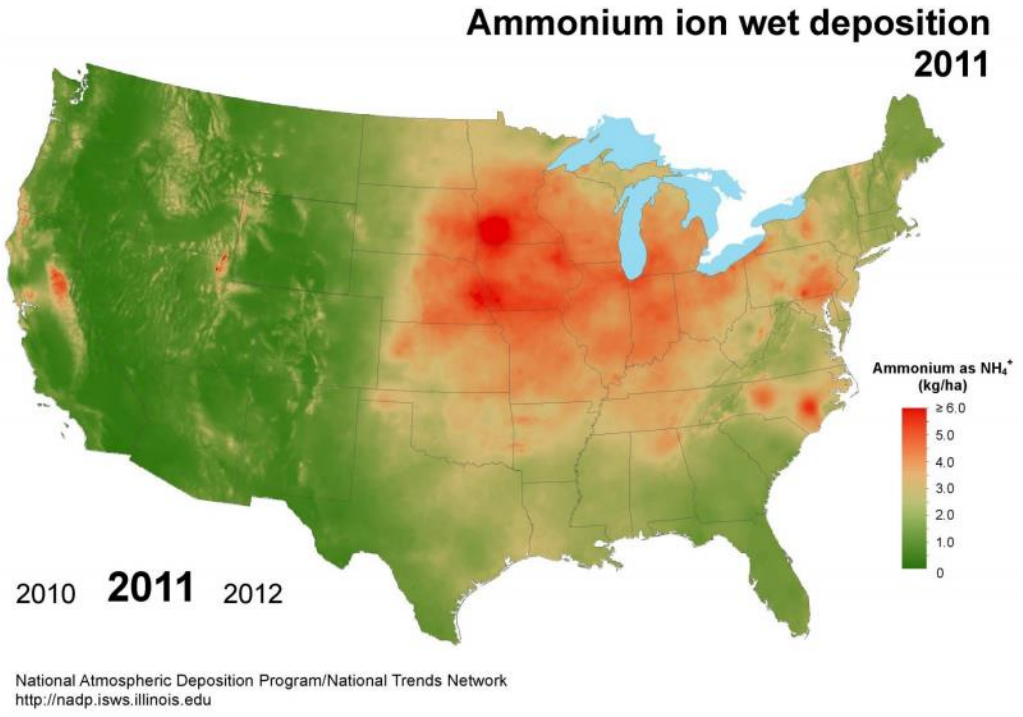

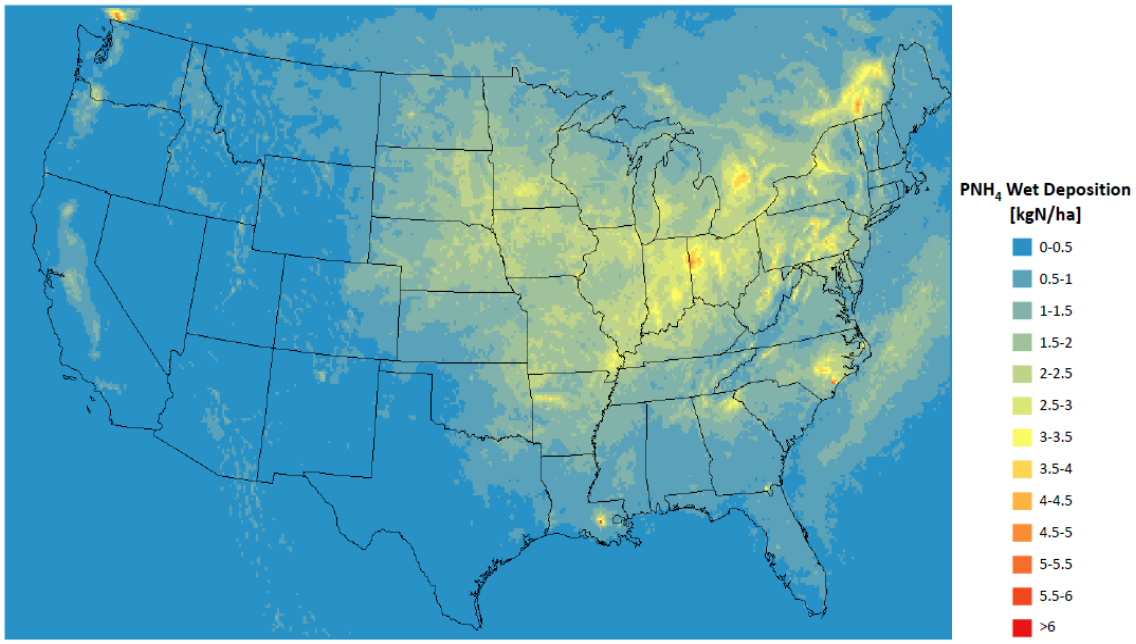

Fig. 3.8 Ammonium Wet Deposited Mass Per Area from NADP and CAMx in the United States in the year 2011, [kgN/ha] (up: NADP; down: CAMx http://nadp.sws.uiuc.edu/data/animaps.aspx)

Great Lakes, Mid-Atlantic, Ohio, and some areas in California and South Atlantic-Gulf watersheds. Our map shows that the watersheds which receive the highest wet deposited mass center on Great Lakes, Ohio, and Upper Mississippi. Other watersheds which receive relatively high wet deposited mass include Mid-Atlantic and South Atlantic-Gulf.

The reasons why the maps have different values and distribution for dry deposition of particulate matter will be further investigated in the future work.

3.4 References

Appel, K.W., Foley, K.M., Bash, J.O., Pinder, R.W., Dennis, R.L., Allen, D.J., Pickering, K. (2011). A multi-resolution assessment of the Community Multiscale Air Quality (CMAQ) model v4.7 wet deposition estimates for 2002e2006. *Geoscience Model Development* 4, 357e371.

Byun, D., Schere, K.L. (2006). Review of the governing equations, computational algorithms, and other components of the Models-3 Community Multiscale Air Quality (CMAQ) modeling system. *Applied Mechanics Reviews* 59, 51e77.

Grell, G., Dudhia, J., Stauffer, D., 1995. A Description of the Fifth-Generation Penn State/NCAR Mesoscale model (MM5). *Boulder, CO*. NCAR/TN-398þSTR.

Meyers, T.P., Finkelstein, P., Clarke, J., Ellestad, T.G., Sims, P.F. (1998). A multilayer model for inferring dry deposition using standard meteorological measurements. *Journal of Geophysical Research* 103, 22645e22661.

National Atmospheric Deposition Program, 2014. Total Deposition Maps, 2011 http://nadp.sws.uiuc.edu/committees/tdep/tdepmaps .

Schwede, D., & Lear, G. (2014). A novel hybrid approach for estimating total deposition in the United States. *Atmospheric Environment*. Retrieved from http://www.sciencedirect.com/science/article/pii/S1352231014002805

Skamarock, W., Klemp, J., Dudhia, J., Gill, D., Barker, D., Wang, W., Huang, X.-y., Duda, M., 2008. A Description of the Advanced Research WRF Version 3. *University Corporation for Atmospheric Research*. NCAR Tech. Note NCAR/TN-475þSTR.

UNC, 2013. SMOKE - Sparse Matrix Operator Kernel Emissions. http://www.smokemodel.org/index.cfm (accessed 5.03.13.).

Chapter 4 RESULTS AND DISCUSSION

In this chapter, 4 bar charts are shown in the main body to quantify the total nitrogen deposited mass per area (kgN/km^2) onto each watershed through dry and wet deposition. Seasonal variation for each species and major contribution from each species are quantified and discussed respectively. Four (4) maps of the deposition onto each of the U.S. watersheds are shown in this chapter as well. Spatial pattern for each species deposited on each watershed is discussed.

The plots of average ambient airborne concentration for each species in each watershed are also included in the main body, which helps to better explain the seasonal variation and spatial pattern for nitrogen deposited mass per area. The time period for each season for concentration files is defined in the same way as the one defined for deposition files, where January to March is winter, April to June spring, July to September summer, and October to December fall.

The bar charts of dry and wet deposition for each specific species and watersheds can be found in Appendix B, which are 24 in total. These 24 bar charts have two different sets of units. The first 12 are in the unit of kgN, which is the nitrogen deposited mass, and the other 12 in the unit of kg/km^2, which is the nitrogen deposited mass per area. Additionally, 4 more bar charts are included in Appendix B showing the total nitrogen deposited mass (kgN) onto each watershed through dry and wet deposition.

Fig 4.1 shows the dry and wet deposition of the total nitrogen-containing species in 18 watersheds. It is noticeable that dry and wet deposition concentrate on the Eastern United States and California where there is higher population,

which leads to higher vehicular combustion and more farmlands, contributing to the emission and deposition of nitrogen oxides (NOx) and ammonia (NH_3), respectively, or where the power plants are mainly located, which also leads to the emission and deposition of NOx.

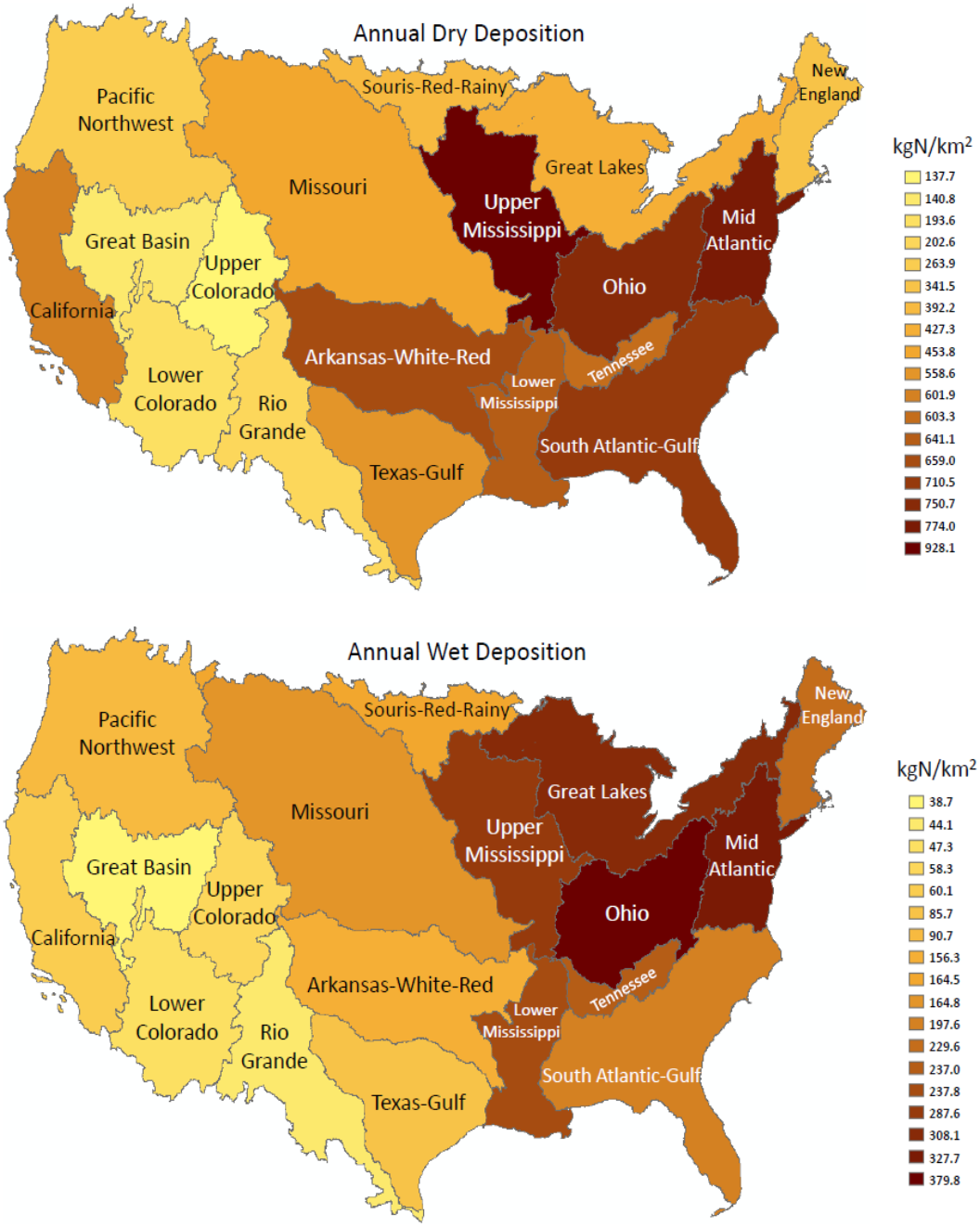

Fig. 4.1 Dry and Wet Deposition Map of U.S. Watersheds (http://viewer.nationalmap.gov/basic/)

The following two maps (Fig. 4.2) show the dry and wet deposition of the total of nitrogen-containing species onto each of the major U.S. watersheds by using the gridded deposition from CAMx. It further illustrates which areas within each watershed receive the most nitrogen deposition throughout the year. It can be seen that the highly concentrated areas for dry and wet deposition are California and eastern United States watersheds, which aligns with the maps shown in Fig. 4.1.

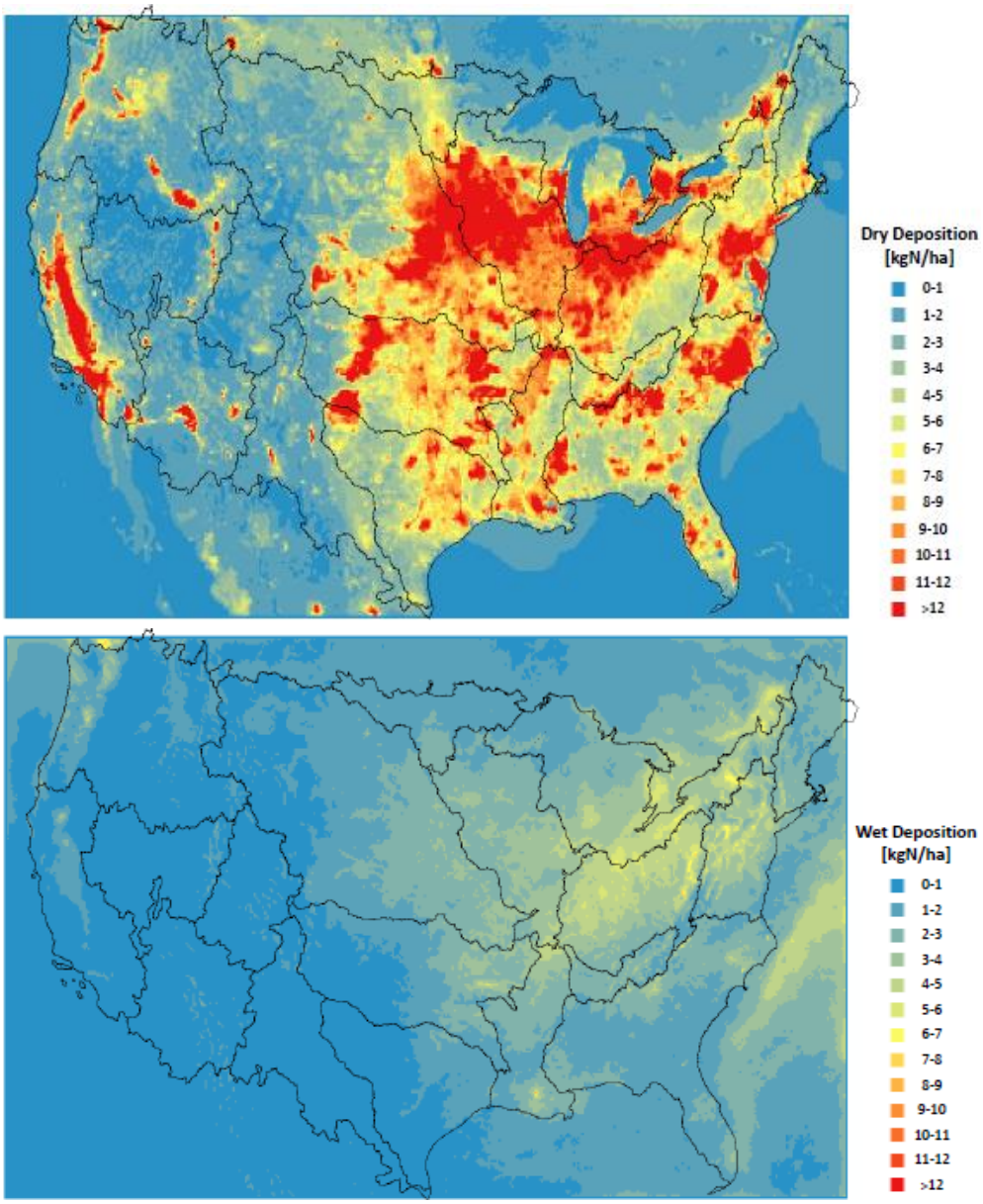

Fig. 4.2 Gridded Dry and Wet Deposition Map of U.S. Watersheds (http://viewer.nationalmap.gov/basic/)

4.1 Deposition Results

4.1.1 Nitrogen Speciation

The following figure (Fig. 4.3) shows the annual total nitrogen deposited mass per area in each season by dry and wet deposition. The amount of dry deposition, which ranges from 110 to 910 kgN/km^2, is over twice that of wet deposition, ranging from 40 to 390 kgN/km^2. There are many factors impacting dry deposition, for instance, the properties of deposited gases and particulates, meteorological conditions, surface properties, and atmospheric concentrations (ENVIRON, 2013; Benedict et al, 2013). For wet deposition, the impacting factors include frequency of rainfall, characteristics of rainfall, gas solubility, particle size, and atmospheric concentrations (Benedict et al, 2013).

Fig. 4.3 also presents that for dry deposition, gaseous species, consisting of ammonia (NH_3, ranging from 10 to 600 kgN/km^2), nitric acid (HNO_3, ranging from 50 to 300 kgN/km^2) and nitrogen dioxide (NO_2, ranging from 10 to 180 kgN/km^2) are the major contributors to the deposited mass, with NH_3 almost twice that of HNO_3 and four times larger than NO_2. NH_3 makes up 40% to 60% of the total nitrogen dry deposition, HNO_3 20% to 40%, and NO_2 about 10%. For wet deposition, the major contributors are nitric acid (HNO_3, ranging from 25 to 190 kgN/km^2) and particulate ammonium (PNH_4, ranging from 10 to 100 kgN/km^2), with HNO_3 almost twice that of NH_3. HNO_3 comprises of 40%-60% of the total nitrogen wet deposited mass per area, PNH_4 20%-40%, and NH_3 and PNO_3 altogether contribute about 10%.

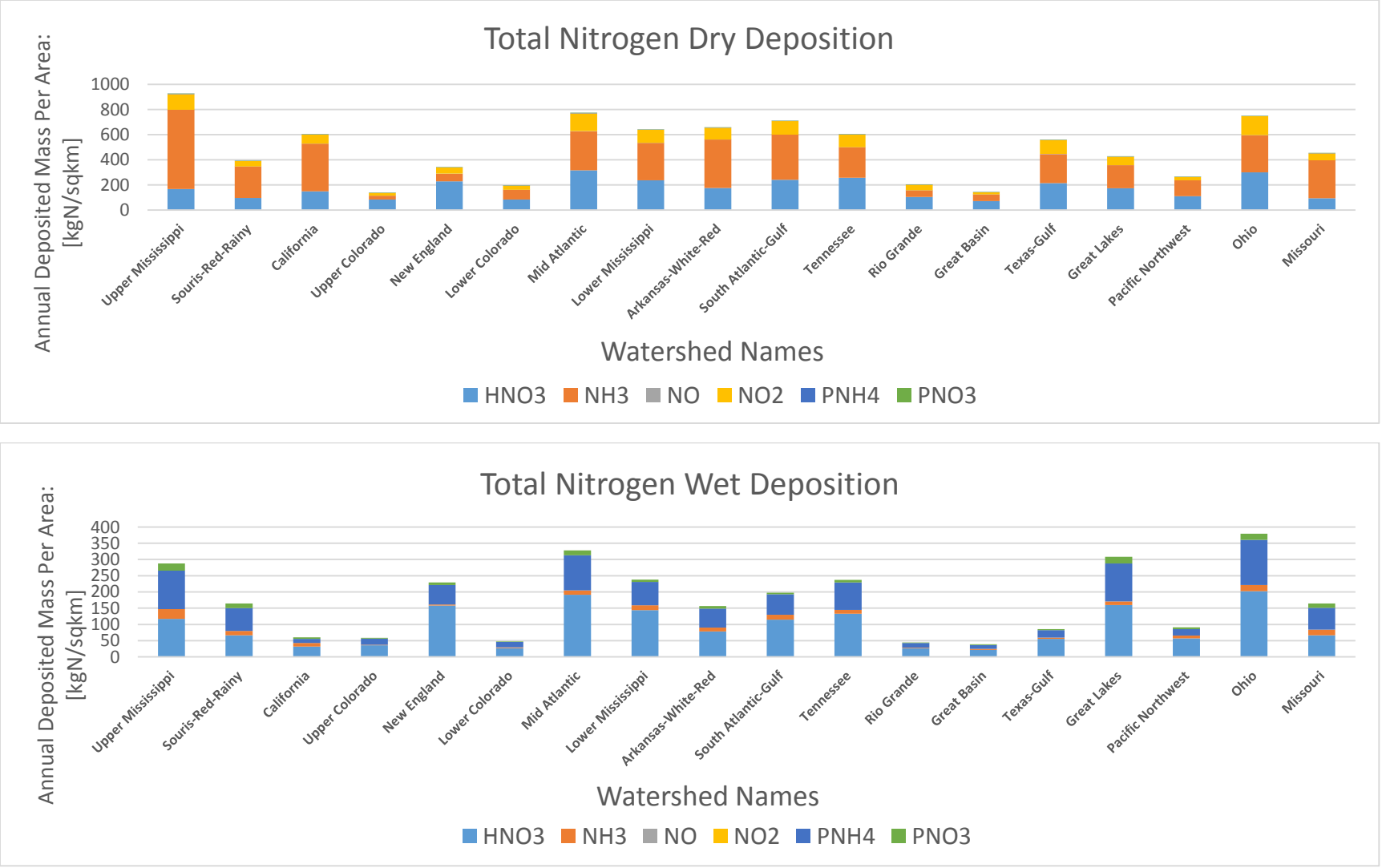

Fig. 4.3 Annual Deposited Mass Per Area of Each Species in Each Watershed, [kgN/km^2]

In CAMx, gaseous species, including nitric acid (HNO_3), nitrogen oxides (NOx) and ammonia (NH_3), are mainly removed from the atmosphere through dry deposition (ENVIRON, 2013). While particulate matter, including particulate nitrate (PNO_3) and particulate ammonium (PNH_4), are mainly removed via wet deposition (ENVIRON, 2013). For gases, they have relatively high deposition velocities compared to particulate matter. Deposition velocity (v_d) is obtained from models which take into account of many factors, including the reactivity, solubility and diffusivity of gases, the size of particles, local meteorological conditions, and season-dependent surface characteristics (ENVIRON, 2013). For a given species, particle size and grid cell, CAMx determines a deposition velocity according to the land use type in that cell and combine the values together based on the fractional distribution of the land use. The files for aerosol size spectra and species-dependent properties, which are needed to calculate deposition velocity, are externally provided to CAMx through the chemistry parameters file; gridded land use is provided for the master grid and optionally for the nested grids; the season is decided by the simulation date and location on earth.

Deposition velocity is the ratio of dry deposition rate and atmospheric concentrations of the chemical species (Hicks et al., 1987). In CAMx, v_d can be calculated through the following equation in terms of three primary resistance:

$$v_d = \frac{1}{r_a + r_b + r_s}$$

r_a , r_b , and r_s represent aerodynamic resistance, quasi-laminar sublayer resistance, and surface resistance, respectively. Each of the resistance term can be calculated in CAMx using different equations. Gases have smaller size, which

makes them less resistant in the atmosphere and easier to move around due to Brownian motion. Brownian motion is the random motion of particles suspended in a fluid (a liquid or a gas), resulting from their collision with the quick atoms or molecules in the fluid (Brown, 1828).

For particulates, they act as cloud condensation nuclei (CCN). As a result, the cloud droplets grow and get into a sufficiently large size and fall as precipitation (ENVIRON, 2013).

Because gaseous nitric acid (HNO_3) is highly soluble and chemically reactive. Its deposition is rapid and irreversible on most surfaces (Seinfeld et al., 2006; Luo et al., 2002; Hicks et al., 1987; Clarke et al, 1997; Meyers et al., 1989). HNO_3 can be mainly removed by wet and dry deposition.

Ammonia (NH_3) is mainly emitted from agriculture, including fertilizer usage, animal wastes, as well as from industrial and vehicular emissions (Erisman et al., 2010; Behera et al., 2013; Zhao et al., 2015; Pitcairn et al., 1995). In spring and summer, fertilizer use is dominant, which leads to high amounts of NH_3 emissions and concentrations in the atmosphere. Aneja et al. (2000) suggested that NH_3 is a major contribution to atmospheric nitrogen loading. Some studies showed the deposition velocity of NH_3 to be similar to or larger than that of nitric acid (HNO_3) (Benedict et al, 2013; Harrison et al, 1991; Anderson et al, 1995; Neirynck et al, 2007). One important consideration for dry deposited NH_3 is that NH_3 has a short lifetime, which is 0.5 to 5 days, resulting from its relatively high dry deposition velocity and also from its rapid gas-to-particle rate of NH_3 to particulate ammonium (PNH_4) (Baek et al., 2004; Aneja et al., 2000; Luo et al., 2002). NH_3 reacts with

strong acids, such as nitric acid (HNO_3) and sulfuric acid (H_2SO_4), to form ammonium nitrate, ammonium sulfate, and ammonium bisulfate aerosols in the atmosphere (Baek et al, 2004; Seinfeld et al, 2006). Ammonium salts obtained through the above reactions can exist in forms of solid particles or liquid droplets, depending on the percentage of water vapor in the air (Baek et al., 2004). Because NH_3 is primarily emitted from animal waste and fertilizer, which means that it has a low source height. It is more likely for NH_3 to deposit near its source (Aneja et al., 2000; Asman et al., 1992).

The rest of ammonia (NH_3), which is not deposited or precipitated by rain, will be converted to particulate ammonium (PNH_4), which has a longer lifetime of 5 to 10 days. PNH_4 can be transported downwind from its sources for a longer distance (Baek et al., 2004).

Particulate ammonium (PNH_4) and particulate nitrate (PNO_3) are formed through chemical reactions of ammonia (NH_3) and nitric acid (HNO_3) in the atmosphere. The formation of PNH_4 and PNO_3, such as ammonium nitrate (NH_4NO_3) and ammonium chloride (NH_4Cl), are favored in higher relative humidity and lower atmospheric temperature. Otherwise, these ammonium salts can be reversed back to their precursor gases (Behera et al., 2013).

The results for the major dry and wet deposited species, which were described above, have quantified what Luo et al. (2002), Hu et al. (1997) and Zhao et al. (2015) estimated the amount of major nitrogen-containing species contribute to dry and wet deposition.

Luo et al. (2002) studied the atmospheric deposition of nitrogen into Long Island Sound from 1991 through 1994, and from 1997 through 1999. They set up four monitoring stations along the Connecticut coastline. They used sensors to collect meteorological information, a two-stage filter pack to collect atmospheric concentration of nitrogen, and wet deposition collector to get the data during rain events. The laboratory analysis was performed in the analytical laboratory at the University of Connecticut. They found that nitric acid was predominant in dry deposition, making up over 70% of the total dry flux, and that wet deposition was the major contributor to the total nitrogen loading along the coastline.

Zhao et al. (2015) used a global transport model, GEOS-Chem, with a meteorological data having a temporal resolution of 6 h and a horizontal resolution of 1/2° latitude by 2/3° longitude. They simulated the data from the year 2008 to 2010 and found that a large percentage (approximately 40%) of nitrogen-containing species deposit into the ocean through wet and dry deposition.

Hu et al. (1997) set up two dry deposition monitoring sites along the shore of Long Island Sound in the year 1991. An Aero-Chem wet-dry sampler and an Anderson wet-dry sampler were employed to collect rain water. Additionally, two three-gallon polyethylene buckets were used in the samplers, one to collect wet deposition, the other dry deposition. Both wet and dry deposition of nitrogen species were sampled and measured every week. All the chemical data analyzed in the laboratory for both wet and dry deposition were conducted under EPA standards. A two layer model developed by Slinn and Slinn (1980) was also adapted to calculate deposition velocities. Hu et al. (1997) estimated that the total

atmospheric nitrogen loading to the Sound was 2240 metric tons per year and that wet deposition was the dominant source of atmospheric contribution to the Sound.

4.1.2 Seasonal Variability

The following figure (Fig. 4.4) is the total nitrogen deposited mass per area from dry and wet deposition in each watershed. It demonstrates that spring and summer are always the seasons contributing most to the deposited mass, each of which is almost twice as large as that in fall and winter. The similar pattern can also be found in the supplement figures in Appendix B from Fig. B.1 to Fig. B.12. In spring and summer, rainfall takes place more frequently, which removes a great amount of soluble gaseous species, such as gaseous nitric acid (HNO_3), and particulate matter, such as particulate nitrate (PNO_3) and particulate ammonium (PNH_4), from the atmosphere (ENVIRON, 2013). Additionally, the amount of deposited mass from dry deposition is dependent on the surface characteristics (ENVIRON, 2013). In spring and summer, trees and plants start to grow and have more leaves, which provide more landing surface for the gaseous species and particulate matter. Besides, in these two seasons, leaves increase the surface roughness, which helps catch gaseous species. Surface roughness is an indication of the smoothness of a surface. It can be examined by eye or rubbed with a fingertip. For example, leaves have more surface roughness than bald branches without any leaves.

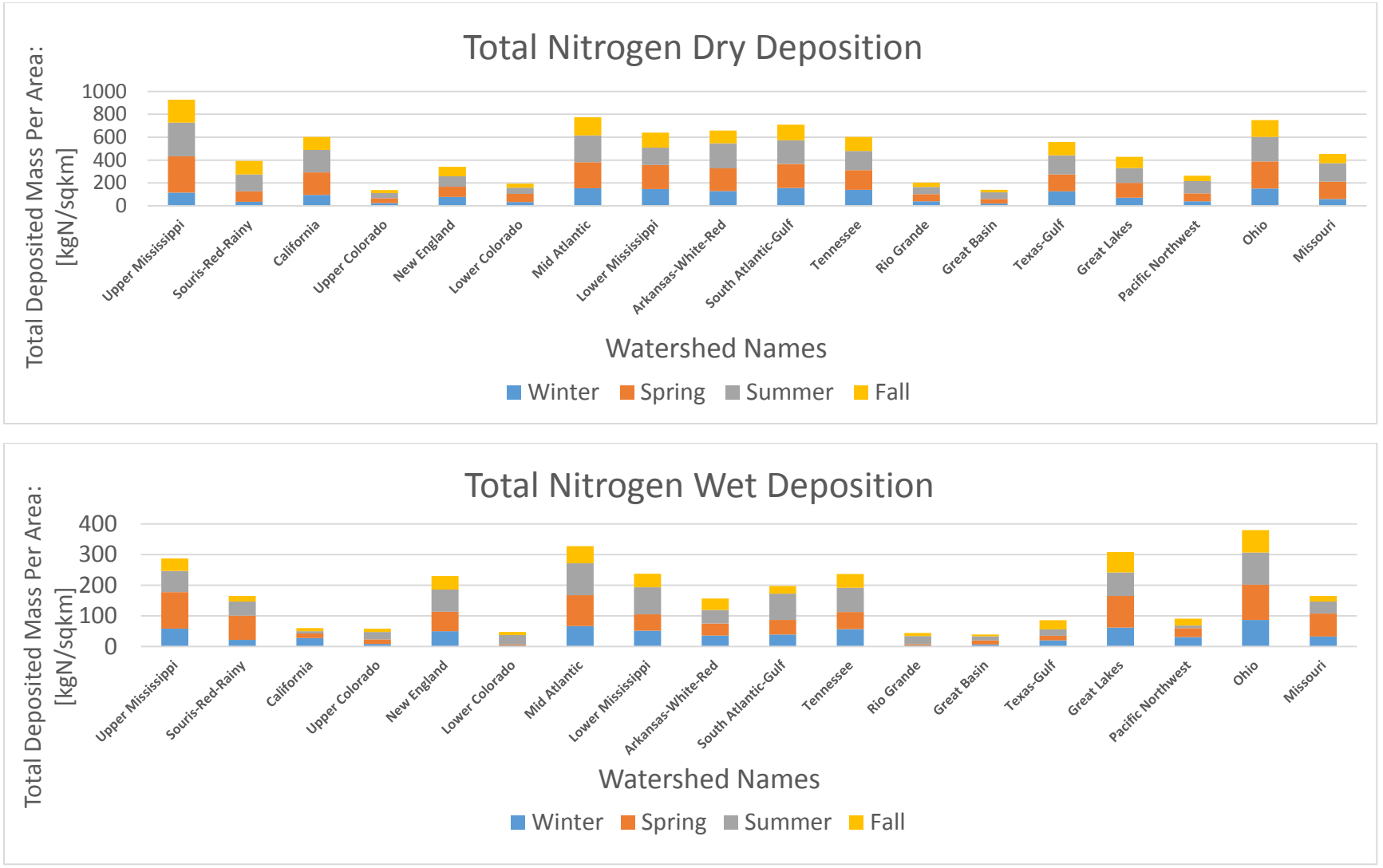

Fig. 4.4 Total Deposited Mass Per Area of Each Season for All Species in Each Watershed, [kgN/km^2]

From Fig. 4.3 and Fig. 4.4, it can be concluded that spring and summer are the seasons when ammonia (NH_3) has the most dry deposited mass per area. As described previously, spring and summer have more landing surface from vegetation for major dry deposited species, ammonia (NH_3) and nitric acid (HNO_3).

The main factors impacting dry deposition of ammonia (NH_3) on vegetation include meteorology conditions (such as relative humidity, temperature) and hours of a day (Behera et al., 2013). Atmospheric moisture deposited on the surface of leaves provide a gateway for atmospheric NH_3. Namely, when there is higher relative humidity in the atmosphere, NH_3 is more easily dry deposited (Behera et al., 2013). Additionally, NH_3 is deposited less at night than during the day because of the physiological and meteorological features of plants. Stomatas of plants close at night, therefore, it stops NH_3 uptake from the atmosphere. Calmer air, lower humidity as well as lower temperature are also the factors which influence the uptake of NH_3 during nighttime (Renard et al., 2004; Beheral et al, 2013).

Cadle (1984) conducted a research on measurements of nitric acid (HNO_3), particulate nitrate (PNO_3), strong aerosol acidity, and ammonia (NH_3) in Warren, Michigan for a one-year period. He found that the greatest variation was for NH_3, which was 8.5 times higher in summer than winter. While PNO_3 had the least variation with the summer maximum 1.8 times higher than the spring maximum.

4.1.3 Spatial Variation

Fig. 4.5 demonstrates the seasonal pattern of the average concentration of two gaseous species, ammonia (NH_3) and nitric acid (HNO_3), in each watershed. Fig 4.6 shows the seasonal pattern of the average concentration of the other two

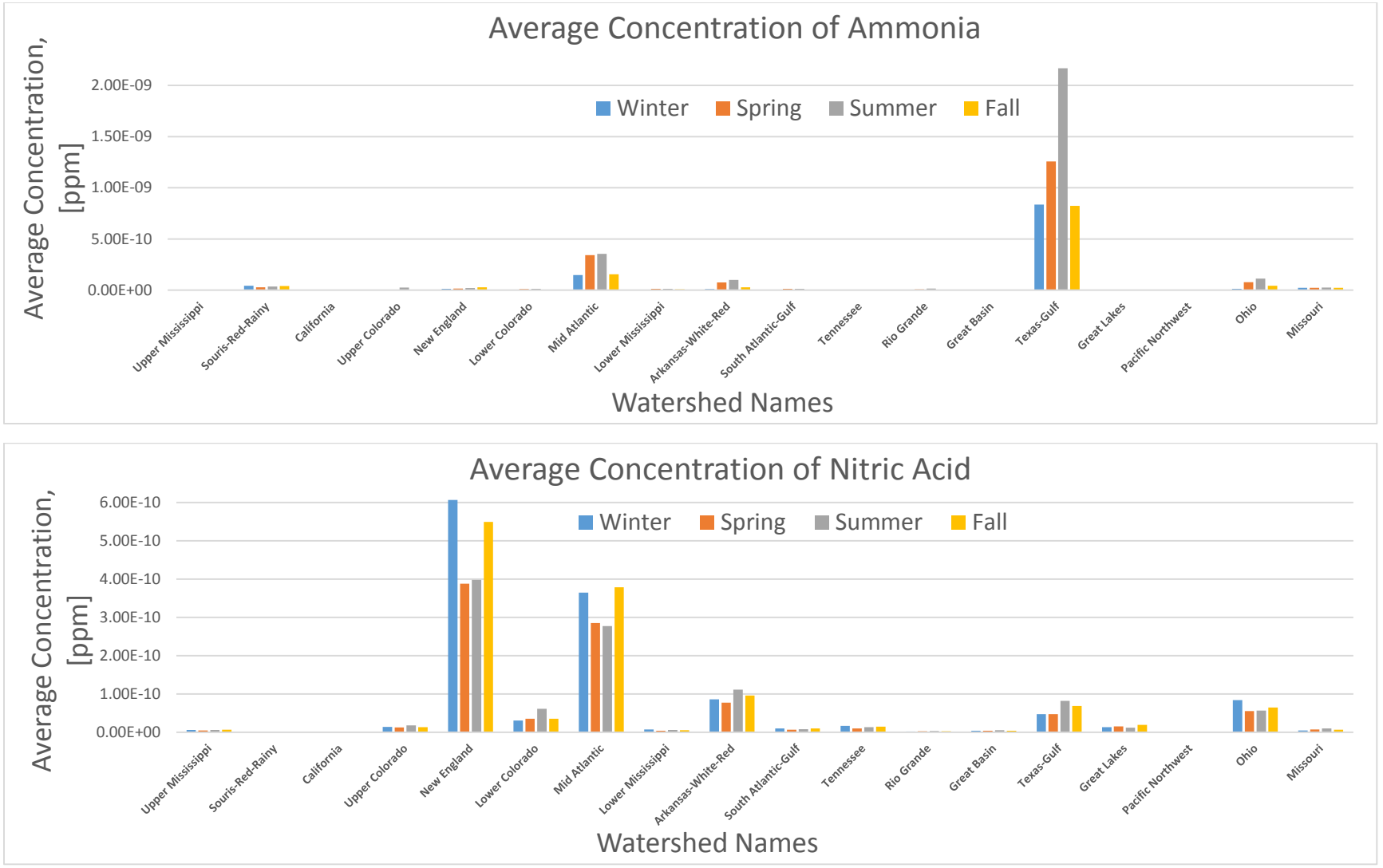

Fig. 4.5 Average Concentration of Ammonia and Nitric Acid in Each Watershed, [ppm]

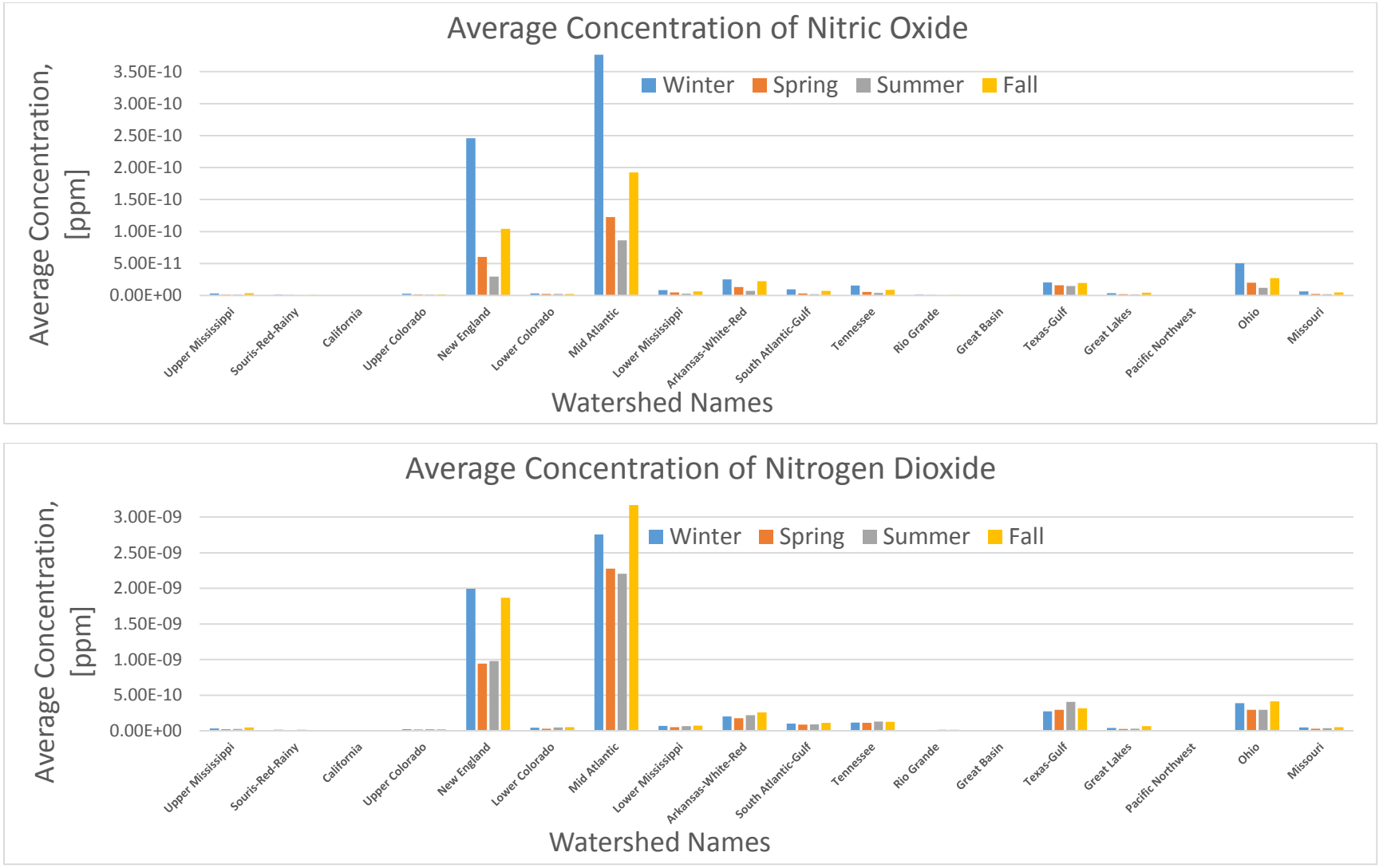

Fig. 4.6 Average Concentration of Nitrogen Oxides in Each Watershed, [ppm]

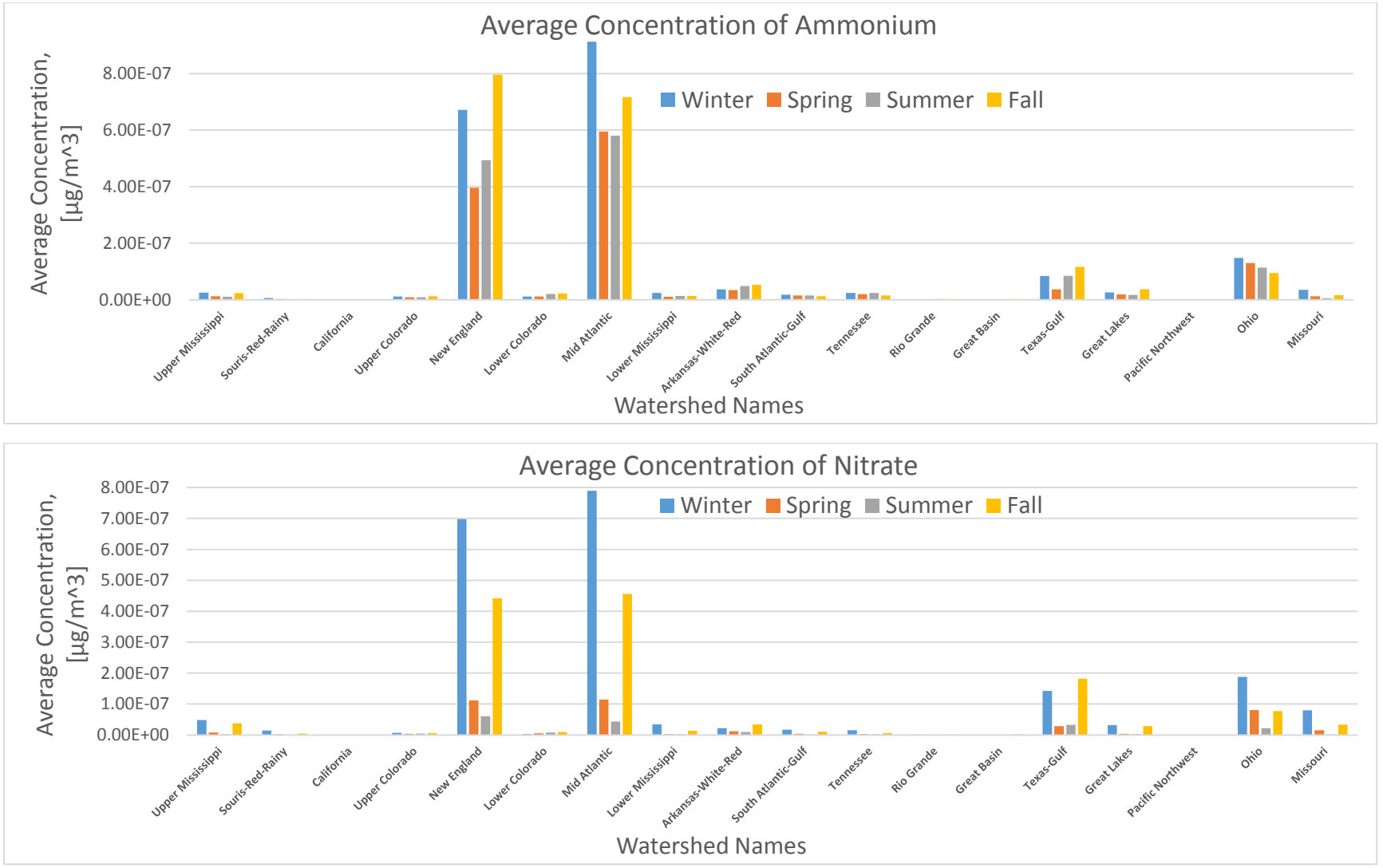

Fig. 4.7 Average Concentration of Ammonium and Nitrate in Each Watershed, [µg/m^3]

gaseous species, nitric oxide (NO) and nitrogen dioxide (NO_2), in each watershed. Fig 4.7 shows the seasonal pattern of the average concentration of two particulate matter, particulate ammonium (PNH_4) and particulate nitrate (PNO_3), in each watershed.

Both Fig. 4.3 and Fig. 4.4 demonstrate that Ohio, Mid Atlantic, Great Lakes, Upper Mississippi, Lower Mississippi, Tennessee and New England watersheds receive more wet deposited mass per area than other regions. Comparing the average concentration for all nitrogen-containing species except for ammonia (NH_3), which are shown in Fig. 4.5 through Fig. 4.7, it can be observed that Mid-Atlantic and New England watersheds have the highest average concentration among all the regions. In the New England watershed, major species emitted to the atmosphere are nitrogen oxides (NOx) from on-road and off-road vehicles, power plants, and smaller combustion sources. Atmospheric nitrogen is also frequently transported into the Northeast U.S. from the Midwest, the Mid-Atlantic, and southern Canada (Fischer et al, 2006; Charles et al, 2003). Meteorology conditions and sea breeze play a major part in determining weather and transport of air pollutants in the New England area (Fischer et al., 2006; Miller et al., 2003). Mid-Atlantic watershed is in the northeastern United States and receives similar pattern as New England watershed.

Fenn et al (2003) studied nitrogen deposition in the western United States and concluded that streamwater nitrate concentrations are elevated in high-elevation catchments in Colorado and are usually high in southern California and in some catchments in the southwestern Sierra Nevada.

The following precipitation map (Fig. 4.8) of the United States shows that Ohio, New England, Mid Atlantic, Upper Mississippi, Lower Mississippi, and Tennessee watersheds receive more precipitation than most of other watersheds. This means that soluble gases, such as nitric acid (HNO_3), nitrogen dioxide (NO_2), and ammonia (NH_3), and particulate matter, such as particulate nitrate (PNO_3), and particulate ammonium (PNH_4), can be greatly removed from the atmosphere by wet deposition.

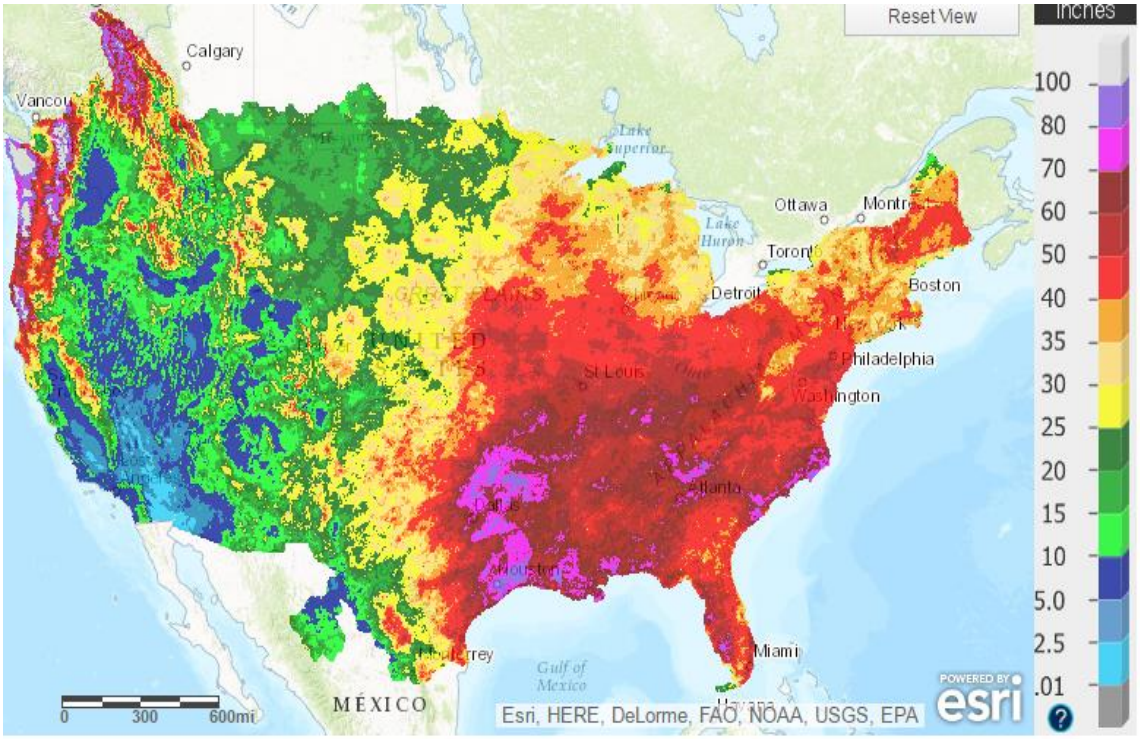

Fig. 4.8 Precipitation Map of the U.S. in the year 2011 (water.weather.gov)

4.2 Average Concentration Results

Fig. 4.6 shows that ammonia (NH_3) has a higher average concentration than nitric acid (HNO_3), which leads to the finding that NH_3 has a higher deposited mass per area than HNO_3 shown in Fig. 4.3.

Additionally, for ammonia (NH_3), the average concentration is higher in spring and summer, than in fall and winter. While nitric acid (HNO_3) has the highest average concentration in fall and winter. NH_3 is directly emitted into the atmosphere, while HNO_3 is a secondary pollutant, which can be formed through chemical reactions in the atmosphere. The major sources of NH_3 emissions are volatilization from synthetic fertilizers and animal wastes, biomass burning, fossil fuel combustion (Behera et al., 2013; Olivier et al., 1998). Because the temperature in summer is higher than other seasons, the volatilization rate of NH_3 from fertilizers and animal husbandry wastes is the highest in summer (Behera et al., 2013).

Nitric oxide (NO) and nitrogen dioxide (NO_2) have higher average concentrations in fall and winter, which are shown in Fig. 3.6. As described in section 3.1.3, NO can be produced during the combustion of fuel cells (Qian et al., 2011). NO_2 comes from traffic emissions and other combustion sources, such as power plants (Son et al., 2004). NO_2 can also be produced by the oxidation of NO in the atmosphere (Seinfeld et al., 2006).

For nitric acid (HNO_3), it can be formed in the atmosphere through oxidation of nitrogen dioxide (NO_2), with the presence of OH. Aneja et al. (1994) monitored and measured the nitric acid, ozone, and hydrogen peroxide in the ambient air at Mt Mitchell State Park, North Carolina. They found that the concentration of gas-phase HNO_3 depends on solar radiation, and temperature and also found that high concentrations of HNO_3 were always linked to low relative humidity (Grosjean et al., 1983). Studies showed that ammonium nitrate (NH_4NO_3) particles are in

equilibrium with NH_3 and HNO_3 in the atmosphere. The equilibrium concentration is directly related to temperature and inversely dependent on humidity (Cadle, 1984; Stelson et al., 1981). If the temperature effects are less significant, concentrations of HNO_3 will be higher. Lower concentrations of NH_3 will counter balance this effect (Cadle, 1984).

The average concentration of particulate nitrate (PNO_3) and ammonium (PNH_4) is shown in Fig. 4.7, both of which have the highest average concentration in fall and winter. PNO_3 and PNH_4 are not emitted in a large quantity but result from the chemical reactions of nitrogen oxides (NOx) and ammonia (NH_3) in the atmosphere (Seinfeld et al., 2006). The formation of PNH_4 and PNO_3, such as ammonium nitrate (NH_4NO_3) and ammonium chloride (NH_4Cl), are favored in higher relative humidity and lower atmospheric temperature. Otherwise, these ammonium salts can be reversed back to their precursor gases (Behera et al., 2013).

4.3 References

Andersen, H. V., and M. F. Hovmand. (1995). Ammonia and nitric acid dry deposition and throughfall. *Water Air and Soil Pollution*, 85:2211–2216.

Aneja, V. P., Claiborn, C. S., Li, Z., & Murthy, A. (1994). Trends, seasonal variations, and analysis of high-elevation surface nitric acid, ozone, and hydrogen peroxide. *Atmospheric Environment*, 28(10), 1781–1790. http://doi.org/10.1016/1352-2310(94)90140-6

Aneja, V. P., Chauhan, J. P., & Walker, J. T. (2000). Characterization of atmospheric ammonia emissions from swine waste storage and treatment lagoons. *Journal of Geophysical Research*, 105, 535–545.

Aneja, V. P., Roelle, P. a., Murray, G. C., Southerland, J., Erisman, J. W., & Fowlder, D. (2000). Atmospheric nitrogen compounds. II. Volatilizations,

transport, transformation, deposition and assessment. *Atmospheric Environment*, 35, 1903–1911.

Asman, W.A.H., van Jaarsveld, J.A. (1992). A variable-resolution transport model applied for NHx in Europe. *Atmospheric Environment* 26A, 445-464.

Baek, B. H., & Aneja, V. P. (2004). Measurement and analysis of the relationship between ammonia, acid gases, and fine particles in eastern North Carolina. *Journal of the Air & Waste Management Association* (1995), 54(5), 623–633. http://doi.org/10.1080/10473289.2004.10470933

Behera, S. N., Sharma, M., Aneja, V. P., & Balasubramanian, R. (2013). Ammonia in the atmosphere: A review on emission sources, atmospheric chemistry and deposition on terrestrial bodies. *Environmental Science and Pollution Research*, 20(11), 8092–8131. http://doi.org/10.1007/s11356-013-2051-9

Benedict, K. B., Carrico, C. M., Kreidenweis, S. M., Schichtel, B., Malm, W. C., & Collett, J. L. (2013). A seasonal nitrogen deposition budget for Rocky Mountain National Park. *Ecological Applications : A Publication of the Ecological Society of America*, 23(5), 1156–69. http://doi.org/10.1890/12-1624.1

Brown, R. (1828). A brief account of microscopical observations made in the months of June, July and August 1827, on the particles contained in the pollen of plants; and on the general existence of active molecules in organic and inorganic bodies. *Philosophical Magazine Series* 2, 4(21), 161–173. http://doi.org/10.1080/14786442808674769

Cadle S. H. (1984).Seasonal Variations in Nitric Acid, Nitrate, Strong Aerosol Acidity, and Ammonia in an Urban Area. *Atmospheric Environment*, 19(1), 181-188. http://doi.org/10.4319/lo.2013.58.2.0489

CHARLES T. DRISCOLL JOHN ABER, ELIZABETH BOYER, MARK CASTRO, CHRISTOPHER CRONAN, CHRISTINE L. GOODALE, PETER GROFFMAN, CHARLES HOPKINSON, KATHLEEN LAMBERT, GREGORY LAWRENCE, and SCOTT OLLINGER, D. W. (2003). Nitrogen Pollution in the Northeastern United States: Sources, Effects, and Management Options. *Bioscience*, 53 (4), 357-374

Clarke, J.F., Edgerton, E.S., Martin, B.E. (1997). Dry deposition calculations for the clean air status and trends network. *Atmospheric Environment*, 31 (21), 3667–3678.

ENVIRON (2013). User's Guide COMPREHENSIVE AIR QUALITY MODEL WITH EXTENSIONS (CAMx) Version 6.0.

Erisman, J. W., & Fowler, D. (2010). Oxidized and Reduced Nitrogen in the Atmosphere. *Encyclopedia of Life Support Systems (EOLSS)*, *I*

Fenn, M., Baron, J. S., Allen, E. B., Rueth, H. M., Nydick, K. R., Geiser, L., Neitlich, P. (2003). Ecological effects of nitrogen deposition in the western United States. *BioScience*, 53(4), 404–420. http://doi.org/10.1641/0006-3568(2003)053[0404:EEONDI]2.0.CO;2

Fischer, E., Pszenny, A., Keene, W., Maben, J., Smith, A., Stohl, A., & Talbot, R. (2006). Nitric acid phase partitioning and cycling in the New England coastal atmosphere. *Journal of Geophysical Research Atmospheres*, 111(23), 1–14. http://doi.org/10.1029/2006JD007328

Grosjean, & Grosjean, D. (1983). Distribution of atmospheric nitrogenous pollutants at a Los Angeles area smog receptor site. *Environmental Science & Technology*, 17(1), 13–19. http://doi.org/10.1021/es00107a006

Harrison, R. M., and A. G. Allen. (1991). Scavenging ratios and deposition of sulfur, nitrogen, and chlorine species in eastern England. *Atmospheric Environment*, 25:1719–1723.

Hicks, B.B., Baldocchi, D.D., Meyers, T.P., Hosker Jr., P., Matt, D.R. (1987). A preliminary multiple resistance routine for deriving dry deposition velocities from measured quantities. *Water, Air and Soil Pollution*, 36, 311–330.

Hu, H. L., Chen, H. M., Nikolaidis, N. P., Miller, D. R., & Yang, X. S. (1997). Estimation of nutrient atmospheric decomposition to Long Island sound. *Water Air and Soil Pollution*, *105*(3-4), 521–538.

Luo, Y., Yang, X., Carley, R. J., & Perkins, C. (2002). Atmospheric deposition of nitrogen along the Connecticut coastline of Long Island Sound: A decade of measurements. *Atmospheric Environment*, *36*(28), 4517–4528. http://doi.org/10.1016/S1352-2310(02)00421-1

Meyers, T.P., Huebert, B.J., Hicks, B.B. (1989). HNO_3 deposition to a deciduous forest. *Boundary-Layer Meteorology*, 49, 395–410.

Miller, S. T. K. (2003). Sea breeze: Structure, forecasting, and impacts. *Reviews of Geophysics*, 41(3), 1011. http://doi.org/10.1029/2003RG000124

Neirynck, J., Kowalski, A. S., Carrara, A., Genouw, G., Berghmans, P., & Ceulemans, R. (2007). Fluxes of oxidised and reduced nitrogen above a mixed coniferous. *Environmental Pollution*, 149(1), 31–43. http://doi.org/10.1016/j.envpol.2006.12.029

Olivier J G J; Bouwmana, A F: van der Hoek, K W; Berdowski, J. J. M. (1998). Global air emission inventories for anthropogenic sources of NOx, NH3, and NO in 1990. *Environmental Pollution*, 102(S1), 135–148.

Pitcairn, C. E. R., Fowler, D., & Grace, J. (1995). DEPOSITION OF FIXED ATMOSPHERIC NITROGEN AND FOLIAR NITROGEN CONTENT OF BRYOPHYTES AND Calluna vulgaris (L.) HULL. *Environmental Pollution*, 88, 193–205.

Qian, F. P., Chyang, C. S., Huang, K. S., & Tso, J. (2011). Combustion and NO emission of high nitrogen content biomass in a pilot-scale vortexing fluidized bed combustor. *Bioresource Technology*, *102*(2), 1892–1898. http://doi.org/10.1016/j.biortech.2010.08.008

Renard, J. J., Calidonna, S. E., & Henley, M. V. (2004). Fate of ammonia in the atmosphere - A review for applicability to hazardous releases. *Journal of Hazardous Materials*, 108(1-2), 29–60. http://doi.org/10.1016/j.jhazmat.2004.01.015

Seinfeld, J. H.; Pandis, S. N. (2006). Atmospheric Chemistry and Physics: From Air Pollution to Climate Change, 2nd ed.; *Wiley-Interscience*.

Son, B., Yang, W., Breysse, P., Chung, T., & Lee, Y. (2004). Estimation of occupational and nonoccupational nitrogen dioxide exposure for Korean taxi drivers using a microenvironmental model. *Environmental Research*, *94*(3), 291–296. http://doi.org/10.1016/j.envres.2003.08.004

Stelson, A. W., & Seinfeld, J. H. (1981). Relative humidity and temperature dependence of the ammonium nitrate dissociation constant. *Atmospheric*

Environment, 41(2007), 126–135. http://doi.org/10.1016/j.atmosenv.2007.10.063

Zhao, Y., Zhang, L., Pan, Y., Wang, Y., Paulot, F., & Henze, D. K. (2015). Atmospheric nitrogen deposition to the northwestern Pacific: Seasonal variation and source attribution. *Atmospheric Chemistry and Physics*, *15*(18), 10905–10924. http://doi.org/10.5194/acp-15-10905-2015

Chapter 5 CONCLUSIONS AND FUTURE WORK

5.1 Conclusions

This study aims to quantify dry and wet deposition of major nitrogen-containing species, including ammonia (NH_3), nitric acid (HNO_3), nitrogen oxides (NOx), particulate ammonium (PNH_4) and particulate nitrate (PNO_3) onto each of the major watersheds in the contiguous United States, and to obtain seasonal variation of each species in each watershed region.

A regional chemical transport model was used, the Comprehensive Air Quality Model with eXtension (CAMx), to obtain the processed deposition data. The watershed shapefile was obtained from National Hydrology Dataset (NHD) website. A Geographic Information System (ArcGIS) was utilized to obtain the features of the watershed file, which includes the area of each watershed and the name of each region, and created a fishnet grid, which uses the same grid information as in CAMx, including using 12x12 km resolution, 396x246 grid cells, and Lambert Conformal Projection. Finally, a program was written in MATLAB to calculate dry and wet deposited mass from nitrogen species onto each watershed.

It is found that gaseous species are dominant in dry deposited mass per area, with ammonia (NH_3) ranging from 10 to 600 kgN/km^2, nitric acid (HNO_3) from 50 to 300 kgN/km^2, and nitrogen dioxide (NO_2, ranging from 10 to 180 kgN/km^2). NH_3, HNO_3, NO_2, contributing 40% to 60%, 20% to 40%, and 10% of the total nitrogen dry deposition. While for wet deposition, the major contribution is from HNO_3 and particulate ammonium (PNH_4), ranging from 25 to 190 kgN/km^2 and 10 to 100 kgN/km^2, respectively. HNO_3 contributes 40%-60% of the total nitrogen wet

deposited mass per area, PNH_4 about 20%-40%, and ammonia (NH_3) and particulate nitrate (PNO_3) altogether contributing about 10%. Gases are easy to be dry deposited due to their high deposition velocity. HNO_3 is highly soluble and can be easily removed from the atmosphere through dry and wet deposition. Particles act as cloud condensation nuclei, resulting in the growth of cloud droplets. After getting to a sufficiently large size, they fall as precipitation (ENVIRON, 2013).

For the annual deposition, the mass of nitrogen deposited per area through dry deposition, which ranges from around 110 to 910 kgN/km^2, is over twice that of wet deposition, which ranges from about 40 to 390 million kgN/km^2.

It is also concluded that spring and summer are the two seasons which consistently receive the most nitrogen deposited mass per area for both wet and dry deposition, while fall and winter receive the least deposited nitrogen mass. The maximum value of spring can be over twice that of fall. This is due to the fact that in spring and summer, fertilizer is heavily used, where ammonia (NH_3) is mainly from. The concentration of NH_3 in the atmosphere is high in these two seasons. While in fall and winter, fuel combustions play a major part in the emissions of nitrogen species, where nitrogen oxides are mainly from. Zhao et al. (2015) studied the atmospheric nitrogen deposition to the northwestern Pacific for 2008-2010. They found that spatial distribution of total nitrogen deposition (ammonium and nitrate) does not show a strong seasonality in the northwestern Pacific.

Another conclusion is drawn that for the annual deposition, the amount of nitrogen deposited mass per area through dry deposition, which ranges from around 110 to 910 kgN/km^2, is over twice that of wet deposition, which ranges from

about 40 to 390 million kgN/km^2. This result is further confirmed by the map (Fig. 4.1) from National Atmospheric Deposition Program (NADP).

Eastern United States, including Ohio, Mid Atlantic, Great Lakes, Upper Mississippi, Lower Mississippi, Tennessee and New England, and other watersheds such as California, Texas-Gulf, and Arkansas-White-Red, receive more deposition throughout the year. Because nitrogen sources are mainly vehicular emissions, power plants, and fertilizer use. These watersheds are highly populated. Additionally, power plants are concentrated in these areas.

5.2 Future Work

Further study on the difference between dry deposition of particulate matter from CMAQ and CAMx is needed. The results show that nitrogen-containing species have different seasonality and spatial patterns. Additionally, different species also contribute differently to the total nitrogen deposition in the atmosphere. It is worth further investigating how meteorological conditions correlate to different seasonal patterns, and how source regions and emission sources contribute to the emissions of major nitrogen-containing species. It is also necessary to perform an evaluation of more highly resolved hydrologic units.

5.3 References

ENVIRON (2013). User's Guide COMPREHENSIVE AIR QUALITY MODEL WITH EXTENSIONS (CAMx) Version 6.0.

Zhao, Y., Zhang, L., Pan, Y., Wang, Y., Paulot, F., & Henze, D. K. (2015). Atmospheric nitrogen deposition to the northwestern Pacific: Seasonal variation and source attribution. *Atmospheric Chemistry and Physics*, *15*(18), 10905–10924. http://doi.org/10.5194/acp-15-10905-2015

Appendix A

```
% This code includes reading deposition data from the excel file and
calculate the deposition mass for each species in each watershed
% The code is using winter as an example, for the other three seasons,
the format of code is the same, just the words 'winter', 'winter_N',
and 'w_' are changed to the name of each season respectively

clear all;
clc;

% The information in the union.xlsx file is as follows
% Col_1: Grid ID    Col_2: Watershed number    Col_3: Calculated areas
% To read and store data in each column
union  = xlsread('union.xlsx','A2:C103389');    % Dataset1
grid_ID = union(:,1);
watershed = union(:,2);
area = union(:,3);

% To read and store the data in winter for each nitrogen-containing
species for dry and wet deposition
% DD means dry deposition; WD means wet deposition; the information after
the underscore is the name of each species
% Col_1: Grid cell ID to match up the information in Dataset1
% Col_2: DD_HNO3      Col_3: DD_NH3
% Col_4: DD_NO        Col_5: DD_NO2
% Col_6: DD_PNH4      Col_7: DD_PNO3
% Col_8: WD_HNO3      Col_9: WD_NH3
% Col_10: WD_NO       Col_11: WD_NO2
% Col_12: WD_PNH4     Col_13: WD_PNO3
winter   = 'depn_winter_data.xlsx';           % Dataset2
winter_N = xlsread(winter,'B2:M97417');

% To store the length of each dataset in a variable
length_dataset2 = length(union(:,1))

% To calculate the dry deposition for each species in summer in each
watershed
w_depn_ttl_species = zeros(23,12);

for k = 1:12
    w_depn(:,k) = winter_N(:,k);          % To store the deposition of
each species in a matrix

    for i = 1:length_dataset2
        watershednum = watershed(i);
        if watershednum == 0   % To replace 0 with 23 for the watershed
            watershednum = 23;
        end
        cellnum = grid_ID(i)+1;
        areanum = area(i);
        w_depn_ttl_species(watershednum,k)                              =
w_depn_ttl_species(watershednum,k)...
            +w_depn(cellnum,k)/0.01*144*(areanum/144);   % To sum up the
values with the same watershed number
    end
end                  % The end of the first MATLAB file
```

```
% From the previous MATLAB file, the units of each species are different
% In this code, it is about the unit conversion to unify the unit of each
nitrogen-containing species to kgN for deposited mass, and kgN/sqkm for
area weighted deposited mass
% We also use the winter data as an example. For the calculation of other
seasons, the format of code is the same, just the words 'winter',
'winter_N', and '_w' are changed to the name of each season respectively

clear all;
clc;
% In the following winter_depn_mass.xlsx file, it has data for each
species in each watershed
% Gases: NO, NO2, NH3, HNO3   [mol]
% PM species: PNO3, PNH4      [g]
% For gases, the data from .xlsx need to be multiplied by the molecular
mass of N in each species, then be muliplied by e-3 to convert g to kg
% For PM species, the data from .xlsx just need to be multiplied by the
percentage of N in each species and then be muliplied by e-3 to convert
g to kg     i.e. PNO3: (14/62)*1e-3   PNH4: (14/18)*1e-3

% To read and store the data for each nitrogen-containing species in fall
% Col_1: DD_HNO3      Col_2: DD_NH3       Col_3: DD_NO
% Col_4: DD_NO2       Col_5: DD_PNH4      Col_6: DD_PNO3
% Col_7: WD_HNO3      Col_8: WD_NH3       Col_9: WD_NO
% Col_10: WD_NO2      Col_11: WD_PNH4     Col_12: WD_PNO3
% Col_13: Watershed Area, [sqkm]
winter   = 'winter_depn_mass.xlsx';
winter_N   = xlsread(winter);

% To store the length of the dataset
length_dataset = length(winter_N);

% Calculation for winter, making all the units to kgN
for i = 1:length_dataset
    for k = 1:4
        depn_w(i,k)      = winter_N(i,k)*14*1e-3;          % Calculation
for gases from dry deposition in winter
        depn_w(i,k+6)    = winter_N(i,k+6)*14*1e-3;        % Calculation
for gases from wet deposition in winter
    end
    depn_w(i,5)     = winter_N(i,5)*(14/18)*1e-3;          % Calculation
for PM species from dry deposition in winter
    depn_w(i,6)     = winter_N(i,6)*(14/62)*1e-3;
    depn_w(i,11)    = winter_N(i,11)*(14/18)*1e-3;         % Calculation
for PM species from wet deposition in winter
    depn_w(i,12)    = winter_N(i,12)*(14/62)*1e-3;
end

% To calculate the area weighted deposition for each season, kgN ->
kgN/sqkm
for m = 1:length_dataset
    for n = 1:12
    area_wei(m,n) = depn_w(m,n)/winter_N(m,13);
    end
end
```

```
% This code includes the calculation for the gridded dry deposition for
HNO3, NH3, PNO3, and PNH4, and wet deposition for PNO3 and PNH4 for the
maps projecting CAMx output data

clear all;
clc;

winter   = 'depn_winter_data.xlsx';    % Dataset1
winter_N = xlsread(winter,'B2:M97417');
spring   = 'depn_spring_data.xlsx';
spring_N = xlsread(spring,'B2:M97417');
summer   = 'depn_summer_data.xlsx';
summer_N = xlsread(summer,'B2:M97417');
fall   = 'depn_fall_data.xlsx';
fall_N = xlsread(fall,'B2:M97417');

% To store the length of the dataset
length_dataset = length(fall_N);

% Calculation for winter, making all the units to kgN
for i = 1:length_dataset
    for k = 1:4
        % To calculate the N percentage for gases
        depn_w(i,k)     = winter_N(i,k)*14*1e-3;          % Winter     %
To calculate the percentage of N in gases for dry deposition, mol/ha ->
kgN/ha
        depn_w(i,k+6)   = winter_N(i,k+6)*14*1e-3;
        depn_spr(i,k)   = spring_N(i,k)*14*1e-3;          % Spring     %
To calculate the percentage of N in gases for dry deposition, mol/ha ->
kgN/ha
        depn_spr(i,k+6) = spring_N(i,k+6)*14*1e-3;
        depn_sum(i,k)   = summer_N(i,k)*14*1e-3;          % Summer     %
To calculate the percentage of N in gases for dry deposition, mol/ha ->
kgN/ha
        depn_sum(i,k+6) = summer_N(i,k+6)*14*1e-3;
        depn_f(i,k)     = fall_N(i,k)*14*1e-3;            % Fall       %
To calculate the percentage of N in gases for dry deposition, mol/ha ->
kgN/ha
        depn_f(i,k+6)   = fall_N(i,k+6)*14*1e-3;                       %
To calculate the percentage of N in gases for wet deposition, mol/ha ->
kgN/ha
    end
    % To calculate the N percentage for PM species
    depn_w(i,5)    = winter_N(i,5)*(14/18)*1e-3;          % Winter     %
To calculate the percentage of N in aerosols, g/ha -> kgN/ha
    depn_w(i,6)    = winter_N(i,6)*(14/62)*1e-3;
    depn_w(i,11)   = winter_N(i,11)*(14/18)*1e-3;
    depn_w(i,12)   = winter_N(i,12)*(14/62)*1e-3;
    depn_spr(i,5)  = spring_N(i,5)*(14/18)*1e-3;          % Spring     %
To calculate the percentage of N in aerosols, g/ha -> kgN/ha
    depn_spr(i,6)  = spring_N(i,6)*(14/62)*1e-3;
    depn_spr(i,11) = spring_N(i,11)*(14/18)*1e-3;
    depn_spr(i,12) = spring_N(i,12)*(14/62)*1e-3;
    depn_sum(i,5)    = summer_N(i,5)*(14/18)*1e-3;        % Summer     %
To calculate the percentage of N in aerosols, g/ha -> kgN/ha
    depn_sum(i,6)    = summer_N(i,6)*(14/62)*1e-3;
```

```
    depn_sum(i,11)    = summer_N(i,11)*(14/18)*1e-3;
    depn_sum(i,12)    = summer_N(i,12)*(14/62)*1e-3;
    depn_f(i,5)     = fall_N(i,5)*(14/18)*1e-3;           % Fall       %
To calculate the percentage of N in aerosols, g/ha -> kgN/ha
    depn_f(i,6)     = fall_N(i,6)*(14/62)*1e-3;
    depn_f(i,11)    = fall_N(i,11)*(14/18)*1e-3;
    depn_f(i,12)    = fall_N(i,12)*(14/62)*1e-3;
end
```

Appendix B

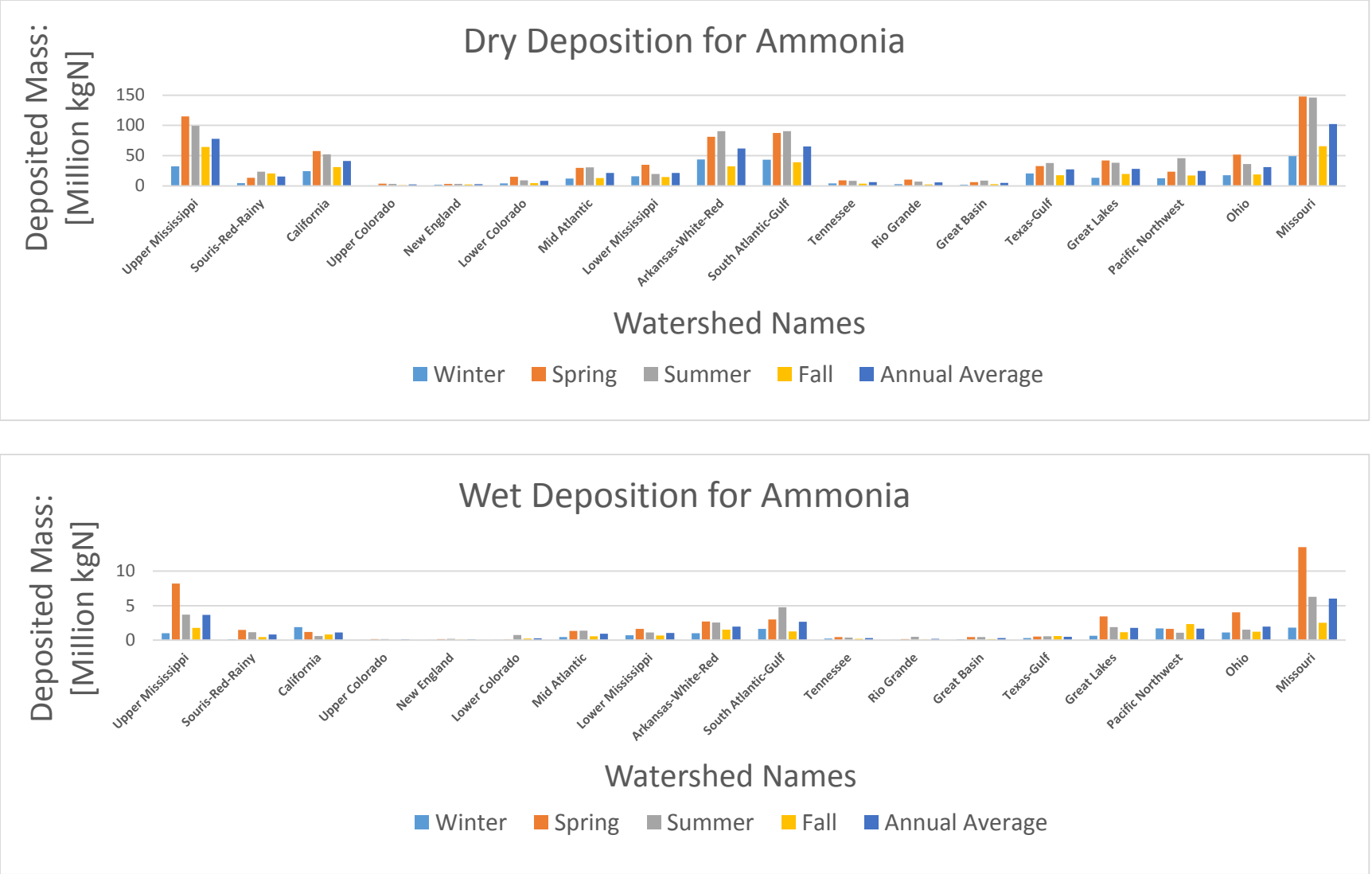

Fig. B.1 Deposited Mass for Ammonia in Each Season in Each Watershed, [Million kgN]

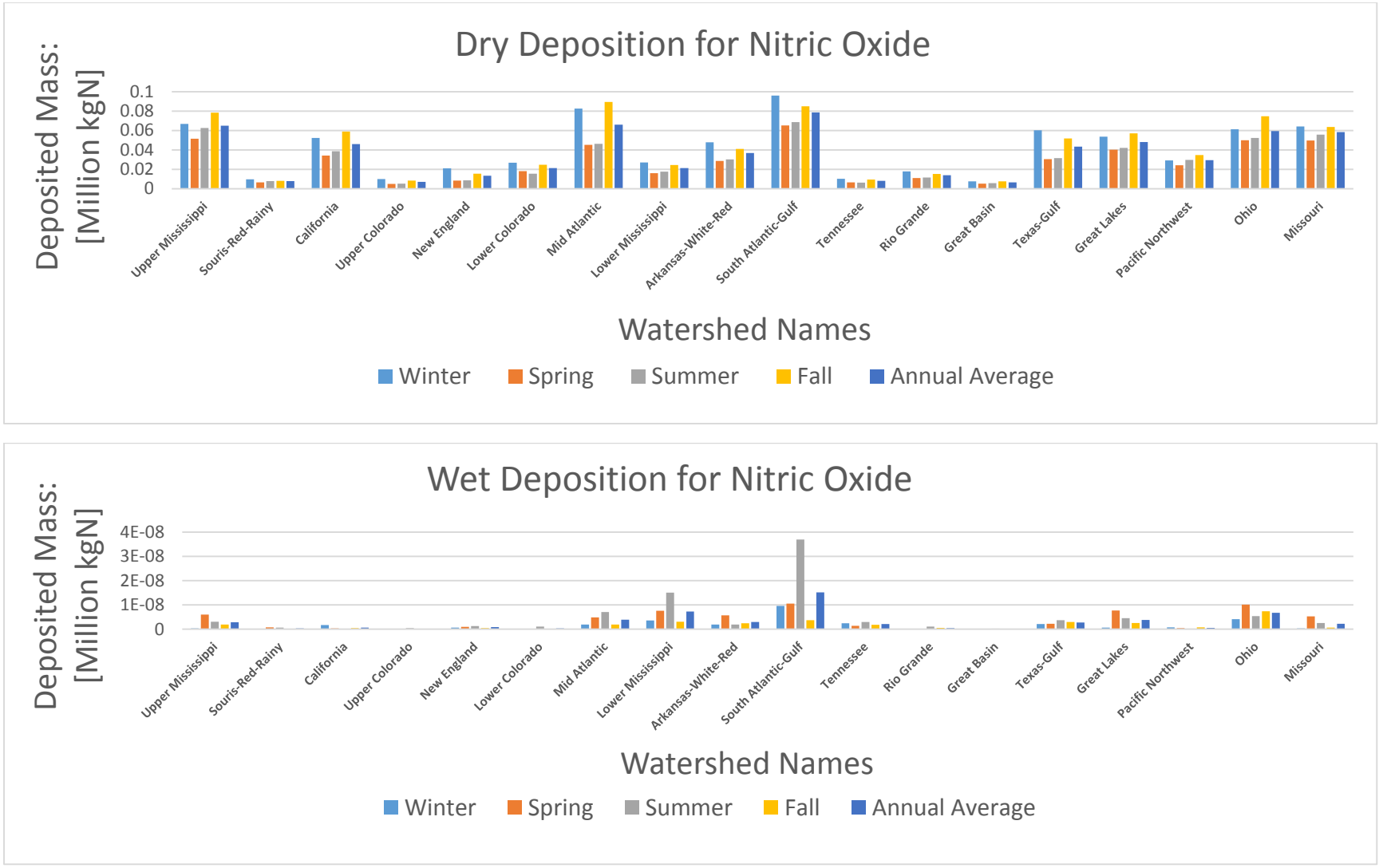

Fig. B.2 Deposited Mass for Nitric Oxide in Each Season in Each Watershed, [Million kgN]

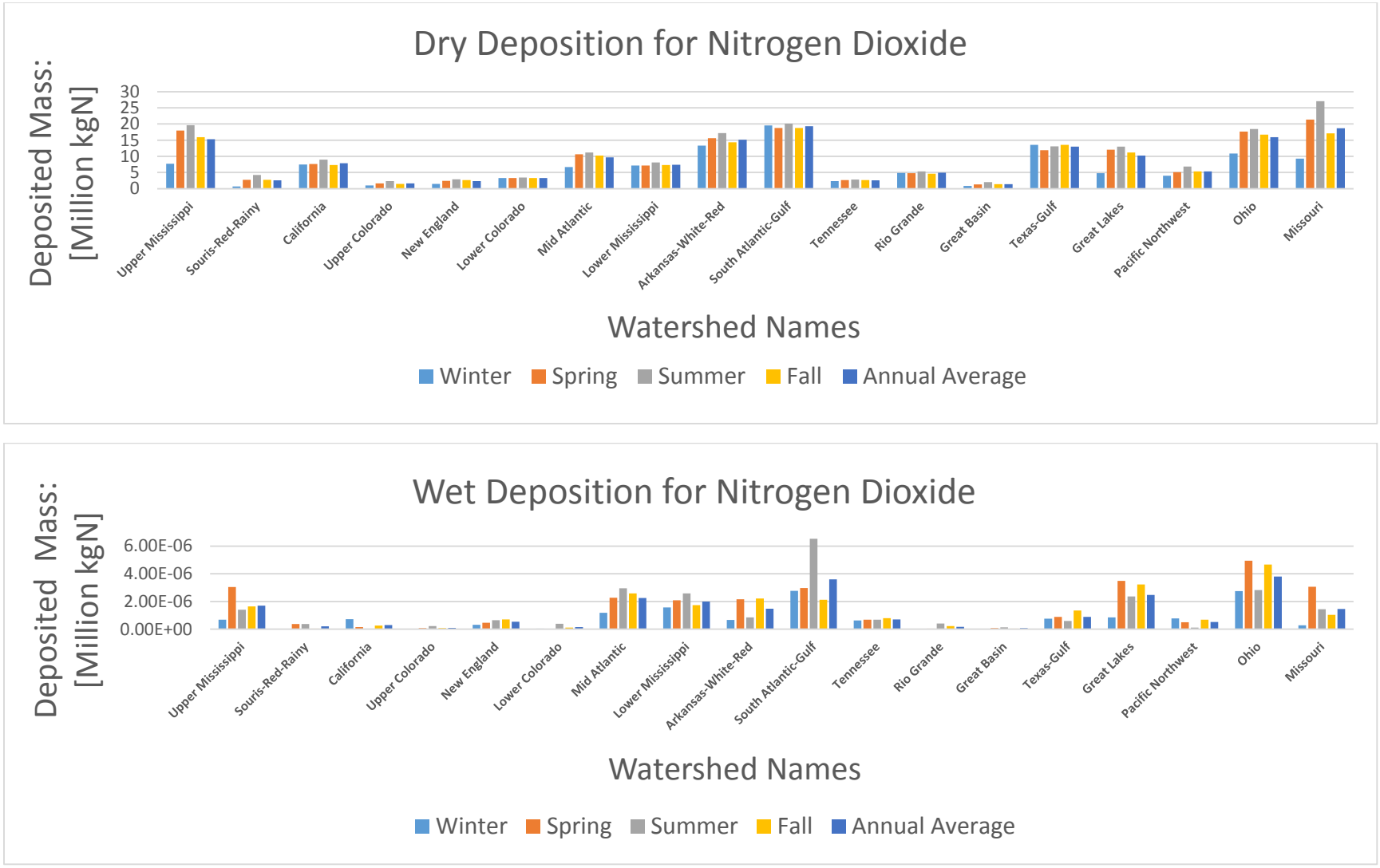

Fig. B.3 Deposited Mass for Nitrogen Dioxide in Each Season in Each Watershed, [Million kgN]

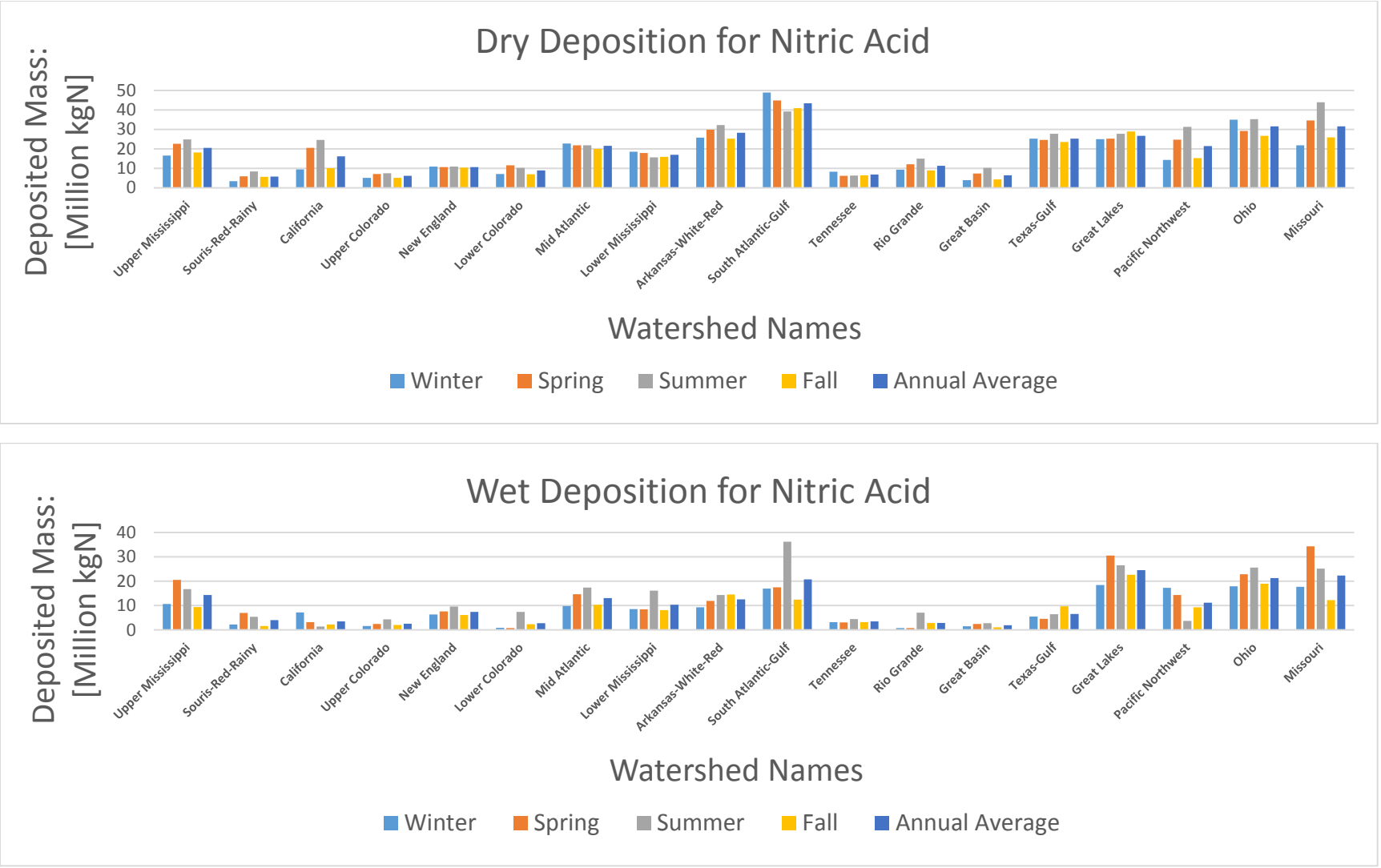

Fig. B.4 Deposited Mass for Nitric Acid in Each Season in Each Watershed, [Million kgN]

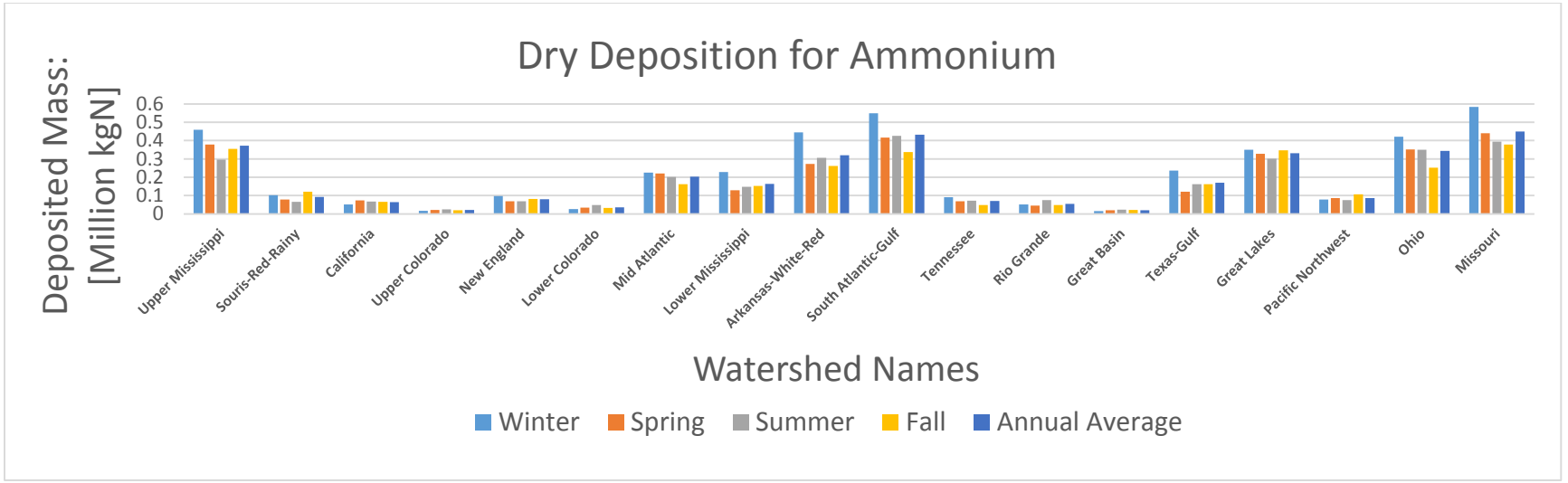

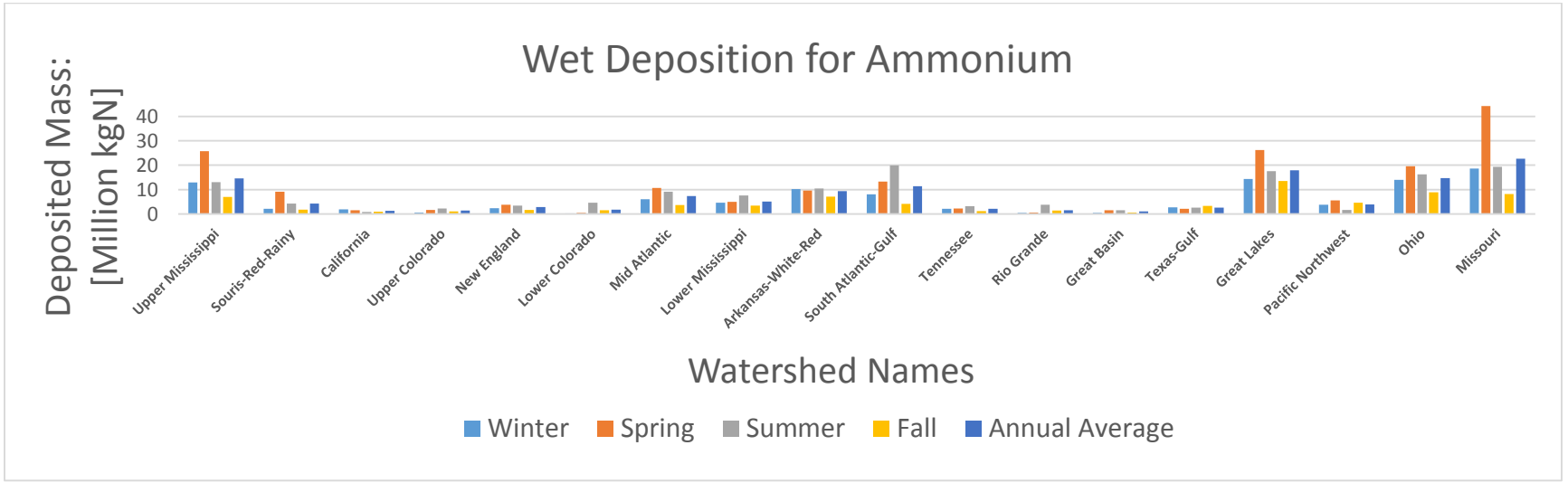

Fig. B.5 Deposited Mass for Ammonium in Each Season in Each Watershed, [Million kgN]

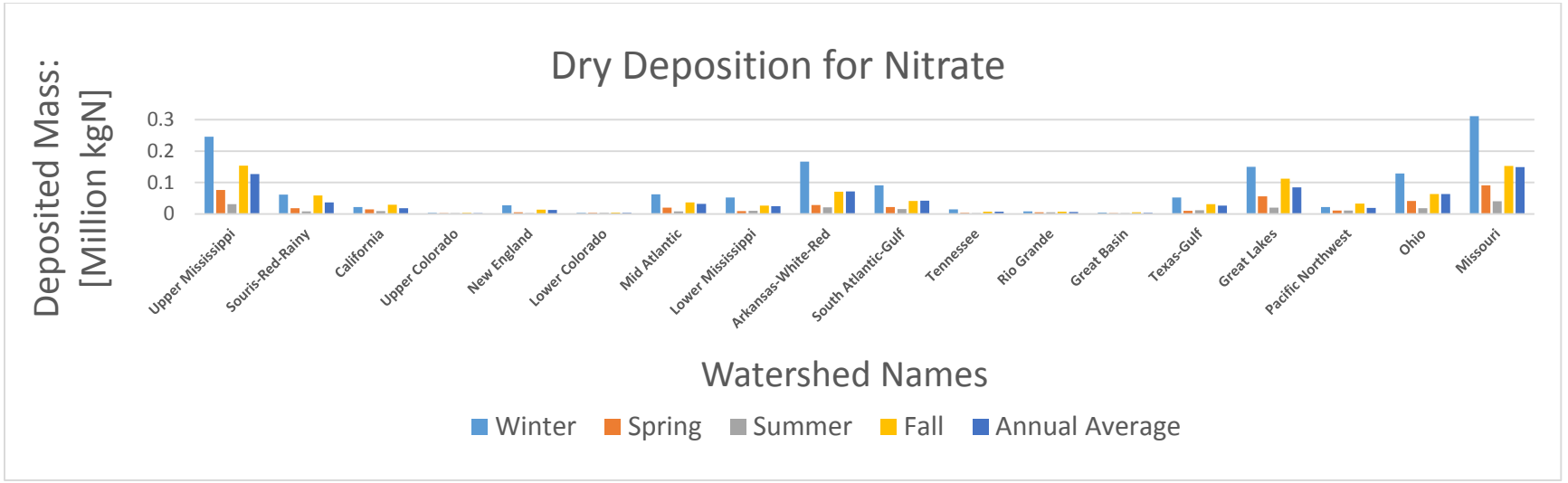

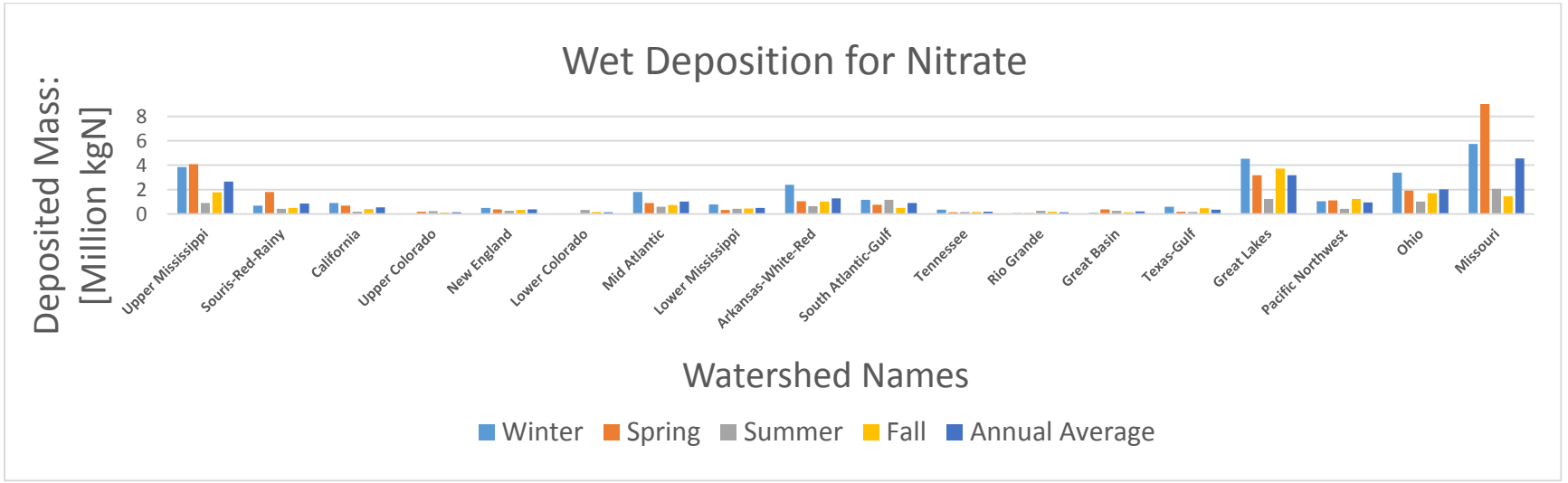

Fig. B.6 Deposited Mass for Nitrate in Each Season in Each Watershed, [Million kgN]

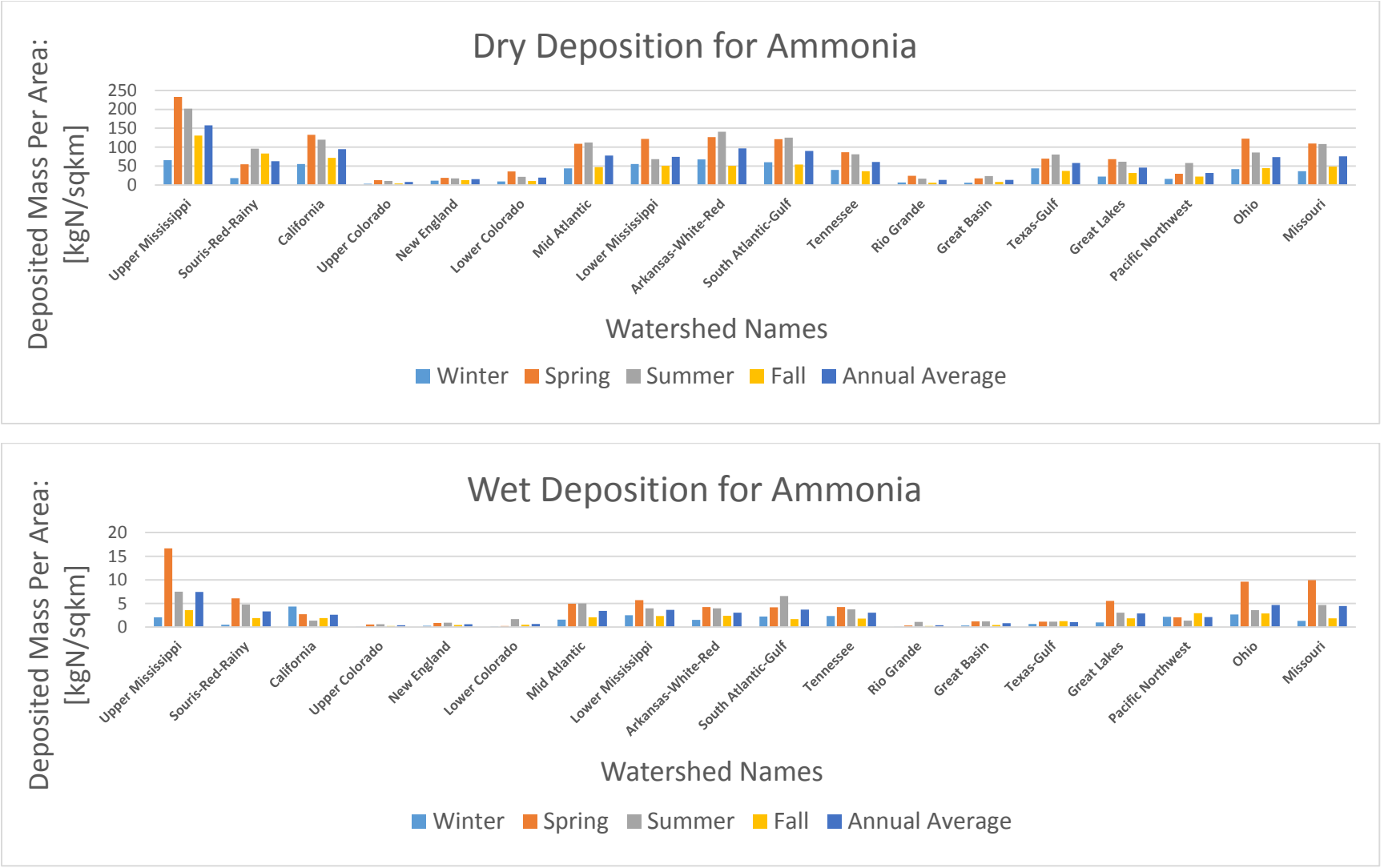

Fig. B.7 Deposited Mass Per Area for Ammonia in Each Season in Each Watershed, [kgN/sqkm]

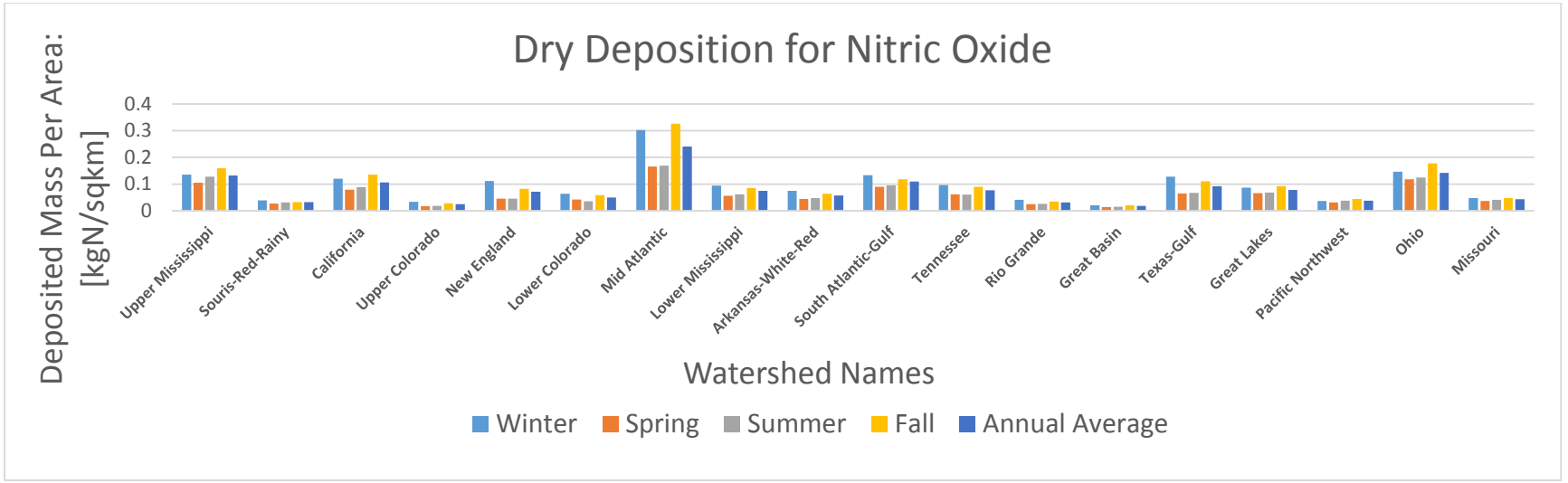

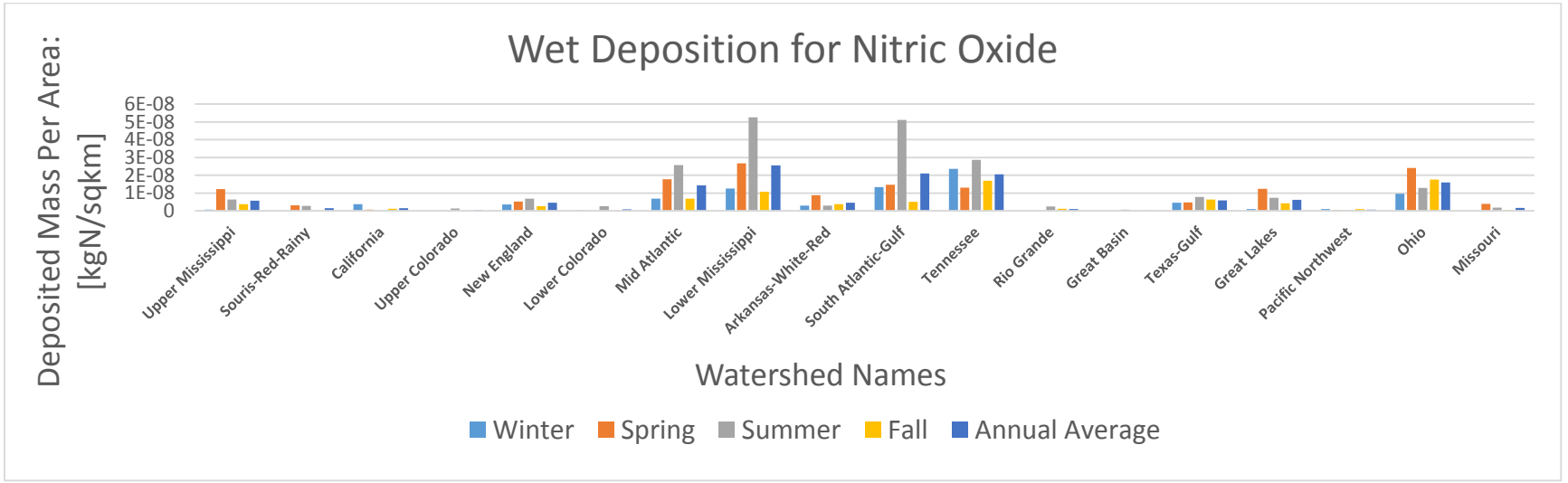

Fig. B.8 Deposited Mass Per Area for Nitric Oxide in Each Season in Each Watershed, [kgN/sqkm]

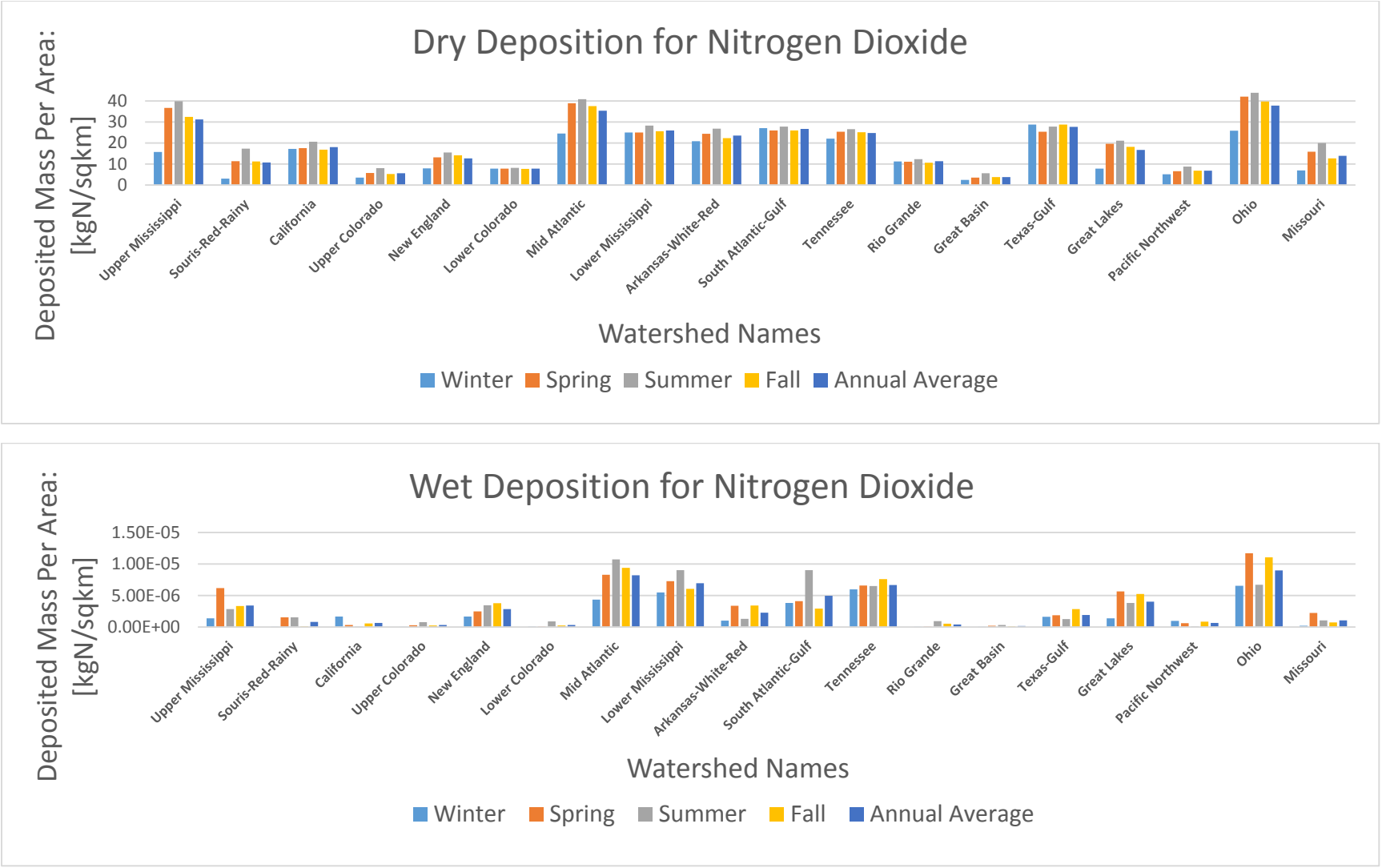

Fig. B.9 Deposited Mass Per Area for Nitrogen Dioxide in Each Season in Each Watershed, [kgN/sqkm]

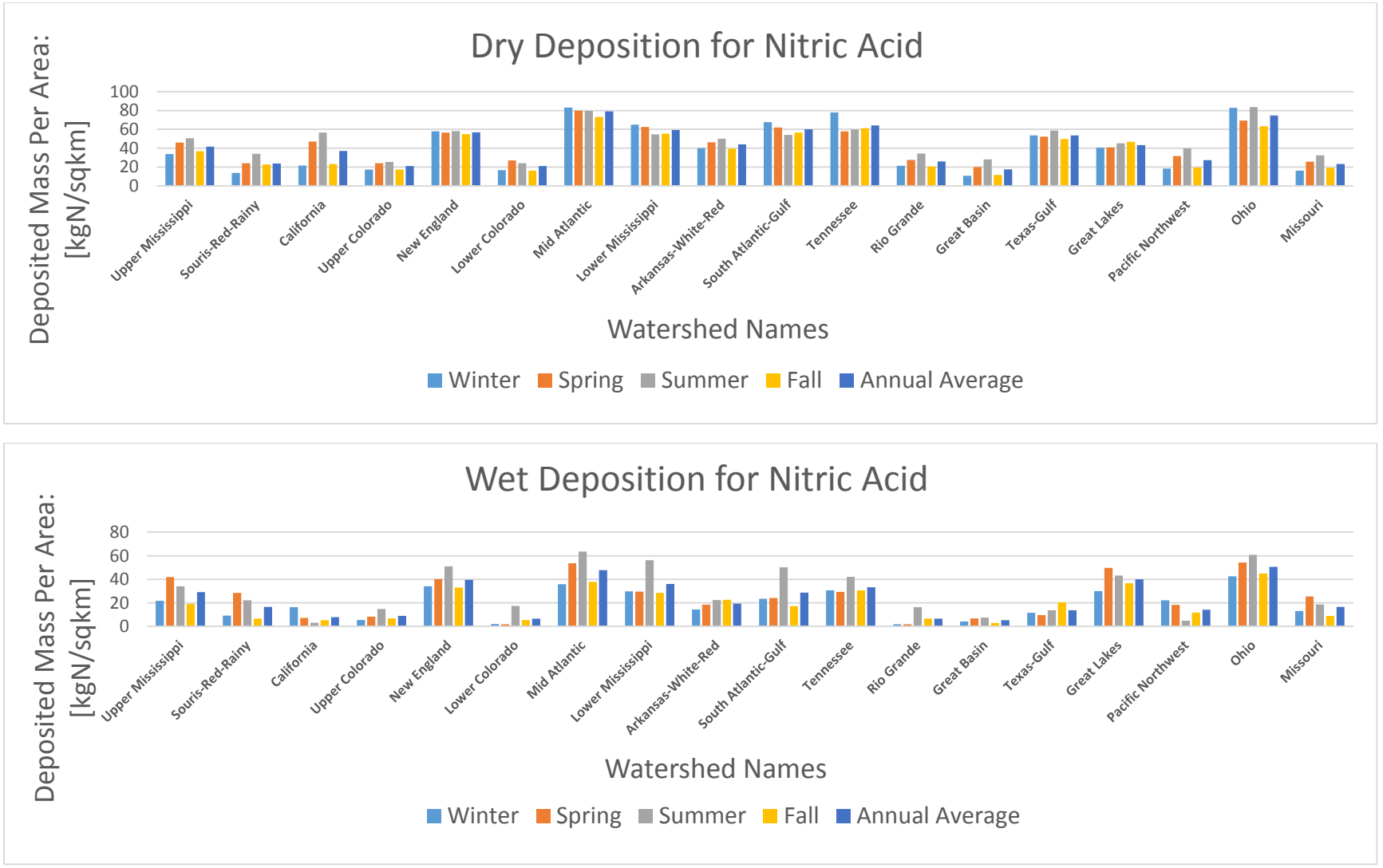

Fig. B.10 Deposited Mass Per Area for Nitric Acid in Each Season in Each Watershed, [kgN/sqkm]

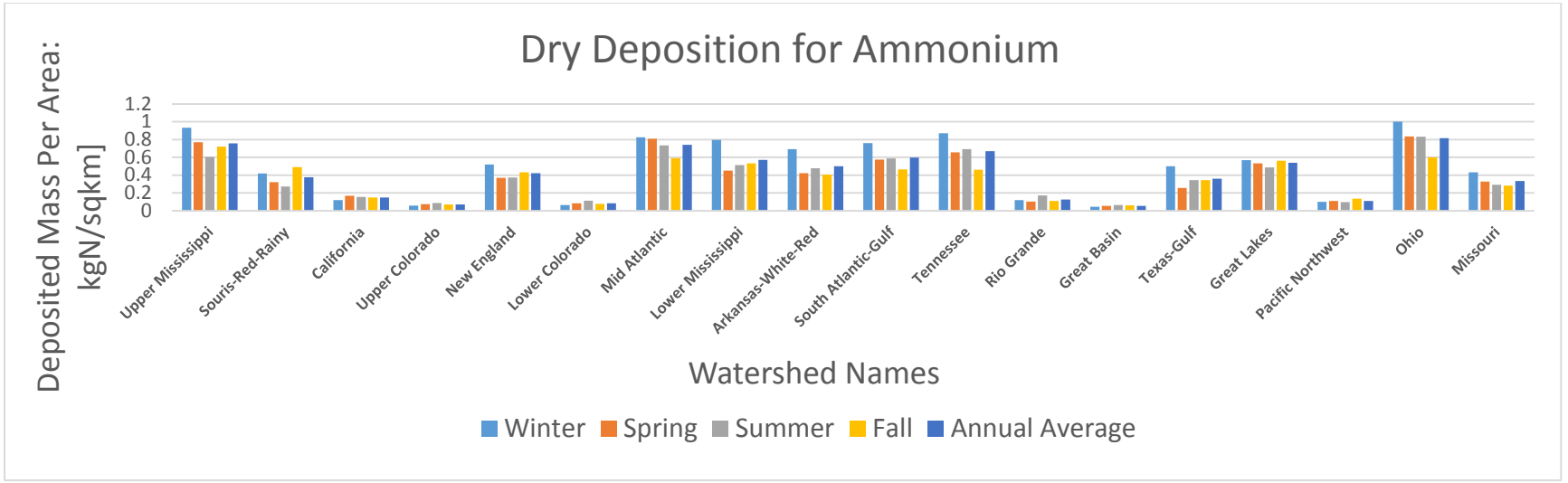

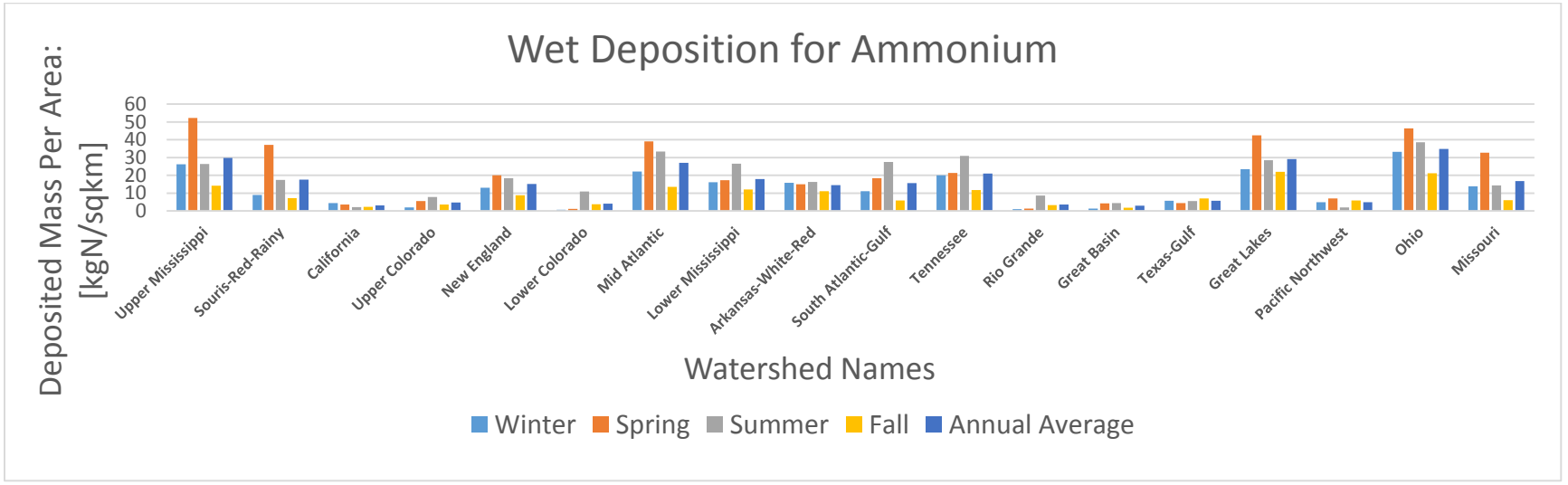

Fig. B.11 Deposited Mass Per Area for Ammonium in Each Season in Each Watershed, [kgN/sqkm]

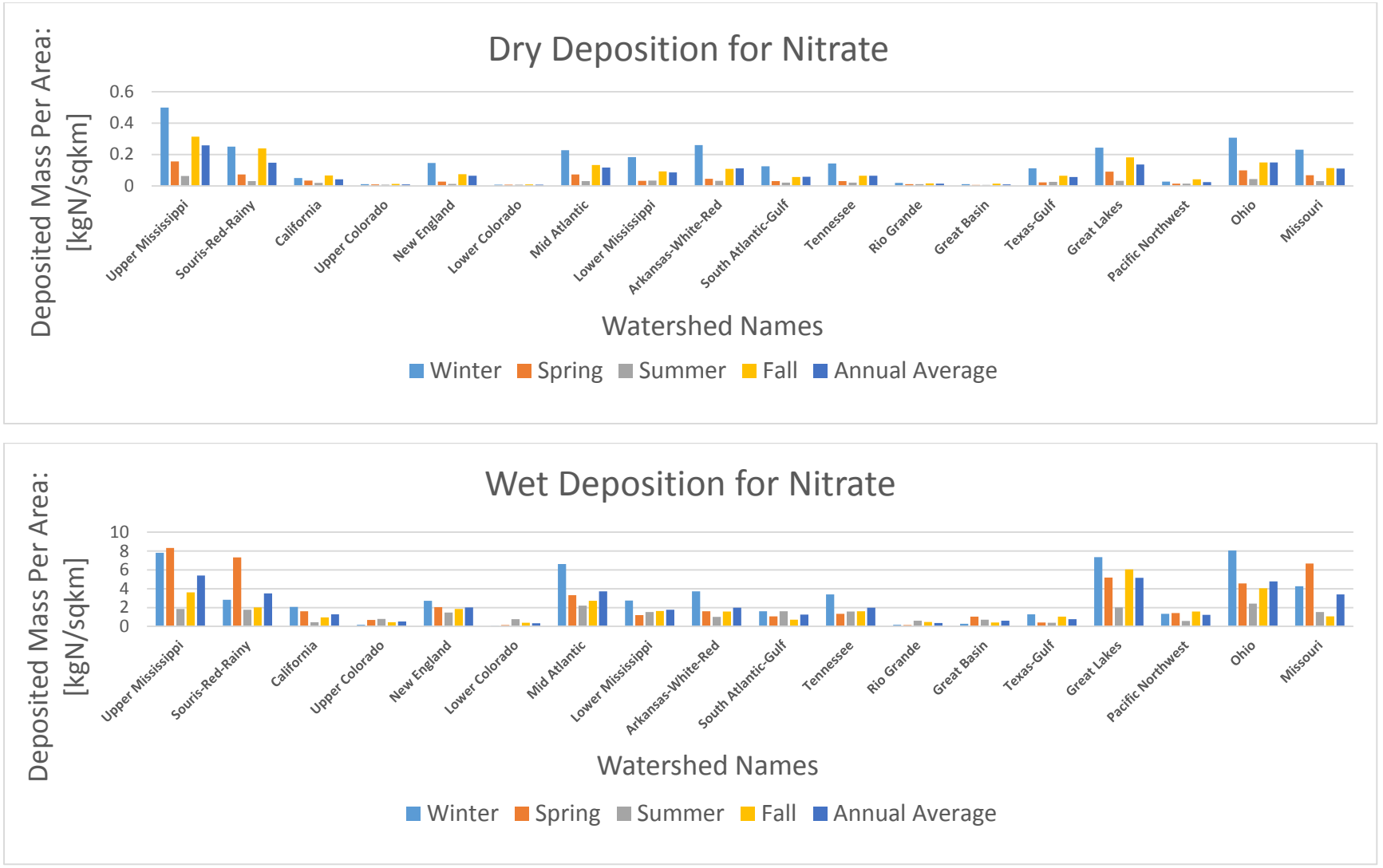

Fig. B.12 Deposited Mass Per Area for Nitrate in Each Season in Each Watershed, [kgN/sqkm]

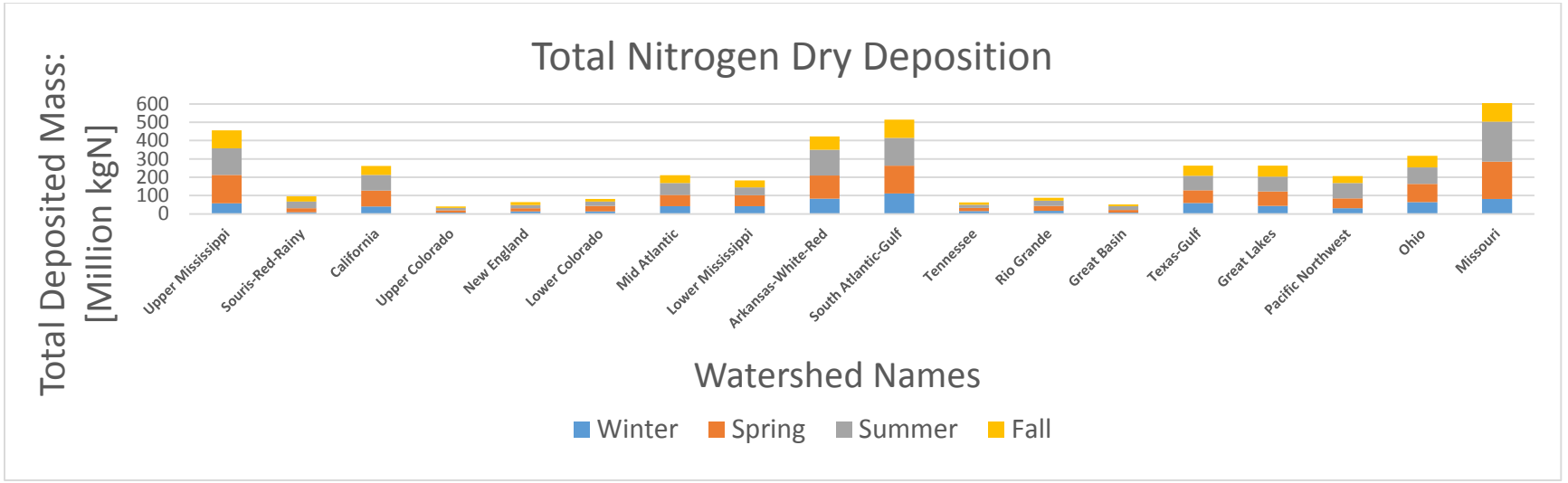

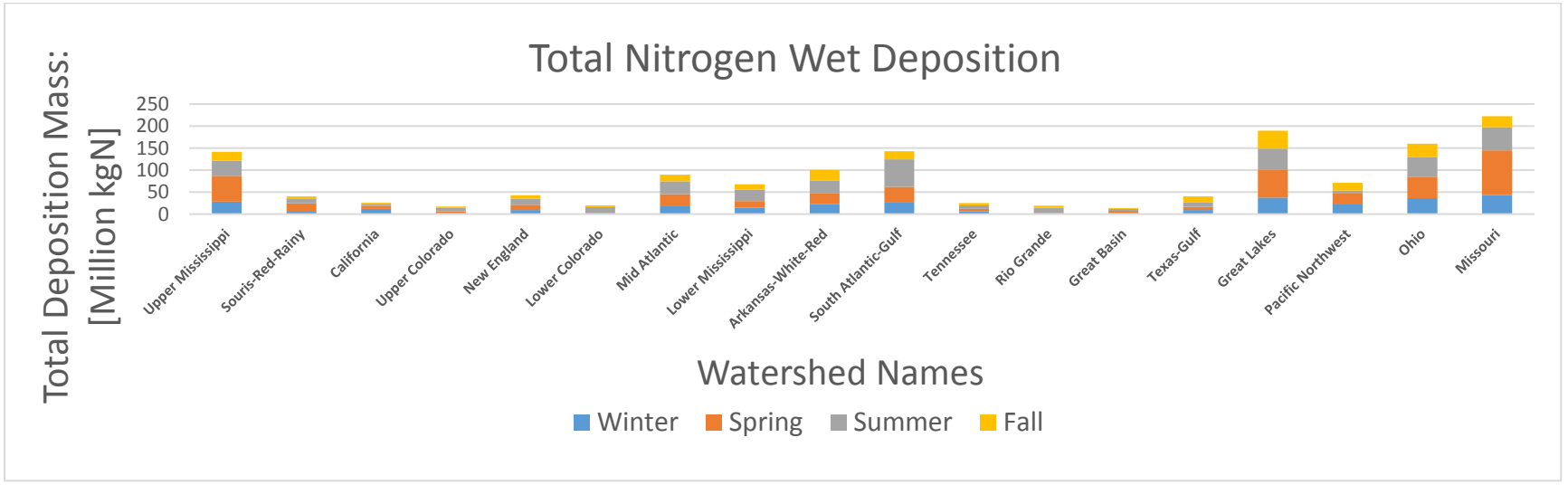

Fig. B.13 Total Deposited Mass of Each Season for All Species in Each Watershed, [Million kgN]

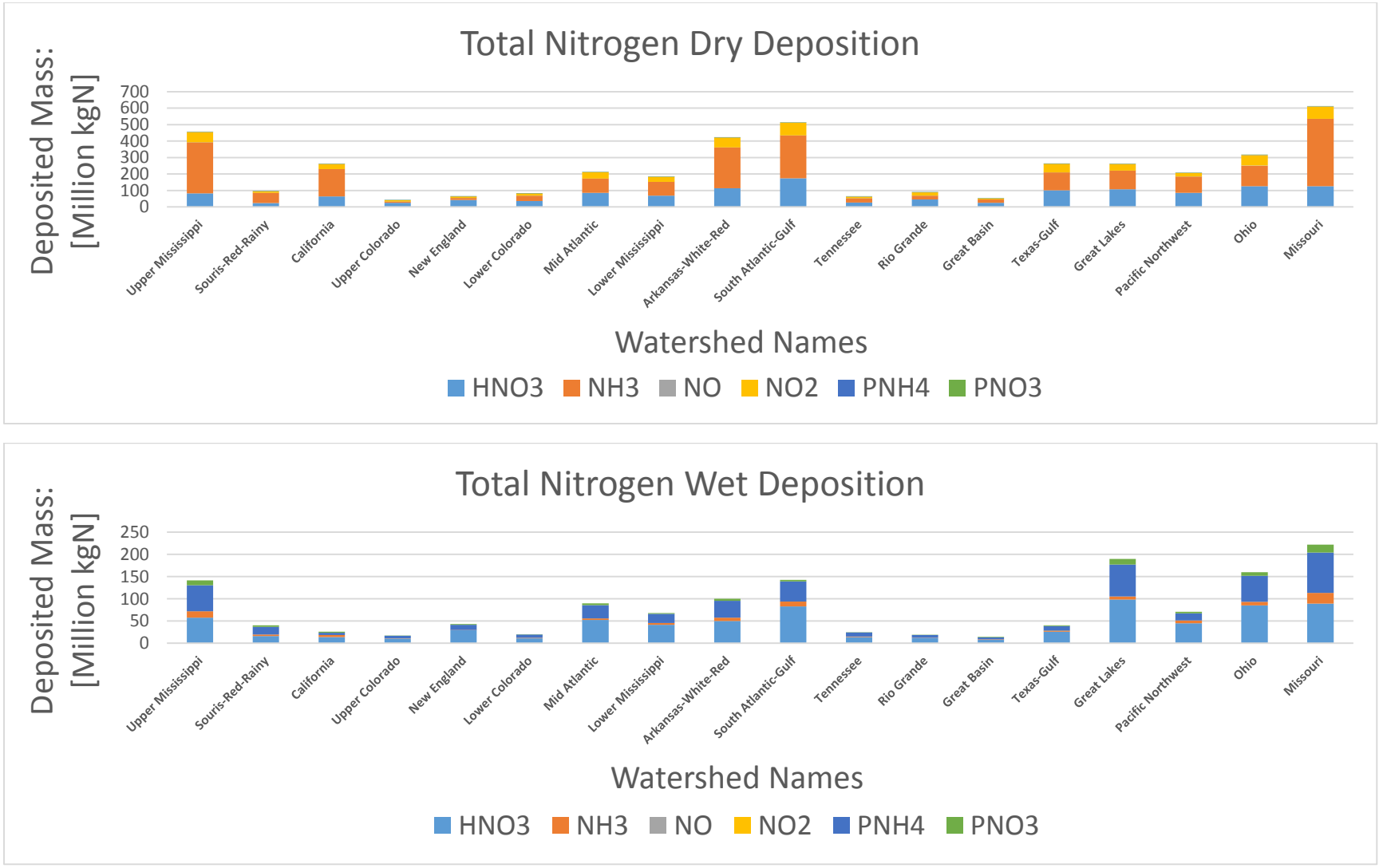

Fig. B.14 Annual Deposited Mass of Each Species in Each Watershed, [Million kgN]